

# **BIOCHEMICAL CHARACTERIZATION OF MURINE QA-1**

by

**KASRA RAMYAR**

A dissertation thesis submitted to Johns Hopkins University in conformity with the requirements for the degree of Doctor of Philosophy

Baltimore, Maryland  
April 2008

© Kasra X. Ramyar 2008  
All Rights Reserved

## Abstract

Qa-1 is a member of the mouse MHC Ib family with roles in both the adaptive and innate arms of immunity. While it is presumed to be quite similar in structure to the class Ia molecules, Qa-1 has limited polymorphism and only presents a limited repertoire of known peptides. Although Qa-1 is the primary ligand for the Natural Killer cell NKG2/CD94 receptors, Qa-1 restricted CD8<sup>+</sup> cytotoxic T cells have also been identified. To better understand the molecular mechanisms of these recognition events and the remarkably short lifetime of the Qa-1/peptide complex, a series of biophysical and biochemical characterizations were made of this molecule. Initial attempts at bacterial expression and *in vitro* reconstitution of the complex led to the identification of a single residue which drastically destabilizes the complex both *in vivo* and *in vitro*. Mutation of this residue results in significant acceleration of Qa-1's maturation rate as well as increased half-life of the molecule. The ability of this mutant to present peptide to T cells and its interaction with the NKG2 receptor have been investigated. While presentation of the cognate peptide predominantly found in complex with Qa-1 has not been altered, the enhanced cell surface expression and the elongated half-life of the mutant molecule provide insights into the normal physiological role of the wild type molecule as a real-time sensor for immunosurveillance by NK cells and rapid cytotoxic response by the effectors of adaptive immunity.

## **Acknowledgements**

I would like to first and foremost thank Mark Soloski, who has been a relentless source of inspiration and excellent advice throughout this process. I would also like to thank the members of my thesis committee, L. Mario Amzel, Michael Edidin, and Schehrazade Sadegh-Nasseri, for their assistance in completion of this work. I am also deeply indebted to Joel Pomerantz for reading this manuscript. Current and previous members of the Soloski lab, especially Adrian Davies, Michael Szperka, and Alena Calm have been invaluable not only with critical assistance and providing reagents, but also in helping me retain my sanity. Lee Blosser and Ada Tam performed most of the preparative sorting described herein. Jason Black and Calvin Chue deserve gratitude well beyond my capabilities for all that they have done over the last two decades. I am also indebted to Samuel Bouyain, Brian Geisbrecht and Lidsay Odell for advice and assistance. I owe an irremediable debt to Ben Perman, who served as mentor when others were notably absent. The unfailing support of my family, especially my sister Roya, has at all times been a tremendous help. Most of all, I owe a tremendous amount to my wife, Michele, for putting up with me.

## Table of Contents

Abstract	ii
Acknowledgements	iii
Table of Contents	iv
List of Figures	v
Chapter 1: Introduction	1
Chapter 2: Heterologous Expression of Qa-1 <sup>b</sup>	15
Chapter 3: The Role of Cysteine 134 in Qa-1 <sup>b</sup> Stability	51
Chapter 4: Biological Significance of the C134S Mutation	87
References	108
Curriculum vitae	115

## List of Figures

1.1 Schematic representation of Mouse MHC region	13
2.1 Alignment of several representative MHC I molecules	34
2.2 The pT7HT bacterial expression vector	36
2.3 Inclusion body purification of $\beta_2m$ and soluble Qa-1 <sup>b</sup> proteins	38
2.4 Inappropriate multimers of $\beta_2m$ and Qa-1 <sup>b</sup> in <i>in vitro</i> refolding reactions	40
2.5 H2-K <sup>b</sup> refolds efficiently around the SIINFEKL peptide	41
2.6 Polycistronic expression of Qa-1 <sup>b</sup> complex components	43
2.7 Baculovirus expression of <i>Hs</i> $\beta_2m$ and Qa-1 <sup>b</sup>	45
2.8 Bacterial QDM, $\beta_2m$ , and Qa-1 <sup>b</sup> linkered constructs	47
2.9 Transient expression of Qa-1 <sup>b</sup> by HEK cells	48
2.10 SDS-PAGE analysis of mammalian expressed Qa-1 <sup>b</sup> complexes	49
2.11 Predicted cleavage of QDM chimeras by mammalian signal peptidase	50
3.1 Comparison of MHC Ia and Qa-1 sequences surrounding cysteine 134	69
3.2 Surface expression of Qa-1 <sup>b</sup> wild type and C134 mutants in L cells	71
3.3 Temperature dependence of Qa-1 surface expression	72
3.4 Stable expression of Qa-1 <sup>b</sup> constructs in B78H1 cells	74
3.5 Relative maturation of B78H1 expressed Qa-1 <sup>b</sup> constructs	75
3.6 Qa-1 <sup>b</sup> maturation in C57BL/6 and H2-K/D <sup>-/-</sup> splenocytes	77
3.7 Co-expression of H2-L <sup>d</sup> as a source of QDM in C1R cells	79
3.8 Maturation and turnover of Qa-1 <sup>b</sup> in B78H1 cells	81
3.9 Maturation and stability of Qa-1 <sup>b</sup> in C1R cells	82
4.1 39.1D7X cytotoxic lysis of C1R transfectants	97
4.2 5D2-T cytotoxic lysis of B78H1 transfectants	99

4.3 5D2-T cytotoxic lysis of C1R and C1R/L <sup>d</sup> transfectants	101
4.4 5D2-T cytotoxic lysis of L(M)Tk <sup>-/-</sup> transfectants	103
4.5 CD94 and NKG2A/C/E expression by CTL clones	105
4.6 CTL activity is enhanced by NKG2A/C/E blockade	106
Table 1 Mouse Class I genes	11
Table 2 Maturation and half-life of Qa-1 <sup>b</sup> in enhanced by the C134S mutation	85

## **Chapter 1**

### **Introduction**

## **Qa-1 is a Novel Member of the Class I Gene Family**

Mammalian Major Histocompatibility Complex (MHC) gene products are often subdivided into three groups. The Class I proteins present cytosol-derived peptides to CD8<sup>+</sup> cytotoxic T cells (CTL), while the Class II molecules present exogenously derived peptides to CD4<sup>+</sup> helper T lymphocytes. The Class III family includes an assortment of molecules predominantly related to immune surveillance, but often unrelated in structure to the immunoglobulin superfamily Class I and II proteins. Class I gene products are further subdivided into the Ia and Ib subfamilies. The Ia molecules are highly polymorphic, invariably associated with  $\beta_2$ microglobulin ( $\beta_2m$ ), and nearly ubiquitously expressed on the surface of nucleated cells. These molecules are evolutionarily ancient, with unambiguous sequence and functional homology found between primate and teleostic fish homologues [1, 2]. The three Ia loci in humans are called HLA-A, B and C, with several hundred known alleles identified so far. The homologous murine Ia loci are H2-K, D, and L, although several inbred mouse strains are H2-L null.

By contrast, there are approximately thirty MHC linked murine MHC Ib family members, which are distinguished from the Ia genes by their relative lack of polymorphism, their spatial and temporal expression profiles, their function, and in some cases, the lack of association with  $\beta_2m$ . Furthermore, several non-MHC linked Class Ib molecules have been shown to present non-peptide antigens such as lipids or glycolipids in lieu of the 8-10 amino acid linear antigens presented by Ia molecules. Included in the MHC-linked Ib subfamily are a large number of pseudogenes and duplicated coding regions, which do encode functional protein in some members of the species, but not in others. This large array of highly similar genes and pseudogenes has arisen over a substantial evolutionary period by single or multiple



gene duplication events[3]. While the Ia gene products have been extensively studied with respect to both function and structure, the diversity and presumably limited or unique function of the MHC Ib family members, as well as the lack of an obvious ligand such as  $\alpha/\beta$  TCR, has hindered similar analyses. Qa-1 is such a murine MHC Ib molecule, yet it shares striking similarities with Ia molecules. Qa-1 shares overall structural homology with Ia molecules based on primary sequence, binds to  $\beta_2m$ , and also shares their ability to present 8-10 amino-acid peptides, which are imported from the cytosol. Unlike Ia molecules, however, Qa-1 is primarily a ligand for innate receptors, therefore this molecule is at the nexus of innate and adaptive immunity. Qa-1 does present its canonical peptide in a TAP and tapasin dependent manner, as is commonly seen with MHC Ia molecules and their cytosol-derived peptide repertoire[4]. This is consistent with the role of this molecule as discussed below. However, the presentation of other peptides may not directly depend on TAP/tapasin interaction.

Several MHC Ib molecule are encoded outside the MHC. One such class Ib molecule is the CD1.1 or CD1d protein. This molecule presents glycolipids, structural constituents of bacterial cell walls, to NKT cells. These effector cells express an invariant  $V\alpha 14$  T cell receptor and mediate a pro-inflammatory response to CD1d ligands [5]. Another particularly interesting Ib protein which has been well characterized is the neonatal Fc receptor, or FcRn. This molecule is the only known Ib with a role in the immune system not as a ligand, but rather as a receptor. FcRn dimers transport maternal immunoglobulin G (IgG) across epithelia in mammary tissues and the gut of nursing infants within vesicles which do not fuse with lysosomes [6], providing the neonate with some measure of acquired immunity. The structurally diverse Ib molecules also include several proteins which have no capacity to present any molecules within their groove to immune effector receptors, such as

the murine Rae (or the human orthologue MIC) proteins, as well as structurally related molecules with no immune function. The latter subset of non-MHC linked Ib molecules includes Zinc  $\alpha_2$ macroglobulin related Glycoprotein (ZAG) [7] and the hemochromatosis factor protein (HFE)[8], which are involved in lipid and iron transport, respectively. An overview of mouse class I proteins can be found in **Table 1**, while the mouse MHC is schematically represented in **Figure1.1**.

Although healthy cells present a variety of self-derived cytosolic peptides in the groove of Ia molecules, infection by intracellular pathogens or transformation leads to the presentation of peptides which are recognized as non-self by CTL. The CD8<sup>+</sup> T cell repertoire which recognizes these peptide/MHC (pMHC) ligands is produced by a tightly regulated and highly complex molecular pathway which stochastically alters the coding sequence of the T cell receptor (TCR) minigenes at the DNA level via V(D)J recombination (reviewed Krangel and colleagues [9] ) and specifically selects for recombination events which lead to weak self-pMHC recognition in the thymus. T cells in the periphery are therefore able to recognize, but not respond fully to self pMHC. Ideally, the presence of non-self peptides initiates the full CTL response in a small subset of these peripheral cells. This response includes maturation of the responding CD8<sup>+</sup> cell, upregulation of cytokines and cytokine receptors, clonal expansion, and the killing of target cells which display that non-self peptide in the context of the restricted MHC [10, 11].

A similar response can also be detected for CTL restricted to Qa-1 pMHC, however it is a significantly smaller number of peripheral CD8<sup>+</sup>  $\alpha\beta$  TCR T cells [12-14] compared to the fraction of cells of the same lineage which recognize peptides presented by H-2K/D/L MHC Ia molecules. The dominant immune surveillance mechanism for Qa-1 is the somatically encoded receptors expressed on Natural Killer (NK) cells [15, 16]. These

receptors, which can be either activating or inhibitory, recognize pMHC via diverse structural mechanisms [17]. Activation of NK cells leads to a cytotoxic response similar to CD8<sup>+</sup> killing, via degranulation and release of perforin and granzymes, and also possibly by induction of Fas ligand (reviewed in Smyth et al. [18]). In light of this recognition by both CTL and NK cells, it can be postulated that Qa-1 recognition forms one mechanism of simultaneous innate and adaptive activation. Qa-1 recognition by somatically encoded NK receptors is distinctly different than MHC/TCR interaction. The invariant nature of the NK receptor repertoire allows Qa-1 surveillance and response by any NK cell, not a small subset of effectors, each with unique MHC restriction and peptide specificity. Furthermore, a small subset of peripheral CD8<sup>+</sup> cells are Qa-1 restricted and could potentially recognize any Qa-1 complexes with a non-self peptide as any canonical CTL would.

### **The Role of pMHC Complexes in Immune Recognition**

Based on the role that MHC Ia molecules play in immunological discrimination between self and non-self, it would be ideal for host survival if pMHC were long-lived complexes. Except in the later stages of an infection, particularly at the focal site of infection or in secondary lymphoid organs, there is only a small probability that a T cell specific for a peptide derived from that pathogen will encounter an infected cell. The likelihood of a successful encounter is therefore increased by prolonged stability of peptide/MHC Ia complexes on the cell surface. This is especially important in light of the fact that many intracellular pathogens have developed immune evasion mechanisms which lead to the loss of surface MHC I expression (reviewed by Antoniou and Powis [19]). The CTL response to infection can be abrogated by degradation of nascent MHC heavy chain, prevention of TAP1/2 import of peptides into the ER lumen, expression of MHC I mimics which cannot present a peptide, or integration into the host genome for a prolonged latency

devoid of protein synthesis. All these mechanisms take a sufficient amount of time to allow some pathogen-derived peptides to be presented on the surface upon initial infection of the cell. A similar downregulation of pMHC occurs in some transformation events [20].

Tumors with significantly reduced or no surface expression of MHC I are protected from T cell mediated deletion directed at peptides derived from oncogenes or other inappropriately expressed proteins. As detection of a non-self pMHC by a responsive CD8<sup>+</sup> T cell is a stochastic process, prolonged exposure on the surface increases the likelihood of positive interactions.

### **Natural Killer Cells and MHC I Recognition**

Downregulation of surface pMHC does not, however, protect an infected or transformed cell for an indefinite period of time. In addition to CD8<sup>+</sup> T cell responses, which can be considered the primary, acquired, cytotoxic response, a secondary immunosurveillance mechanism exists in vertebrates. Natural Killer cells affect this response via non-TCR mediated recognition of MHC Ia and Ib ligands. The complicated mechanism by which the large repertoire of somatically encoded NK receptors recognizes and responds to targets has yet to be completely elucidated. One complicating factor is that a large number of these receptor molecules have overlapping functions, while another is the fact that within a family of receptors (for example the NKG2 family), some are activating, while others are inhibitory. Furthermore, not all receptors have been identified or classified by function as yet (reviewed by Deng and Mariuzza [17]). Compounding the issue is that rodents and primates express distinct receptor families, in addition to ones common to both. The presumed trigger for NK cytotoxicity is stronger activating signals than inhibitory signals. These signals, often due to the phosphorylation of Immune Tyrosine Inhibitory Motif (ITIM) or Immune Tyrosine Activating Motif (ITAM) sequences in the cytoplasmic

tails of receptors, do not directly correlate with killing or ignoring the target. The mechanisms of both the extracellular recognition and intracellular signaling pathways in NK cells are tantalizing areas of investigation due to the potential benefits in targeting intracellular infections and cancers which alter pMHC biogenesis.

In primates, HLA expression is monitored by the KIR and LIR receptors. In mice, the Ly49 family of lectin-like receptors recognizes MHC Ia, often in an allele-specific, but peptide independent manner [21-24]. There are at least 23 known Ly49 molecules, the majority of which are inhibitory receptors. These receptors bind to their ligand MHC below the peptide binding platform, at least in cases where a structure has been determined [25-27]. As these recognition events are predominantly peptide-independent, presentation of non-self peptides will not lead to NK lysis via these receptors. However, downregulation of the MHC will lead to ablation of the inhibitory signal provided by these molecules. Some yet to be elucidated mechanism exists to integrate the sum of the inhibitory and activating signals received from the totality of pMHC complexes on the surface of a target cell.

A second class of lectin-like molecules, the NKG2 receptors, interacts with MHC Ib molecules in both rodents and primates[28-32]. The NKG2 receptors usually form heterodimers with CD94, a structurally related molecule with no capacity for signal transduction. The only known exception is NKG2D, which exclusively forms homodimers, and whose only known ligands are the Ib molecules MICA/MICB or Rae1 $\alpha$ - $\epsilon$  (in primates and rodents, respectively)[33]. NKG2D is capable of initiating a cytotoxic response despite any inhibitory signals, as its ligands are only expressed by cells in extreme distress. Other NKG2 receptors, particularly the well characterized NKG2A/CD94, NKG2C/CD94, and NKG2E/CD94, recognize Qa-1, or its human functional homologue, HLA-E [15, 16]. The NKG2A/CD94 heterodimer is inhibitory due to the presence of an ITIM sequence in its

cytoplasmic tail, while the C and E receptors are activating via ITAM sequences. One distinguishing feature of these receptors is that they bind across the top of the peptide presentation groove, and are therefore able to interact directly with the peptide inside the groove of the MHC Ib molecule [34].

### **Biogenesis of Qa-1 Complexes**

To better appreciate the nature of this recognition, it is critical to understand the biogenesis of Qa-1 and its human functional homologue, HLA-E. Unlike the polymorphic Ia molecules, Qa-1 and HLA-E present a very limited repertoire of peptides. In fact, in healthy cells, the dominant peptide that should be presented, according to our current model of this system, is a hydrophobic nonamer derived from the leader sequence of MHC Ia molecules. In mice, this peptide has been called QDM, for Qa-1 Determining Motif [35]. The QDM sequence of AMAPRTLLL is found in the signal sequence of all known H2-D alleles, as well H2-L<sup>d</sup>. One known variant, NH<sub>2</sub>-AMVPRTLLL-COOH, is found in H2-D<sup>k</sup> and is therefore called QDM<sup>k</sup>. Humans, which have at least two orders of magnitude more HLA alleles than commercially available inbred mouse strains, present a remarkably similar peptide, also derived from the leader of HLA-A, B and C propeptides. The human peptide is most frequently VMAPRT(L/V)(V/L)L, but there are several similar variants. It is interesting that in mice, QDM is only encoded by Ia genes and a single MHC-linked Ib, H2-Q10, however several MHC Ib genes in humans have peptides that are similar enough to be presented by HLA-E. In no known instance does the leader sequence of any Qa-1 or HLA-E allele encode a suitable peptide. The reason for this is obvious, in light of the function of these molecules. As the combination of both the leader peptide and the Qa-1 or HLA-E MHC is a protective signal, it would be futile for either of these MHC to present their own leader peptide and affect the same response from NK or CD8<sup>+</sup> T cells.

The current model is that HLA-E and Qa-1, when presenting the cognate leader peptide, protect cells from the cytotoxic response of NK cells via engagement of NKG2A/CD94. When MHC Ia propeptides are not being produced, or MHC biogenesis has otherwise ceased, Qa-1 or HLA-E are expressed on the cell surface with a different peptide, or they simply fail to mature due to the lack of an appropriate ligand in the ER. As already stated, infection or transformation can lead to reduction or ablation of MHC Ia biogenesis. It is the very lack of Qa-1/QDM, or HLA-E/leader peptide, which leads to NK cytotoxic lysis of MHC Ia deficient cells when any activating ligand is present. Clearly, this is not a completely accurate model of NK activation, as MHC Ia null cells, such as erythrocytes, are not targeted by NK cells. Based on these pieces of evidence, one can propose that some activating signal must be present on the surface of the potential target cell, while the absence of an inhibitory signal is neither sufficient nor necessary for NK mediated killing.

At the outset of the experiments outlined below, our interest was to elucidate the molecular basis for Qa-1/QDM recognition by the two distinct receptors encoded on T cells and NK cells. Based on the primary sequence of Qa-1 alleles, they are unambiguously members of the MHC I superfamily. They are distinct from Ia molecules, however, in their extremely high peptide binding selectivity. There are many potential peptides capable of being presented by any given MHC Ia allele. By contrast, to date only five peptides have been identified within the groove of Qa-1 or HLA, not including the cognate peptides derived from the signal sequence of MHC Ia propeptides. In order to better understand the molecular mechanisms of this exacting peptide specificity and the resulting surfaces interrogated by the NK receptors, several approaches were used to generate crystallizable quantities of Qa-1<sup>b</sup>/QDM complexes. We also hoped to compare the murine and human

NK recognition events in light of two recently published descriptions of HLA-E in complex with the NKG2A/CD94 receptor [34, 36]. For our experiments, the *b* allele (Qa-1<sup>b</sup>) was selected due to the availability of a large body of experimental work, as well as existing reagents such as antibodies and cell lines, including alloreactive CTL clones. Chapter two details heterologous expression systems used in these attempts at producing biochemical quantities of the complex of Qa-1<sup>b</sup> and QDM, with particular emphasis on the most recent advances, which may yet result in successful generation of this complex. During the course of these experiments, a single residue was identified as an important determinant of Qa-1 pMHC stability. Characterization of this residue is detailed in chapter three. Chapter four summarizes the experimental evidence for recognition of the synthetic mutant by Qa-1<sup>b</sup> restricted T cells and NK receptors and also includes a discussion of the importance of wild type Qa-1's inherent instability.



### **Table 1 Mouse Class I Genes**

A partial list representing known mouse Class I molecules encoded within the MHC and elsewhere. Excluded are a large number of predicted or hypothetical translation products from various genomic and expressed tag sequencing efforts. Many such entries are alleles, truncations, or mis-sequenced variants of known Class I molecules. This table is based on extensive concatenation of data from various sources by the IMGT Repository currently located at [imgt.cines.fr](http://imgt.cines.fr) [37, 38]. Non-MHC linked gene positions were identified in the Entrez Gene database at NCBI [39].

**Table 1**

<i>Gene</i> <sup>1</sup>	<i>Class</i>	<i>Location</i> <sup>2</sup>	<i>Gene</i> <sup>1</sup>	<i>Class</i>	<i>Location</i> <sup>2</sup>
H2-K	Ia	<b>17</b> 18.4	H2-T17	Ib	<b>17</b> 19.8
H2-K2	Ia	<b>17</b> 18.4	H2-T18	Ib	<b>17</b> 19.8
H2-D1	Ia	<b>17</b> 19.1	H2-T19	Ib	<b>17</b> 19.8
H2-D2	Ia	<b>17</b> 19.1	H2-T20	Ib	<b>17</b> 19.8
H2-D3	Ia	<b>17</b> 19.1	H2-T21	Ib	<b>17</b> 19.8
H2-D4	Ia	<b>17</b> 19.1	H2-T22	Ib	<b>17</b> 19.7
H2-L	Ia	<b>17</b> 19.1	H2-T23 <sup>3</sup>	Ib	<b>17</b> 19.7
H2-Q1	Ib	<b>17</b> 19.1	H2-T24	Ib	<b>17</b> 19.7
H2-Q2	Ib	<b>17</b> 19.2	H2-M1	Ib	<b>17</b> 20.2
H2-Q3	Ib	<b>17</b> 19.2	H2-M2	Ib	<b>17</b> 20.4
H2-Q4	Ib	<b>17</b> 19.2	H2-M3	Ib	<b>17</b> 20.4
H2-Q5	Ib	<b>17</b> 19.2	H2-M4	Ib	<b>17</b> 20.3
H2-Q6	Ib	<b>17</b> 19.2	H2-M5	Ib	<b>17</b> 20.3
H2-Q7	Ib	<b>17</b> 19.2	H2-M6	Ib	<b>17</b> 20.3
H2-Q8	Ib	<b>17</b> 19.2	H2-M7	Ib	<b>17</b> 20.3
H2-Q9	Ib	<b>17</b> 19.2	H2-M8	Ib	<b>17</b> 20.3
H2-Q10	Ib	<b>17</b> 19.2	H2-M9	Ib	<b>17</b> 20.3
H2-T1	Ib	<b>17</b> 20.1	H2-M10-1	Ib	<b>17</b> 19.8
H2-T2	Ib	<b>17</b> 20.0	H2-M10-2	Ib	<b>17</b> 20.2
H2-T3	Ib	<b>17</b> 20.0	H2-M10-3	Ib	<b>17</b> 20.3
H2-T4	Ib	<b>17</b> 20.0	H2-M10-4	Ib	<b>17</b> 20.2
H2-T5	Ib	<b>17</b> 20.0	H2-M10-5	Ib	<b>17</b> 20.3
H2-T6	Ib	<b>17</b> 20.0	H2-M10-PS1	Ib	<b>17</b> 19.5
H2-T7	Ib	<b>17</b> 20.0	H2-M10-PS2	Ib	<b>17</b> 20.2
H2-T8	Ib	<b>17</b> 20.0	H2-M10-PS3	Ib	<b>17</b> 20.3
H2-T9	Ib	<b>17</b> 20.0	Non-MHC linked		
H2-T10	Ib	<b>17</b> 20.0	CD1.1	Ib	<b>3</b> 48.0
H2-T11	Ib	<b>17</b> 20.0	HFE	Ib	<b>13</b> 15.0
H2-T12	Ib	<b>17</b> 19.9	ZAG	Ib	<b>5</b> 78.0
H2-T13	Ib	<b>17</b> 19.9	FcRn	Ib	<b>7</b> 23.0
H2-T14	Ib	<b>17</b> 19.9	Rae-1 ( $\alpha$ - $\epsilon$ )	Ib	<b>10</b> A3
H2-T15	Ib	<b>17</b> 19.9	H60	Ib	<b>10</b> 16.0
H2-T16	Ib	<b>17</b> 19.8	MULT-1	Ib	<b>10</b> A3

<sup>1</sup> Genes encoded within the MHC are prefixed with H2-, as opposed to the deprecated yet ubiquitous H-2 designation.

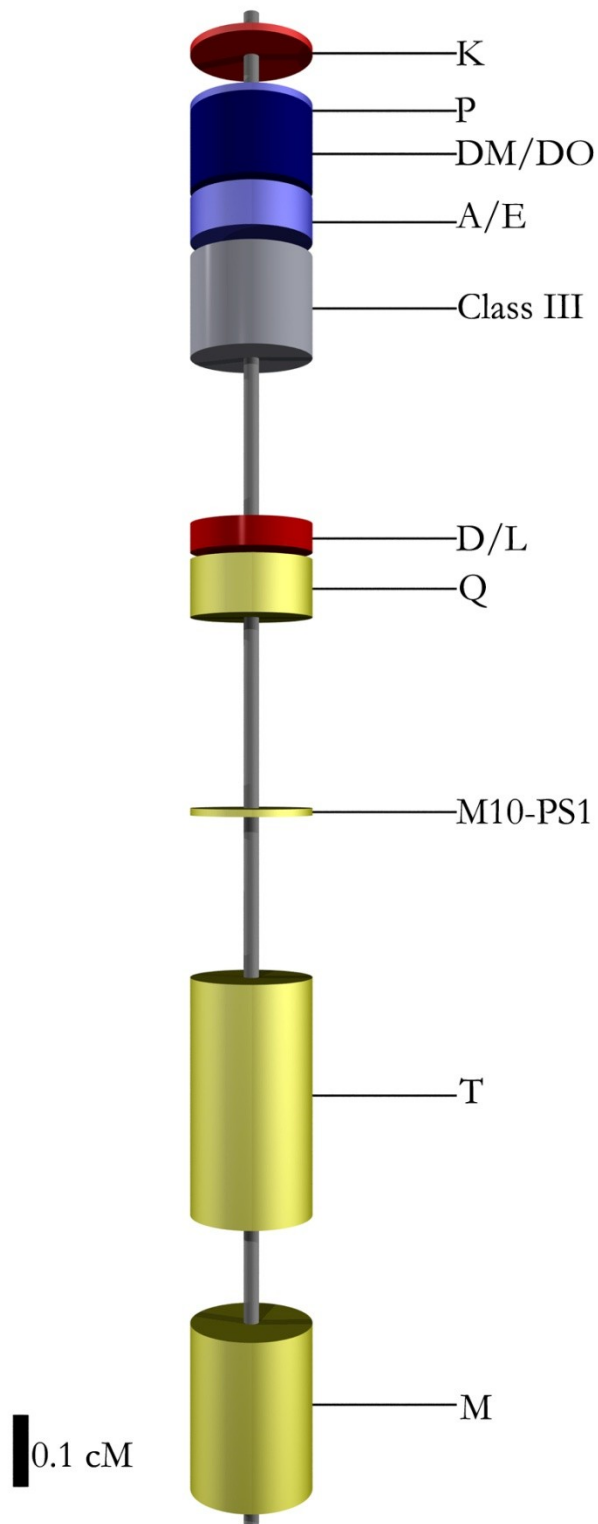
<sup>2</sup> Chromosome number is indicated in bold and the approximate physical location is indicated in cM, where known. Rae-1 and MULT-1 (also known as ULBP-1) are currently assigned to an unassembled fragment designated A3.

<sup>3</sup> Qa-1 is the product of the T23 gene.

### **Figure 1.1 Schematic Representation of Mouse MHC Region**

A schematic representation of the mouse MHC region on chromosome 17, located between 18.43 and 20.43 cM. The Class Ia and Ib regions are colored red and yellow respectively, while the IIa and IIb are light and dark blue. The Class III region, which includes a large number of disparate genes including complement components and immunological proteasome subunits, is represented in gray. Relative positions are based on the data in Table 1 as well as the positional markers found at the IMGT and NCBI websites. The figure was generated using the POV-Ray ray tracer ([www.povray.org](http://www.povray.org)).

Figure 1.1 The Mouse MHC Region



## Chapter 2

### Heterologous Expression of Qa-1<sup>b</sup>

## Introduction

### Qa-1 pMHC Are Fundamentally Different from MHC Ia Complexes

A striking disparity between MHC Ia proteins and Qa-1/HLA-E is the exquisite peptide specificity displayed by the latter. Clearly the distinct roles of these closely related proteins have largely defined their evolutionary provenance. The overall similarity between the Ia molecules and Qa-1/HLA-E belies the mechanistic details of peptide binding within the groove formed by the  $\alpha_1$  and  $\alpha_2$  helices and platform. There are typically many ionic and van der Waals interactions between the peptide and the residues which line the peptide binding groove, however a large number of these bonds involve backbone atoms, and are therefore peptide sequence independent. These generic interactions allow a substantial variety in the identity of the peptide, as the major determinant of peptide specificity is therefore constrained to the two or three side-chains which are buried within the deep pockets found on the platform.

By limiting the molecular interactions to the almost uniform peptide backbone, the MHC Ia are potentially capable of binding a staggering repertoire of peptide sequences per allele. An overly simplified mathematical reduction of the constraint that any one of the nineteen amino acids or proline could occupy the six non-anchor positions would allow 64 million possible peptides ( $6^{20}$  possible combinations). In practice, however, the potential peptide repertoire is likely much smaller. For examples, certain side-chains are preferred when that residue faces the walls of the binding groove and steric clashes with large side-chains are likely to destabilize the pMHC. Nonetheless, even if the actual potential pool of peptides is five orders of magnitude smaller, it would still dwarf the miniscule peptide repertoire which has been experimentally identified for Qa-1 or HLA-E [40-43]. The structure of HLA-E in complex with the human Ia leader peptide VMAPRTVLL describes

the molecular details of this peptide selectivity [44]. Unlike Ia molecules, which only constrain the peptide via two or three pockets, HLA-E forms a novel set of molecular contacts with the peptide at almost every residue. Comparing the primary sequence of the  $\alpha_{1-2}$  domains of Qa-1<sup>b</sup> and HLA-E highlights the subtle differences between these two molecules (**Figure 2.1**), therefore we proposed to solve the structure of Qa-1<sup>b</sup>/QDM at atomic resolution. There are three substantial differences between these mouse and human functional orthologues: firstly, there are important allelic variants of Qa-1 despite the presence of only two QDM alleles. Secondly, only Qa-1 and its rat homologue, RT-BM1, have an unpaired cysteine at positions 134. Lastly, the murine system provides a far more tractable framework for *in vivo* analyses. Despite the enormous polymorphism of the human MHC Ia loci, there are only two known alleles of HLA-E, which differ at position 107 [45].

To better understand the molecular basis of peptide selectivity of Qa-1, and to establish the preliminary work for exploring Qa-1/NKG2 co-crystals, we began experimenting with heterologous expression systems. Several approaches have been successfully used to generate crystallizable quantities of pMHC complexes, including purification from endogenous sources [46, 47], insect expression systems [48], and bacterial expression followed by *in vitro* complex reconstitution [44, 49, 50]. It was not foreseen that all but the first approach would eventually be attempted for Qa-1<sup>b</sup>.

## **Results and Discussion**

### **Bacterial Expression of Soluble Qa-1<sup>b</sup>**

There is a substantial body of experimental evidence for successful bacterial expression of MHC Ia and Ib heavy chains, as well as  $\beta_2$ microglobulin, followed by *in vitro*

refolding [49-52]. Of direct interest is the production of soluble HLA-E pMHC by this method [44]. This method of pMHC generation is now commonly used to produce a large variety of tetramer complexes by enzymatic biotinylation of a short peptide genetically linked to the carboxy terminus of the Class I molecule, followed by streptavidin capture [49]. Initially, it was believed that Qa-1<sup>b</sup>/QDM complexes could simply be produced using a similar approach.

In practice, this approach requires a substantial excess of solubilized, denatured heavy chain, which is refolded *in vitro* in the presence of  $\beta_2m$  and synthetic peptide, typically in a 1:5:20 molar ratio. Properly refolded pMHC are then purified by gel filtration to remove large aggregates, as well as excess  $\beta_2m$  and peptide. To produce the starting material, the open reading frames of Qa-1<sup>b</sup> and mouse  $\beta_2m$  (allele *a*) were cloned into a bacterial expression vector (**Figure 2.2**) which encodes a cleavable amino-terminal hexahistidine tag which can be removed following the refolding reaction using the Nla protease[53] from Tobacco Etch Virus (TEV protease). In my previous experience with both prokaryotic and eukaryotic systems, the combination of an Immobilized Metal Affinity Chromatography (IMAC) tag and a highly specific protease cleavage site has proved extremely effective at the production of highly pure crystallizable protein. The cleavable tag is invaluable in a simple, readily scalable purification and concentration step which can produce greater than 95% pure protein with two sequential IMAC steps.

The first attempts at protein expression produced very good yields of highly pure tagged protein as inclusion bodies. Neither the MHC heavy chain, nor  $\beta_2m$  are produced as soluble protein in standard inducible bacterial expression systems. Inclusion bodies are initially isolated by differential solubility, which typically results in greater than 90% purity (**Figure 2.3**). Following solubilization in urea, the tagged protein is then purified by the first



IMAC step. A second IMAC purification following the refolding reaction results in highly pure protein which is then digested with TEV protease. Any bacterial proteins which co-purify with the complex in the second IMAC step, as well as uncleaved complex and the protease, which has a non-cleavable tag, are removed by a third IMAC step. Ideally, this produces a highly purified preparation that is suitable for biophysical analysis.

Qa-1<sup>b</sup>, unfortunately, did not behave as an ideal complex. Typically, pMHC complexes produced with this *in vitro* approach are reported to produce final yields of 20-40%. The best refolding reactions using Qa-1<sup>b</sup> resulted in approximately 5% yield with the remainder of the starting material forming multimers and large aggregates. Following enzymatic removal of the tag and re-purification of the complex, the final yield of potentially crystallizable material was approximately 1% of the initial protein as assessed by spectrophotometry. That corresponds to nearly 500 µg complex per liter of initial refolding solution. That is an acceptable yield for a 44,000 Dalton mammalian protein complex, however the subsequent concentration resulted in further aggregation of the purified complex. Analytical gel filtration of the complex revealed that soluble monodisperse complex is an ephemeral species which rapidly converts irreversibly to insoluble aggregates. This was the primary reason for exploring the theoretical model of the Qa-1<sup>b</sup> structure for residues that might destabilize the complex and precipitated the work discussed in chapter 3.

In light of the experimental evidence detailing the average lifetime of Qa-1<sup>b</sup> complexes [54], as well as personal observations made during successive refolding experiments, several approaches were used to improve the yield to acceptable levels. The most obvious problem with the *in vitro* refolding reactions is the misformation of the two canonical disulfide bonds in the  $\alpha 2$  and  $\alpha 3$  domains of the heavy chain, as well as the single disulfide in  $\beta_2 m$ . The initial purification of the inclusion bodies is performed in the presence

of either dithiotriethol or  $\beta$ -mercaptoethanol, therefore producing fully reduced polypeptides. Non-reducing, denaturing PAGE analysis of refolded material, however, reveals multimers of both the heavy chain and  $\beta_2m$  form during the reaction (**Figure 2.4**). It should be noted that only a very small fraction of the  $\beta_2m$  formed covalent multimers, yet this indicates a systemic failure of the oxidation process critical to the success of this approach. This suggested that the initial redox conditions were not effective in producing the correct pairing of cysteines, even in  $\beta_2m$ , which only has two cysteine residues and is refolded prior to the introduction of the MHC heavy chain into the reaction. Several modifications and variations of the glutathione redox reagent pair were then explored in an effort to enhance correct pairing, and, hopefully, the final yield of complexes.

Where there is detailed description of the refolding reaction components, the redox pair is universally reported to be glutathione in a ratio of  $5\mu\text{M}:0.5\mu\text{M}$  for reduced to oxidized peptide. Neither changing the ratio nor total amounts of the redox pair improved the yield of monomeric complex following concentration and gel filtration analysis. Cysteine:cystine was also assessed as a redox pair, however the already dismal yields were even further reduced in these experiments. An alternative approach to forming correct disulfide pairs is to dissolve the denatured and fully reduced polypeptides in the presence of the ionic detergent sodium laurylsarcosine, then promote disulfide bond formation using catalytic metal ions [55]. The detergent is then removed after the oxidation reaction by dilution to below the critical micelle concentration in 8 molar urea and the protein is purified and concentrated using weak ion exchange chromatography under non-reducing condition. The formation of internal disulfide bonds can then be assessed by non-reducing SDS-PAGE. This approach did not produce an appreciable fraction of properly disulfide bonded  $\beta_2m$ . At this point the suitability of the glutathione refolding reaction was assessed by attempting to

reproduce published results using an MHC I molecule which is known to generate crystallizable complexes using these conditions.

The mouse MHC Ia molecule H2-K<sup>b</sup> was cloned into the pT7 expression vector and purified in a manner identical to Qa-1<sup>b</sup>. Refolding this protein around the chicken ovalbumin peptide SIINFEKL (residues 257 to 264) produced 40% purified, concentrated, monodisperse complex (**Figure 2.5a**). This is comparable to published reports of 25-35% yield using this heavy chain and peptide. H2-K<sup>b</sup> is a suitable control for Qa-1<sup>b</sup> refolding, as this allele also includes an unpaired cysteine, although this is located at position 142 (relative to the complete ORF). It is clear from the crystal structure of H2-K<sup>b</sup>/SIINFEKL that this free cysteine is located at the beginning of loop six and is highly solvent accessible (**Figure 2.5b**). The successful refolding of this MHC Ia complex, compared to Qa-1<sup>b</sup>, is further evidence for the intractability of this approach to generating biochemical quantities of the latter's complex.

A second prokaryotic expression approach was then attempted. A lesser explored advantage of bacteria is their ability to simultaneously translate multiple proteins from the same message [56, 57]. QDM, mouse  $\beta_2m$ , and the Qa-1<sup>b</sup> cDNAs were cloned into the polycistronic vector pST39 after genetically appending the *Escherichia* pelB leader sequence to the N-terminus of each ORF. This leader peptide is analogous in function to the mammalian signal sequence, sorting polypeptides to the oxidizing bacterial lumen [58] prior to enzymatic cleavage by the host peptidases. The entire polycistronic cassette was then transferred to pET28b(+) due to the incompatibility of the pST39 origin of replication with the pRARE plasmid in the inducible host bacteria strain (**Figure 2.6**). It was hoped that simultaneous co-expression of all three components and their co-localization to the lumen would allow formation of complexes due to the action of host chaperones, including the

GroEL chaperone, the protein disulfide isomerases DsbA/DsbC and peptidylprolyl isomerases. To further ensure disulfide bond formation, the *E. coli* strain RosettaGami, which is deficient in two reductases, was used as the expression host. Defects in thioredoxin reductase (*trx*) and glutathione oxidoreductase (*gor*) produce an oxidizing environment not only in the luminal space, but also alter the pH of the cytosol to promote disulfide bond formation. Initial attempts at transfection of the polycistronic vector were uniformly unsuccessful at producing colonies unless glucose, an inhibitor of the *lac* operon, was added to both solid and liquid media.

Upon induction of T7 polymerase by the addition of IPTG, these cells would rapidly lyse in a manner reminiscent of bacteriophage induced lysis. Within two hours of IPTG addition, the only remaining evidence of bacteria was a single viscous spindle of genomic DNA and cellular debris. By comparison, the same host strain readily produced large amounts of inclusion bodies when transformed with plasmids encoding  $\beta_2m$ , Qa-1<sup>b</sup>, or a pST39-based plasmid which only encodes these two polypeptides. As the toxicity observed was limited to expression of QDM and its targeting to the luminal space, this approach to complex formation proved no more useful than the independent expression of each polypeptide.

### **Insect Expression of Qa-1<sup>b</sup> Complexes**

Yet a third approach to generating pMHC complexes is to produce them in insect cells. The earliest known occurrence of MHC in evolution is in teleosts, or bony fish [2], therefore it is not surprising that insects lack the MHC-specific chaperones tapasin and the peptide transporter TAP1/2. Despite this potential impediment to successful biogenesis of mature complexes, biochemical quantities of pMHC have been successfully produced in *Drosophila* S2 cells by stable transfection, and in *Trichoplusia* and *Sfungidoptera* cells infected

with recombinant baculovirus[19, 59-61]. The Qa-1<sup>b</sup> ectodomain and human  $\beta_2m$ , which produced slightly higher amounts of soluble complex in bacterial refolding experiments, were genetically modified by the addition of the honeybee melittin signal sequence[62]. Qa-1<sup>b</sup> was also modified to encode an amino-terminal octahistidine tag and TEV consensus site downstream of the melittin sequence. The two modified reading frames were cloned into the commercial dual promoter baculovirus transfer vector pACuW51 (**Figure 2.7**). The presence of a polyhistidine tag on the heavy chain allows IMAC purification of the complex from conditioned media which has been supplemented with excess synthetic QDM following removal of the infected cells. Although both proteins were readily produced upon infection with high-titer virus, a large fraction of the complex was highly aggregated and distinct multimers of Qa-1<sup>b</sup> could be observed by Western analysis of gel filtration fractions. Furthermore, the observed yield did not inspire confidence in the tractability of this approach. Following several unsuccessful large scale preparations of conditioned media, this approach was also abandoned. At this point, the results of the *in silico* analysis were used to design the point mutations at residue 134 as detailed in chapter 3.

Initial purification of the Qa-1<sup>b</sup> Cys134Ser ectodomain inclusion bodies were very similar to the wild type protein in the bacterial expression system. Comparisons between *in vitro* refolding reactions of the wild type and C134S mutant show a marked reduction in large aggregate formation and a very promising improvement in the amount of monodisperse complex. The mutant complex, however, is still relatively unstable and readily aggregates during all efforts at concentration. It is unclear from the refolding reactions and subsequent purification steps whether the aggregation and insolubility of the Qa-1<sup>b</sup>/QDM complex is due to the instability of the complex, or accumulation of failed refolding products which cannot be separated by our purification scheme.

## Generation of Chimeras

It is reasonable to assume that pMHC complexes are highly unstable when either the peptide or  $\beta_2m$  dissociates. This is supported by experimental observations, specifically the absence of surface pMHC expression in cellular models lacking functional TAP1/2 peptide transporter or deficient in  $\beta_2m$ . This is reflected in mouse knock-out models of TAP1/2, or  $\beta_2m$ [63]. These mice are profoundly deficient in peripheral CD8<sup>+</sup> T cells and yet the thymus has the expected distribution of CD4<sup>+</sup>CD8<sup>+</sup> double positive precursors. TAP1/2 deficiency can also be induced by transduction or transfection of the Herpes Simplex virus ICP47 protein, which blocks peptide transport via the TAP1/2 complex [64]. In either the serendipitous or induced models of either phenotype, there is drastically reduced surface expression of MHC Ia molecules, despite significant accumulation of the heavy chain within the endoplasmic reticulum. Since both the peptide and the light chain are required for proper maturation and, therefore, stability of the complex, we proposed to generate chimeric molecules where all three components of the pMHC were covalently attached via flexible tethers, markedly reducing the possibility that any one component would dissociate during purification stages.

Previously, a single chain transgenic mouse model of Qa-1<sup>b</sup> had been generated in our lab. The construct used is a chimera of mouse  $\beta_2m$ , including its normal signal sequence, attached at the DNA level to the entire mature ORF of Qa-1<sup>b</sup> via the 15-mer flexible spacer (Gly<sub>4</sub>Ser)<sub>3</sub>. Two different versions of this synthetic ORF were generated, one encoded by the cDNA, and the second using the C57BL/6 Qa-1<sup>b</sup> gene, modified to prepend the  $\beta_2m$  ORF to exon 1 [13]. Previous characterization of these constructs in tissue culture, as well as in the resultant transgenics, uniformly indicated reduced protein levels compared to wild type full length Qa-1<sup>b</sup> constructs. There is, however, unambiguous surface expression by

FACS and Western analysis, and once crossed into the  $\beta_2m$  deficient background, a small number of  $CD8^+$  cells restricted to Qa-1 can be detected in the periphery. Using the cDNA chimera as an initial model, several constructs with modifications were made in an attempt to produce crystallizable material. The 15-mer spacer was lengthened to twenty residues to alleviate any torsional constraints on  $\beta_2m$  binding. Additional constructs were made which encoded QDM and a 15-mer linker immediately after the  $\beta_2m$  signal sequence [65]. Both wild type and C134S versions of these constructs were made (**Figure 2.8**), as were analogous constructs which encoded the entire carboxy terminus of Qa-1<sup>b</sup>, such that their biological significance could be assessed in T cell killing assays. As these latter constructs are extensively described in the later chapters, the following discussion will focus entirely on the soluble versions, which were used to make protein in bacteria and mammalian tissue culture.

Bacterial expression of these single chain constructs was quite robust; however they failed to ameliorate the yield of soluble, monodisperse complex in refolding reactions. There was a diminished solubility of the resultant proteins during the *in vitro* refolding reaction, likely due to the decreased probability of forming the correct ternary and quaternary structure due to the increased size and additional pair of cysteines in  $\beta_2m$ . Several experiments using the Qa-1<sup>b</sup> wild type and C134S mutant refolded around a QDM-(G<sub>4</sub>S)<sub>3</sub>- $\beta_2m$  protein that had already been refolded and purified were attempted. This seemed an optimal effort at producing complexes which would be easy to generate *in vitro* and would have an increased lifetime as both the peptide and the  $\beta_2m$  would be less likely to dissociate. Obviously, this approach is not as ideal as a proper refolding of the three component chimera, however that proved experimentally intractable. Unfortunately, the yield of complex using QDM<sub>15</sub> $\beta_2m$  was disheartening, even if the refolding reaction was performed in the presence of excess synthetic QDM.

## High-level Expression in Mammalian Cells

Despite the relatively high cost and limited production capacity of tissue culture expression systems, there is a decided advantage in using mammalian cells to produce difficult proteins or complexes. Cells which are capable of expressing Qa-1<sup>b</sup> complexes on their surface are obviously capable of generating modified versions which are not tethered to the plasma membrane. This approach to protein production for crystallography has the distinct advantage of producing complexes that are as similar to those produced *in vivo* as is reasonably possible. Both the chaperone mediated refolding and the glycosylation state of secreted complexes would approximate events which occur during their generation in murine cells. Two different mammalian systems were used to generate soluble QDM/Qa-1<sup>b</sup> pMHC.

The first system was based on stable transfectants of dihydrofolate reductase deficient Chinese hamster ovary cells (CHO DHFR<sup>-</sup>), as well as the related cell line Lec1, which does have endogenous DHFR, but is deficient in N-acetylglucosaminyltransferase [66]. Proteins secreted by Lec1 cells have not been fully matured by the Golgi glycoprocessing enzymes and are therefore only modified with high-mannose N-linked glycosylation. Vectors encoding Qa-1<sup>b</sup> as a carboxy-terminal fusion with human growth hormone (hGH) were generated and co-transfected with a non-selectable DHFR plasmid into both CHO DHFR<sup>-</sup> and Lec1 cells [67]. Following an initial drug resistance selection and single-colony cloning step, the DHFR/Qa-1<sup>b</sup> insertion sites were amplified by several cycles of increasing methotrexate treatment.

In addition to the high cost and demanding labor required for this approach, an additional disadvantage is the prolonged period of time between the initial transfection and any indication of the viability of this system for the production of a given complex. While



protein production levels can easily be assessed by ELISA or Western analysis of the tissue culture supernatant, the sequential cloning steps and the marked reduction in growth rates which accompany each successive methotrexate (MTX) amplification cycle typically take 10-15 weeks before protein yields near acceptable levels. Further complicating this approach is the occasional, and inexplicable, lack of protein expression level increases following each additional MTX amplification step. Initial transient transfections of CHO cells produced nearly 100 µg/L of hGH, however following four successive MTX amplifications in selected stable clones, the total hGH yield never exceeded 450 µg/L in CHO DHFR<sup>-</sup>. Protein expression by Lec1 cells, which is consistently lower, did not exceed 100 µg/L after MTX amplification. This method of complex generation was therefore abandoned as well.

### **Transient Protein Expression**

The prolonged period between construct generation and maximal protein production can be significantly reduced by using transient expression systems [68]. Qa-1<sup>b</sup> soluble constructs and chimeras were cloned into a high-level expression mammalian plasmid kindly provided by Samuel Bouyain and Brian Geisbrecht. DNA:polyethylimine complexes were then used to transiently transfect nearly confluent cultures of human HEK293 cells as well as the derivative cell line HEK293-S, which is deficient in the GnT I gene. This method allows scalable production of soluble protein within one week of plasmid construction. Conditioned media were initially assessed for Qa-1<sup>b</sup> expression by Western analysis using the 6A8.6F10 monoclonal. Surprisingly, media conditioned for three days following transient transfection included approximately 2 milligrams per liter hGH-Qa-1<sup>b</sup> (**Figure 2.9**). This was a very pleasant surprise compared to previous experiences with Qa-1<sup>b</sup> complexes, which had largely diminished any expectations that the protein levels observed by Western analysis of reduced, denatured samples were in fact correctly folded to a substantial degree.

Following buffer exchange and CFF purification of the hGH-his-TEV tagged complex, the eluate was separated by gel filtration chromatography to determine the fraction of the product which is monodisperse. SDS-PAGE and Western analysis of the resultant fractions revealed that the product of this experimental approach is quantitatively and qualitatively well folded. In fact, protein expression levels and the total yield following CFF purification and tag cleavage is sufficiently high to allow observation of a dispensable fraction of the sample by Coomassie staining (**Figure 2.10**), a heretofore unparalleled event.

The success of this heterologous expression system is undoubtedly due in large part to the intact MHC I processing pathway in HEK293 cells. As expected, the glycosylation-defective cell line HEK293-S produces less total protein (Bouyain and Geisbrecht, personal communication), however the product of these cells can be easily deglycosylated using recombinant EndoH enzyme, which is highly active under physiological conditions. By contrast, protein produced in HEK293 cells must be treated with PNGaseF, an endoglycosidase which is optimally active following reduction and denaturation of the substrate protein. In practice, I discovered that PNGaseF is fully capable of quantitative deglycosylation of Qa-1<sup>b</sup> complexes if the enzyme is used in moderate excess of the quantities normally required and furthermore that cleaved polysaccharides, an inhibitory product, are removed by ultrafiltration and buffer exchange. TEV protease was included in the deglycosylation reaction, as it is sufficiently active at 4° C.

The best yields were observed with the  $\beta_2m$ -(Gly<sub>4</sub>Ser)<sub>4</sub>-Qa-1<sup>b</sup> C134S construct in HEK293 cells. Final yields from pooled conditioned media are in the range of 2-4 milligrams per liter, which corresponds to two media collections from approximately 3,000 cm<sup>2</sup> total cultured surface area. Following deglycosylation and tag removal, purified protein was used in a limited crystallographic grid screen using different PEG<sub>3350</sub> concentrations and

varying the pH from 3 to 10. Vapor diffusion hanging drops were set up with 1 mg/ml pMHC, but no crystals or potentially interesting precipitates were observed in the 96 experimental conditions. Higher protein concentrations and a much larger volume of precipitant space may have to be explored in order to generate useful crystals. This approach to generating the complex is by far the most tractable among the previously discussed. It should be noted that the HEK293 cells do not express QDM, but rather the human leader sequence, therefore synthetic peptide has to be added to the preparation throughout the processing steps to promote peptide exchange. To alleviate this problem, H2-L<sup>d</sup> has been transfected stably into both cell lines and individual high expressing single cell clones have been isolated.

One additional observation made during these transient expression experiments was the reduced comparative yield of the QDM<sub>15</sub>β<sub>2</sub>m<sub>20</sub>Qa-1<sup>b</sup> constructs. While they express well and mature easily in surface expression experiments detailed in chapter 3, these chimeric molecules are expressed at much lower levels by HEK293 cells. The most likely explanation for the disparity between surface expression and secretion of the soluble protein is that the amino terminus of the tethered peptide is not accessible in the secreted chimeras. Computer simulations predict that signal peptidase will cleave the β<sub>2</sub>m signal sequence-QDM chimera at the desired position immediately amino-terminal to the first alanine (**Figure 2.11**) [69, 70].

## Materials and Methods

### Generation of Soluble Constructs

Soluble versions of full length constructs were generated by PCR using the sense Qa-1<sup>b</sup>(Sal) primer (GGGGTCGACAAGCCCACACTCGCTGCGG) and antisense Qa-1<sup>b</sup>(NotTGA) primer (CCGCGGCCGCTCACCATCTCAGGGTGAGGGGCTCAGG) using plasmid pAD30.2 as a template. SalI/NotI cut amplicons were cloned into the T7 driven low-copy expression vector pT7HT [71] and sequenced to confirm ORF integrity. Mouse  $\beta_2m$  was cloned into pT7HT in an analogous fashion, again with the addition of flanking 5' SalI and 3' NotI sites during PCR amplification. Mutant ORF's were generated by using the full length mutants as PCR templates. Human  $\beta_2m$  was cloned by RT-PCR from total human RNA derived from peripheral blood mononuclear cells. Soluble chimeric constructs for bacterial expression were generated by PCR from pCI-Neo templates. The same ORFs were cloned into pSGHV1 (Geisbrecht and Bouyain, personal communication) using the SalI/NotI flanking restriction sites. In order to clone the QDM<sub>15</sub> $\beta_2m$ <sub>20</sub>Qa-1<sup>b</sup> ORF into the mammalian expression system, plasmid pSGHV2 was generated from pSGHV1 by introducing a silent EcoRV site at position 3313 using overlap mutagenesis PCR. The pSGHV2/QDM<sub>15</sub> $\beta_2m$ <sub>20</sub>Qa-1<sup>b</sup> plasmid was generated by ligating an EcoRV/EcoRI PCR fragment to the EcoRI/NotI 3' ORF fragment derived from  $\beta_{20}$ Qa-1<sup>b</sup>.

### Bacterial Expression

Protein was expressed in Rosetta pLysS bacteria (Novagen) host strain by induction with 1 mM IPTG for 4 hours at 37°C. Insoluble inclusion bodies were purified essentially as described [49] except that the partially purified inclusion bodies were dissolved in 6 M guanidine buffer and further purified by immobilized metal affinity chromatography (IMAC)

using Chelating Fast Flow resin (GE Healthcare) loaded with Ni<sup>++</sup> and pre-equilibrated with guanidine buffer. Retained protein was eluted with 50 mM EDTA in 6 M guanidine-HCl, 100 mM Tris-HCl, pH 8.0 and quantified spectrophotometrically at 280 nm using the theoretical absorption coefficient for fully reduced, denatured polypeptide ([www.expasy.org](http://www.expasy.org)). Small aliquots of the purified proteins were stored at -80°C.

### ***In vitro* Refolding Reactions**

Refolding reactions were performed essentially as described [49, 72, 73]. Refolding reactions were carried out in a rapidly stirring solution of 400 mM arginine, 100 mM Tris-HCl, pH 8.0, and typically 5 μM:0.5 μM glutathione (reduced:oxidized, respectively) at 4° C. Synthetic peptide and guanidine or urea solubilized β<sub>2</sub>m were rapidly injected at final concentrations of 20 and 5 μM, respectively. Heavy chain was injected in three steps at 12 hour intervals with continuous stirring to a final concentration of 1 μM. After an additional twelve hours of stirring, large precipitates were removed by centrifugation followed by vacuum filtration through 0.22 μm polyethylsulphone filters. The refolding reaction was concentrated 10-fold using an Amicon pressure cell equipped with a 10,000 dalton nominal molecular weight filter, then buffer exchanged twice using 200 mM NaCl, 20 mM imidazole and 50 mM Tris-HCl, pH 8.0. In some experiments, QDM peptide was added during the buffer exchange steps to a final concentration of 5 μM.

### **Insect Protein Expression**

The mature human β<sub>2</sub>m and the soluble Qa-1<sup>b</sup> open reading frames were first modified by the amino-terminal addition of the honeybee melittin signal sequence. Upon confirmation of sequence integrity, each ORF was sequentially transferred into the pAcUW51 dual-promoter commercial expression vector (BD Biosciences). CsCl purified DNA was co-transfected into 80% confluent SF9 cells along with the BaculoBright

linearized viral DNA. Transfected cells were preparatively sorted into 96-well plates containing uninfected SF9 cells and productive wells were screened by dot-blot analysis of supernatants. Several positive virus clones were expanded in SF9 cells to produce high titer stock for preparative infection of High Five *Trichoplusia ni* cells as described by the manufacturer, with the exception that synthetic QDM was added to preparative cultures at a final concentration of 2-5 $\mu$ M.

### **Mammalian Protein Expression**

HEK293 and HEK293S cells were maintained in high glucose (4.5g/L) Dulbecco's Modified Eagle Media supplemented with 2 mM L-Glutamine, 10 mM HEPES pH 7.4 and 10% (v/v) newborn calf serum. On the day of transfection, 60-90% confluent cells were briefly washed with HBSS or PBS, then fed with media containing only 2% (v/v) serum. Supercoiled DNA and linear 25K Da MW polyethylimine (Polysciences) were mixed in a 1:1 (w/w) ratio and allowed to form complexes for 10 minutes at room temperature in DMEM with no additives prior to being added to the cultured cells at a final concentration of 625 ng/cm<sup>2</sup>. Conditioned media were removed after three days and cells were incubated for an additional four days using fresh media. Pooled conditioned media were concentrated and simultaneously buffer exchanged to CFF binding buffer using an Amicon pressure cell with a 30,000 NMW filter. Initial protein concentrations were estimated by Western analysis of total conditioned media.

### **Chromatographic Purification of pMHC Complexes**

Buffer exchanged reactions were mixed with pre-equilibrated Chelating Fast-Flow (CFF) resin loaded with Ni<sup>2+</sup> and nutated at 4° C for a minimum of four hours. Captive complexes were washed by gravity flow using the starting buffer prior to elution in the same buffer augmented with 100 mM EDTA. TEV protease was added to the eluate and the

cleavage reaction was allowed to proceed to completion at 4° C in an Amicon 10,000 NMW centrifugal concentrator with several buffer exchanges to the initial binding buffer in preparation for a second, reverse capture CFF step, to remove any uncleaved starting material as well as the His-tagged protease. In some experiments, additional QDM was added at a concentration of 5  $\mu\text{M}$  during the proteolysis and buffer exchange step. Following reverse purification of the cleaved complex, the sample was concentrated to approximately 1/400<sup>th</sup> of the initial starting volume of the reaction and resolved by gel chromatography using a 10/30 Superdex S-200 column (GE Healthcare) equilibrated in 200  $\text{mM}$  NaCl, 25  $\text{mM}$  Tris-HCl, pH 8.0. Fractions were analyzed by SDS-PAGE and Coomassie Brilliant Blue R250 staining, and those corresponding to the 44,000 dalton monodisperse pMHC complex were pooled and concentrated to a volume corresponding to 1-5 mg protein per milliliter using 10,000 NMW centrifugal filters (Millipore). Protein concentrations were determined by spectrophotometric analysis at 280 nm using predicted molar absorption coefficients as determined by the ProtParam algorithm [74].

### **Crystallization Trials**

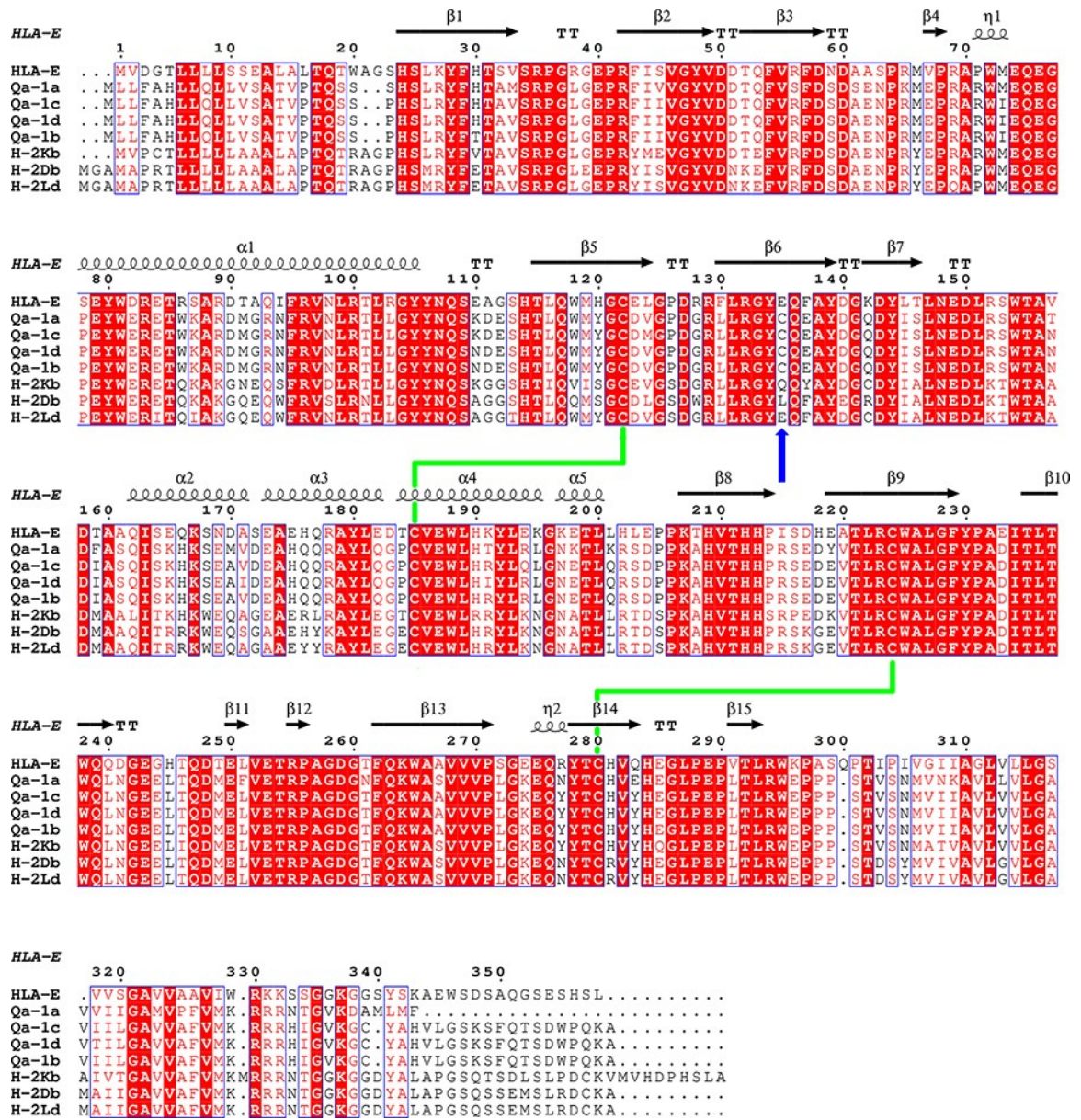
Samples were prepared for crystallographic analysis by concentration and buffer exchange to 10  $\text{mM}$  NaCl, 1  $\text{mM}$  Tris-HCl, pH 8.0 using Amicon Microcon centrifugal concentrators. 3  $\mu\text{l}$  mixtures of protein solution: mother liquor: water (1:1:1) were used in hanging drop vapor diffusion experiments. The precipitant screen was a sparse matrix composed of PEG<sub>3350</sub> at 10-30% (w/v) and buffers ranging from pH 3.0 to 10.0 at 100  $\text{mM}$  concentration. Duplicate trays were used which included 2% (w/v) saturated ammonium sulfate as an additional precipitant. Trays were equilibrated and maintained at 4° C.

### **Figure 2.1 Alignment of Several Representative MHC I Molecules**

All four published Qa-1 alleles were aligned with representative H2-K,D, and L alleles, as well as the human and rat functional homologues, HLA-E and RT-BM1, respectively. Canonical disulfide bonds are identified by green lines and the lone cysteine located in the  $\beta 6$  loop of Qa-1 and RT-BM1 is marked with a blue arrow. Note that the canonical leader peptide presented by Qa-1 (AMAPRTLLL) is only found in the H2-D<sup>b</sup> and H2-L<sup>d</sup> sequences, not within the leader of any of the Class Ib molecules or any H2-K alleles, including K<sup>b</sup>. This alignment was performed using the program MUSCLE v3.6 [75] and the output was rendered using ESPript v.2.2 [76]. Chain A of the HLA-E structure described by O'Callaghan and coworkers [77] was used to automatically determine secondary structure motifs for this alignment.

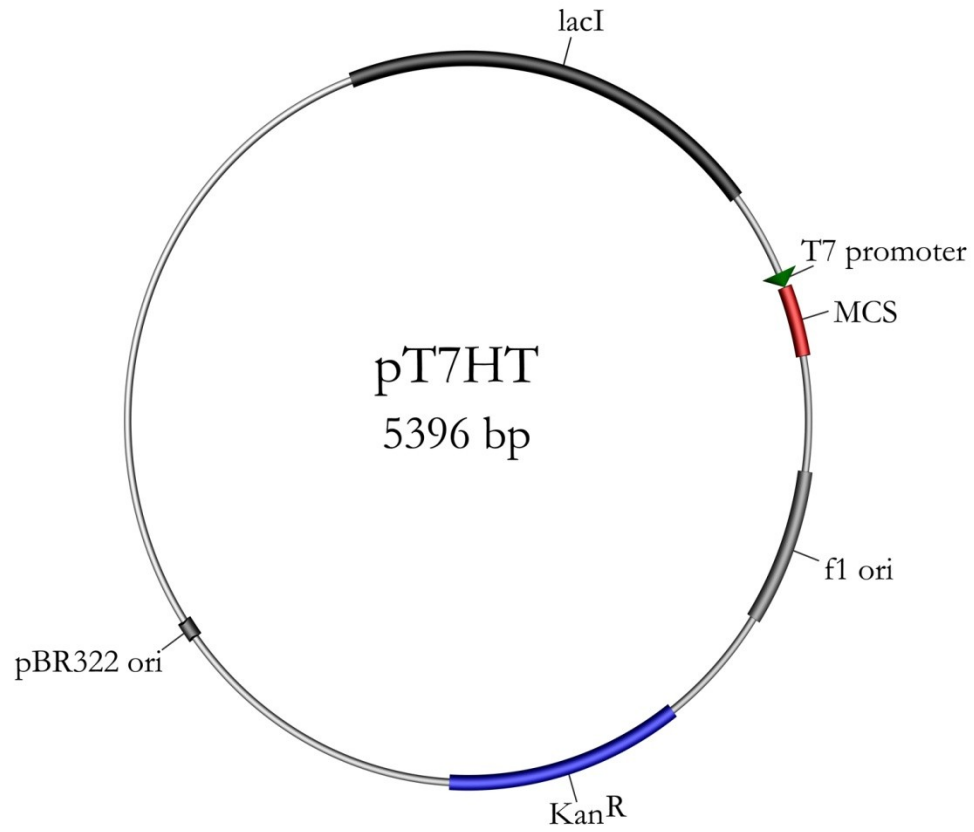


Figure 2.1 Multiple Sequence Alignment of Several MHC Molecules



**Figure 2.2 The pT7HT bacterial expression vector.**

Schematic representation of the pT7HT expression vector and the entire multiple cloning site (MCS). The TEV protease recognition site is colored blue and the resultant amino-terminal glycine following proteolysis is in red. Endonuclease restriction sites are underlined. The protein of interest is expressed with an enzymatically cleavable N-terminal polyhistidine tag following induction of T7 polymerase in suitable *E. coli* strains, such as the *DE3* T7 lysogens. The lacI repressor reduces baseline transcription from the *lac* operon, limiting basal expression of T7 RNA polymerase.



ATG GGC AGC AGC CAT CAT CAT CAT CAT CAC AGC AGC GGC CTG GTG  
M G S S H H H H H H S S G L V

NdeI

CCG CGC GGC AGC CAA CAT ATG GGC ATG GAG CAG AAG CTG ATC AGC  
P R G S Q H M G M E Q K L I S

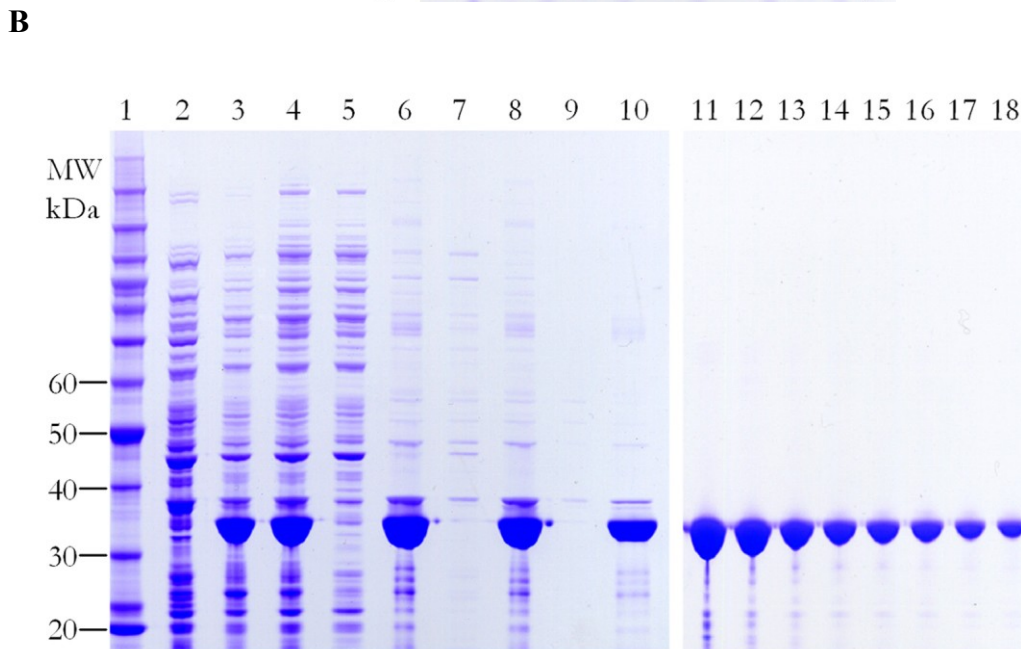
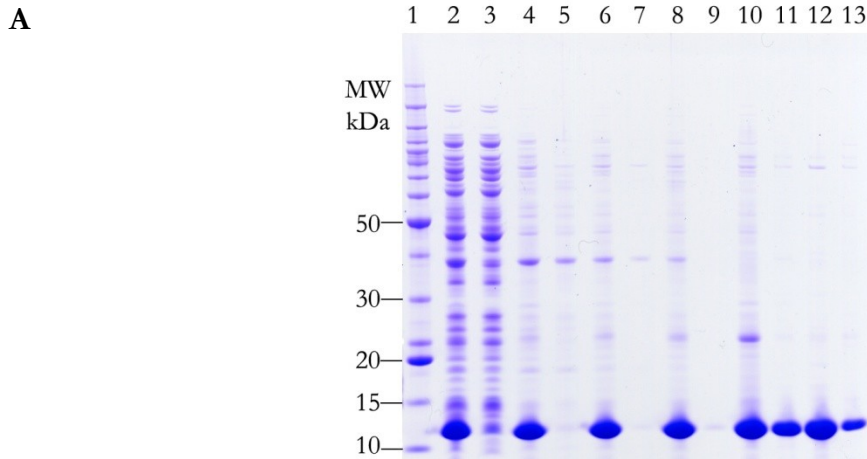
SalI

GAG GAG GAC CTG AAC GGC GAG AAC CTG TAC TTC CAG GGG TCG ACA  
E E D L N G **E N L Y F Q G** S T

BamHI	NheI	SacII	NotI	XhoI
<u>GGA TCC</u>	<u>GCT AGC</u>	<u>CCG CGG</u>	<u>GCG CGG CCG</u>	<u>CAC TCG AGC</u>
G S	A S	P R	A R P	H S S

**Figure 2.3 Inclusion body purification of  $\beta_2m$  and soluble Qa-1<sup>b</sup> proteins.**

SDS-PAGE analyses of bacterially expressed human  $\beta_2m$  and soluble Qa-1<sup>b</sup> ectodomain proteins following induction and purification by differential solubility. The poly-histidine tagged induction product is first separated from the majority of bacterial proteins by physical disruption of the cells in the presence of detergents. Subsequent resuspension of the insoluble inclusion bodies in detergent and salt containing buffered washes significantly increases the purity of the protein of interest prior to denaturing IMAC purification or ion exchange chromatography in 8 M urea.



**A.**

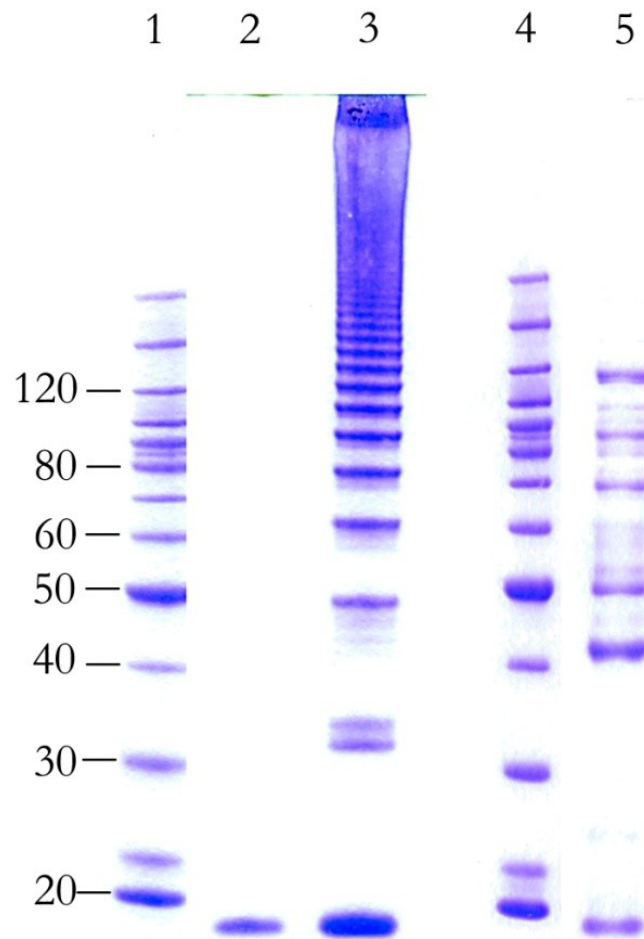
- |                             |                             |                             |
|-----------------------------|-----------------------------|-----------------------------|
| 1. Molecular Weight markers | 5. Soluble fraction 2       | 9. Soluble fraction 4       |
| 2. Total protein            | 6. Pellet 2                 | 10. Final pellet            |
| 3. Soluble fraction 1       | 7. Soluble Fraction 3       | 11. IMAC elution fraction 1 |
| 4. Pellet 1                 | 8. Pellet 3                 | 12. IMAC elution fraction 2 |
|                             | 13. IMAC elution fraction 3 |                             |

**B.**

- |                             |                           |                           |
|-----------------------------|---------------------------|---------------------------|
| 1. Molecular Weight markers | 7. Soluble fraction 2     | 13. MonoQ peak fraction 3 |
| 2. Uninduced lysate         | 8. Pellet 2               | 14. MonoQ peak fraction 4 |
| 3. Induced lysate           | 9. Soluble fraction 3     | 15. MonoQ peak fraction 5 |
| 4. Total protein            | 10. Final pellet          | 16. MonoQ peak fraction 6 |
| 5. Soluble fraction 1       | 11. MonoQ peak fraction 1 | 17. MonoQ peak fraction 7 |
| 6. Pellet 1                 | 12. MonoQ peak fraction 2 | 18. MonoQ peak fraction 8 |

**Figure 2.4 Inappropriate Multimers of  $\beta_2m$  and Qa-1<sup>b</sup> in *In Vitro* Refolding Reactions**

Non-reducing SDS-PAGE analysis of Tris/Arginine refolding reactions reveals the presence of specious multimers. Supernatant and insoluble pellet fractions from a  $\beta_2m$  refolding reaction and the soluble supernatant from a QDM/ $\beta_2m$ /Qa-1<sup>b</sup> refolding reaction were denatured in Laemmli buffer without any reducing reagents. Apparent molecular weights in kilodaltons are indicated on the left.



Lane 1: Benchmark molecular weight marker

Lane 2:  $\beta_2m$  supernatant

Lane 3:  $\beta_2m$  insoluble pellet

Lane 4: Benchmark molecular weight marker

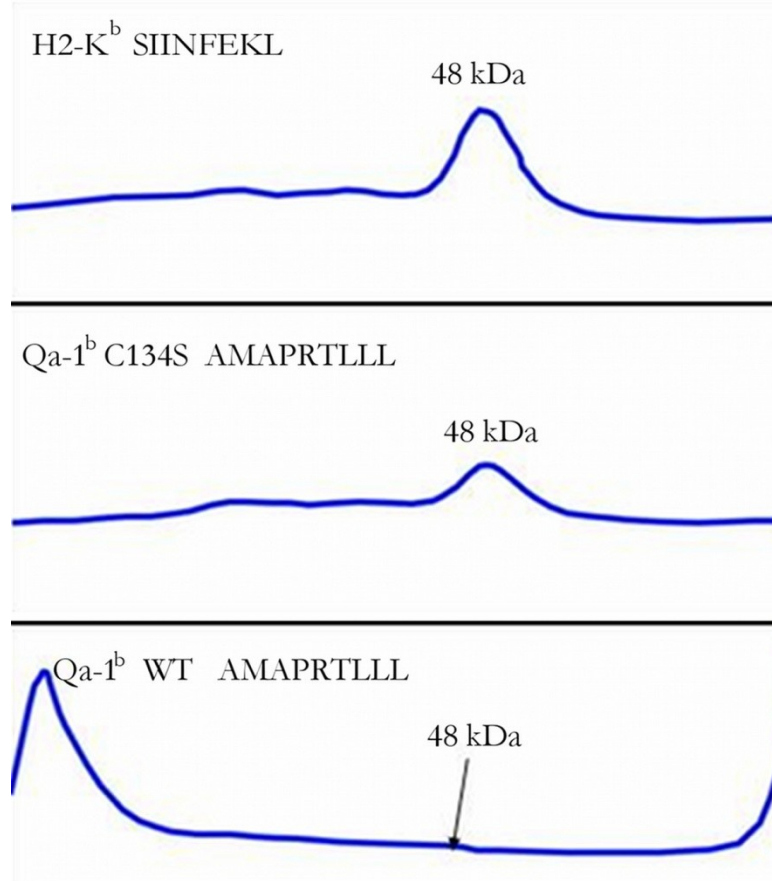
Lane 5: QDM/ $\beta_2m$ /Qa-1<sup>b</sup> soluble supernatant

### Figure 2.5 H2-K<sup>b</sup> Refolds Efficiently Around the SIINFEKL Peptide

Unlike QDM/Qa-1<sup>b</sup> complexes, SIINFEKL/H2-K<sup>b</sup> can be generated easily *in vitro* and purified by gel filtration chromatography. (A) The salient portion of an H2-K<sup>b</sup> refolding reaction and a QDM/Qa-1<sup>b</sup> C134S *in vitro* refolding reaction are shown, along with a wild type QDM/Qa-1<sup>b</sup> refold (not zoomed). The calculated mobility of monodisperse pMHC trimers is indicated, based on molecular weight standard calibration. For the purpose of clarity both traces were enhanced in Adobe Photoshop. The wild type chromatogram clearly depicts the large aggregate peak at  $V_0$  and the beginning of the  $\beta_2m$  monomer peak. (B) Model of H2-K<sup>b</sup> bound to the SIINFEKL peptide based on the coordinates from PDB file 1VAC [61].  $\beta_2m$  is represented in black and the MHC heavy chain in grey, while the peptide backbone is drawn as a yellow tube. All five cysteine residues are rendered as van der Waals spheres and colored according to atom type. The unpaired cysteine is easily identifiable at the beginning of strand  $\beta_6$ , with the sulfhydryl moiety projecting away from the remainder of the molecule, into the solvent.



**A**



**B**

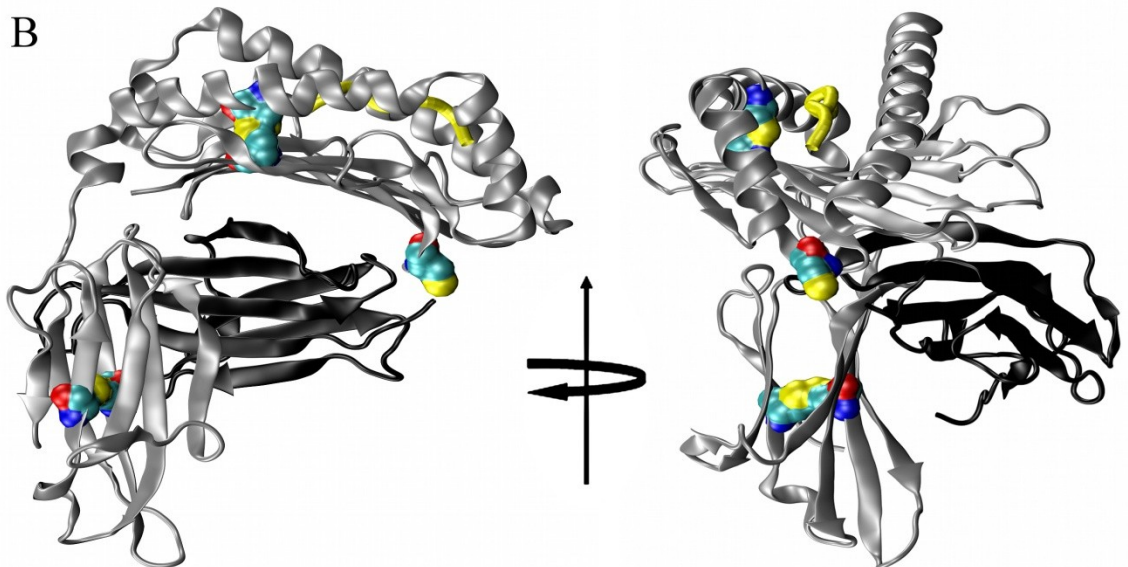
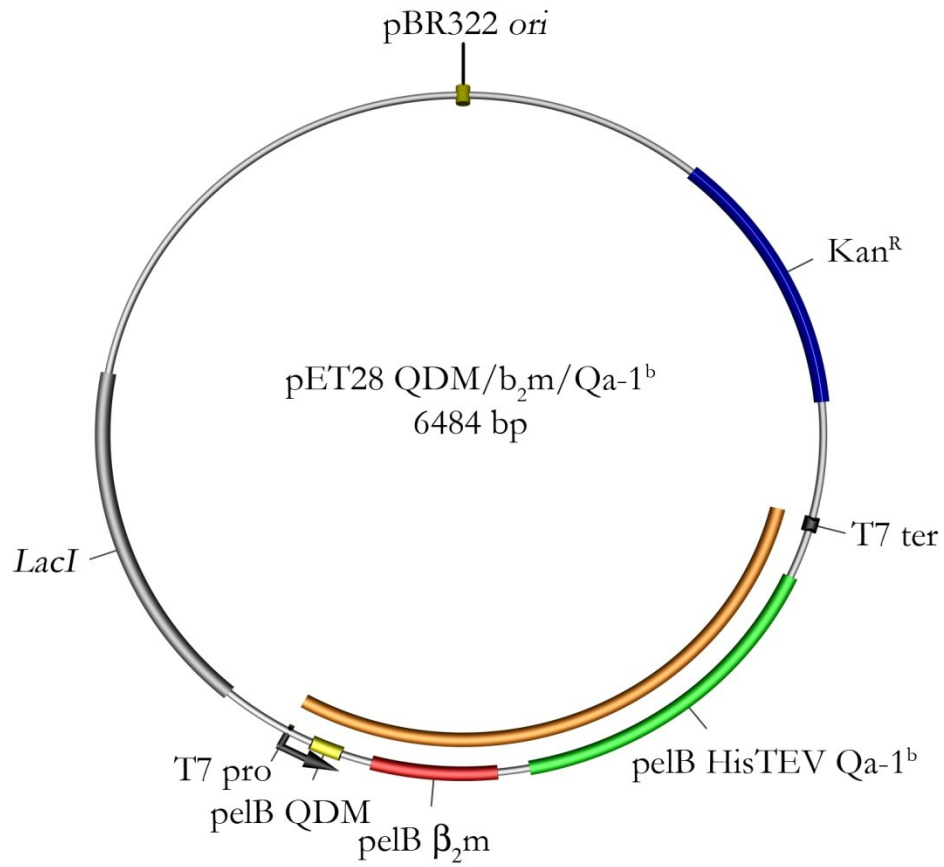


## Figure 2.6 Polycistronic Expression of Qa-1<sup>b</sup> Complex Components

The pelB leader sequence was appended to the amino termini of all three Qa-1<sup>b</sup> complex components. Additionally, a polyhistidine cassette and the TEV consensus sequence were added to the Qa-1<sup>b</sup> ORF to facilitate purification of resultant trimeric complexes by IMAC.

(A) Schematic representation of the pet28 QDM/ $\beta_2$ m/HisTEVQa-1<sup>b</sup> plasmid. (B) Amino acid sequences of the pelB and pelB-His<sub>8</sub>-TEV chimeras. The pelB leader is underlined and the TEV recognition sequence is double underlined. The polycistronic message is under the control of the T7 promoter, allowing rapid, high level transcription following induction of T7 polymerase. Additionally, the presence of the *E. coli* *LacI* inhibitor reduces pre-induction transcription by limiting basal transcription of T7 polymerase message in *DE3* lysogens.

A



B

pelB-QDM  
MKYLLPTAAAGLLLLLAAQPAMAAMAPRTLLL\*

pelB-β<sub>2</sub>m  
MKYLLPTAAAGLLLLLAAQPAMAMEKTPQIQVYSRHPPENGKPNI...WDRDM\*

pelB-His<sub>6</sub>TEV-Qa-1<sup>b</sup>  
MKYLLPTAAAGLLLLLAAQPAMAMGSSHHHHHHSSGLVPRGSQHMENLYFOGSTSPH...PL  
TLRW\*

### **Figure 2.7 Baculovirus Expression of *Hs* $\beta_2m$ and Qa-1<sup>b</sup>**

The human  $\beta_2m$  and Qa-1<sup>b</sup> ectodomain open reading frames were genetically modified to encode an amino-terminal honeybee melittin signal peptide. The Qa-1<sup>b</sup> ORF was further prepended with a TEV cleavable polyhistidine tag (A). Both sequences are shown in their entirety, with the co-translationally cleaved melittin leader underlined. The canonical TEV recognition sequence is double underlined and the carboxy terminal glutamine is indicated in red. Both open reading frames were directionally cloned into the pAcUW51 dual-promoter transfer vector for simultaneous expression late in the infectious cycle of recombinant baculovirus using *Tricoplusia ni* derived High Five cells (B).

## A

Melittin *Hs*  $\beta_2$ m

MKFLVNVALVFMVVYISYIYADGSSIQRTPKIQVYSRHPAENGKSNFLNCYVSGFHPSD  
IEVDLLKNGERIEKVEHSDLSFSKDWSFYLLYYTEFTPTEKDEYACRVNHVTL SQPKIV  
KWDRDM\*

Melittin His<sub>6</sub>TEV Qa-1<sup>b</sup>

MKFLVNVALVFMVVYISYIYADGSSHHHHHHSSGLVPRGSQHMENLYFQGSTSPHSLRY  
FTTAVSRPGLGEPFRIIVGYVDDTQFVRFDSDAENPRMEPRARWIEQEGPEYWERETWK  
ARMDGRNFRVNLRLTLLGYYNQSNDESHTLQWMYGCDVGPDGRLLRGYCQEAYDGQDYIS  
LNEDLRSWTANDIASQISKHKSEAVDEAHQQRAYLQGPCVEWLHRYLRLGNETLQORS DP  
PKAHVTHHPRSEDEVTLRCWALGFYPADITL TWQLNGEELTQDMELVETRPAGDGT FQK  
WAAVVVPLGKEQYYTCHVYHEGLPEPLTLRW\*

## B

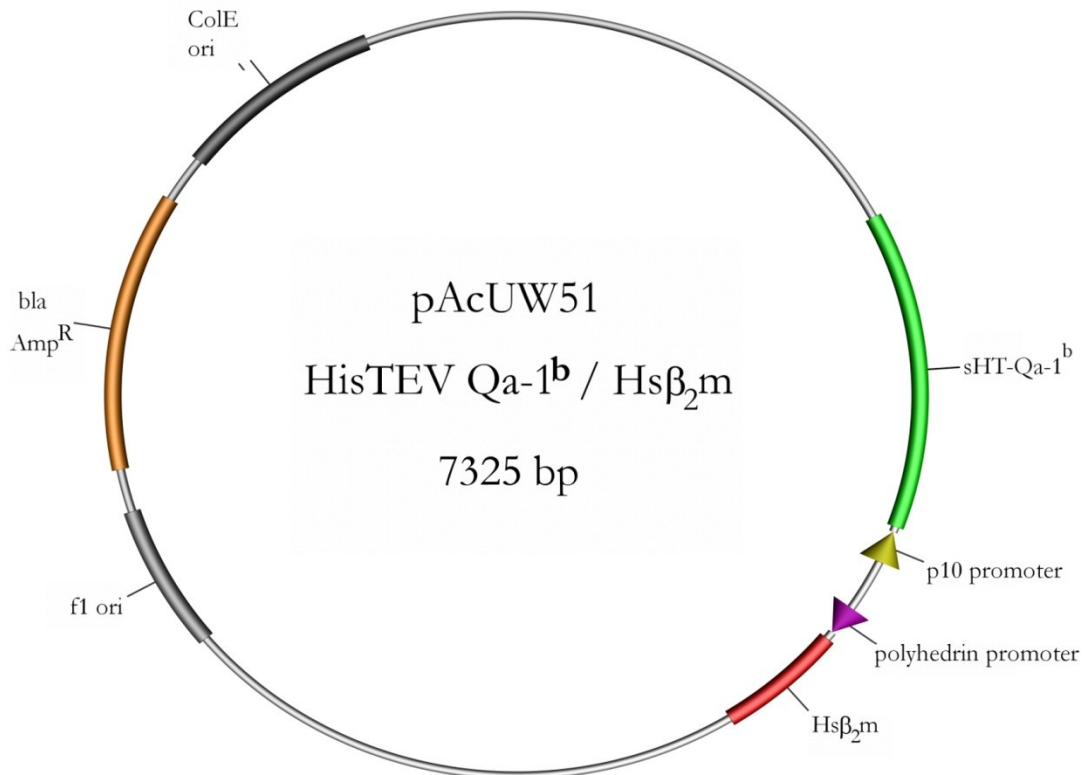


**Figure 2.8 Bacterial QDM,  $\beta_2m$ , and Qa-1<sup>b</sup> linked constructs.**

Soluble chimeras were produced for bacterial expression by genetically linking QDM,  $\beta_2m$ , and the Qa-1<sup>b</sup> ectodomain open reading frames with Gly<sub>4</sub>Ser linkers. In the following schematics, the amino-terminal polyhistidine TEV tag used for initial purification is indicated in black, while the QDM nonamer (AMAPRTLLL) is indicated in yellow and the (G<sub>4</sub>S)<sub>n</sub> linkers are colored blue. The mature  $\beta_2m$  ORF is red and the Qa-1<sup>b</sup> ectodomain green. Both wild type and C134S variants of the constructs which include Qa-1<sup>b</sup> were generated.

QDM - (G<sub>4</sub>S)<sub>3</sub> -  $\beta_2m$



$\beta_2m$  - (G<sub>4</sub>S)<sub>4</sub> - Qa-1<sup>b</sup>



QDM - (G<sub>4</sub>S)<sub>3</sub> -  $\beta_2m$  - (G<sub>4</sub>S)<sub>4</sub> - Qa-1<sup>b</sup>



### Figure 2.9 Transient Expression of Qa-1<sup>b</sup> by HEK Cells

HEK-293 or HEK293S cells were transiently transfected with different concentrations of pSGHV1  $\beta_2m_{20}Qa-1^b$  or pSGHV2 QDM<sub>15</sub> $\beta_2m_{20}Qa-1^b$  using polyethylimine. After 72 hours, conditioned media was removed and clarified by centrifugation. 5  $\mu$ l aliquots were analyzed by Western blot using the 6A8.6F10 anti-Qa-1 monoclonal antibody. The glycosylated chimeras, with amino-terminal human growth hormone (~22 kDa) fusions, have an expected polypeptide molecular weight of 74 and 76 kDa, respectively. The apparent altered migration is due to batch to batch variations of prestained markers, as well as retardation by glycosylation. The HEK-293S protein migrates slightly faster due to immature terminal glycosylation by this cell line.

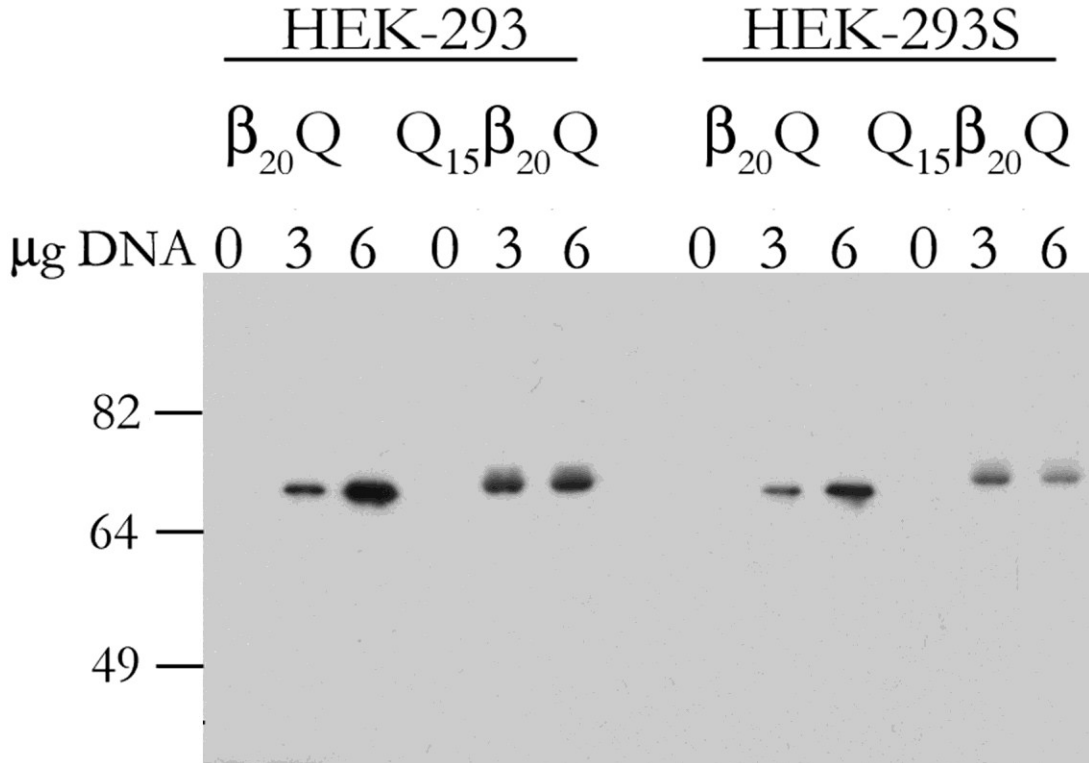


**Figure 2.10 SDS-PAGE analysis of mammalian expressed Qa-1<sup>b</sup> complexes.**

PAGE analysis of Sephadex S-200 Gel Filtration purified  $\beta_2m-(G_4S)_4$ -Qa-1<sup>b</sup> C134S complexes digested with MBP-Endoglycosidase H. 1% (10  $\mu$ l/ milliliter) of each gel filtration fraction was loaded on a 4-12% Bis-Tris/MES gel and stained with Coomassie Brilliant Blue R250. Starting material was initially purified by a single IMAC step from approximately 500 milliliters of media conditioned for 72 hours following transient transfection of HEK293 human cells.

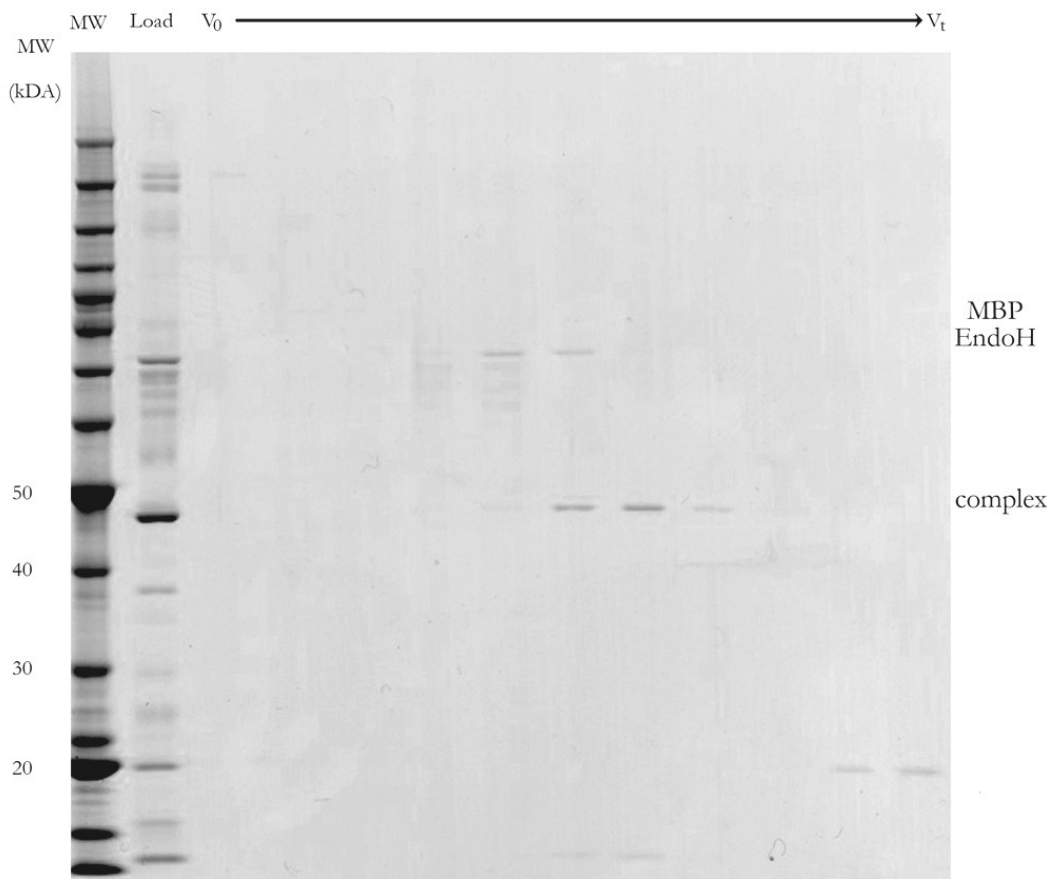
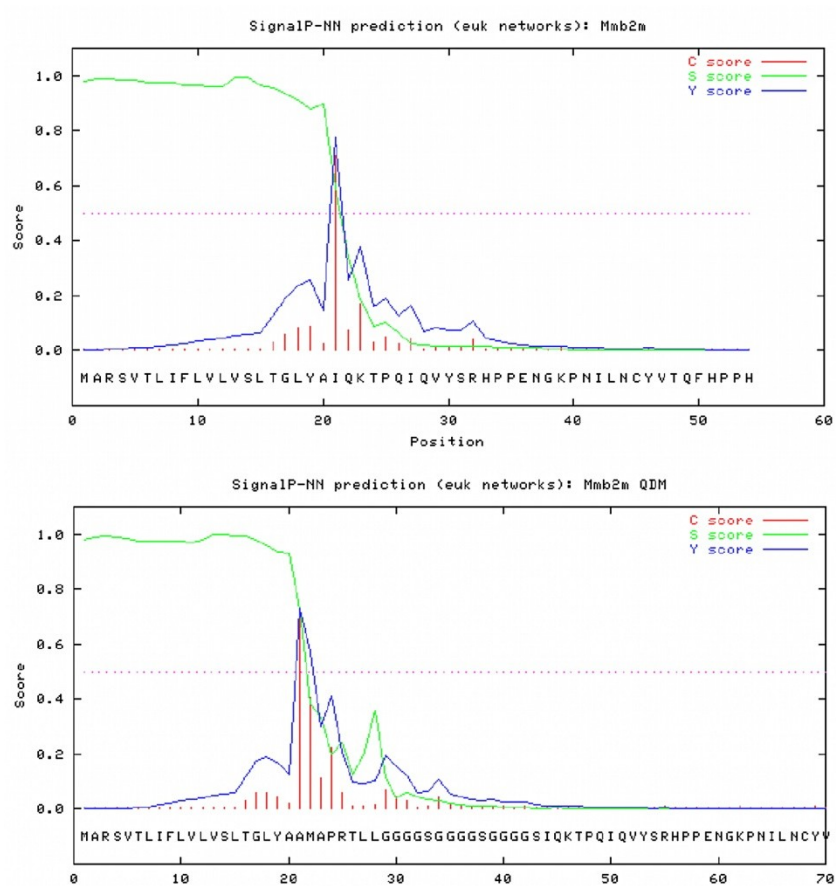




### Figure 2.11 Predicted cleavage of QDM chimeras by mammalian signal peptidase

The murine  $\beta_2m$  and the chimeric  $\beta_2m$  leader-QDM-(Gly<sub>4</sub>Ser)<sub>3</sub>- $\beta_2m$  sequences were analyzed using the program SignalP, version 3.0. Predicted cleavage site probabilities are indicated by the vertical red line, and in both cases the preprotein is most likely to be cleaved between residues 20 and 21. In the case of the chimeric molecules, this would leave an intact amino terminal AMAPRTLLL, the QDM sequence. The new amino terminal residue following cleavage is indicated in red.



Mouse  $\beta_2$  microglobulin preprotein sequence:

MARSVTLIFLVLVSLTGLYA IQKTPQIQVYSRHPPENGKPNILNCYVTQFHPPH...

Mouse  $\beta_2$  microglobulin leader peptide and QDM-(Gly<sub>4</sub>Ser)<sub>3</sub>  $\beta_2m$

MARSVTLIFLVLVSLTGLYA A MAPRTLLGGGGSGGGGSGGGGS IQKTPQIQVYSR...

## **Chapter 3**

### **The Role of Cysteine 134 in Qa-1<sup>b</sup> Stability**

## Introduction

In the process of attempting various approaches to purify biochemical quantities of Qa-1<sup>b</sup> pMHC, we observed a very short half-life for these complexes. We postulated that this instability is an inherent property of the Qa-1 heavy chain and sought to understand its molecular basis. By comparing the primary sequences of murine MHC Ia molecules, as well as their known atomic resolution structures where available, we categorized sequence differences that could potentially alter the stability of heavy chain interactions with the bound peptide or  $\beta_2$  microglobulin. There are obviously a large number of polymorphisms in MHC Ia molecules, however they were excluded from our analyses. We focused primarily on residues which would interact directly with the peptide, especially backbone atoms, as well as heavy chain residues below the peptide binding platform and along the  $\alpha 3$  domain which would stabilize interactions with  $\beta_2$ m. There is a high degree of identity ( $\sim 77\%$ ) and similarity ( $\sim 88\%$ ) between Qa-1<sup>b</sup> and murine Ia molecules by direct comparison of ectodomains using BLAST [78]. There was one striking difference between Qa-1 molecules and other MHC sequences: a lone cysteine at position 134.

Although several MHC Ia molecules contain unpaired cysteines, only Qa-1 and the rat homologue RT-BM1 contain a lone cysteine at a unique position (134 in the Qa-1 molecule). This residue is predicted to line a peptide binding pocket and therefore become completely solvent inaccessible once a peptide is loaded into the molecule. As no other differences between Ia molecules and Qa-1 readily supported our hypothesis that the primary sequence of the heavy chain is responsible for the short half-life of Qa-1, we focused on Cys134. We further postulated, based on non-reducing PAGE analysis of *in vitro* refolding reactions, that an odd number of cysteines did not facilitate the production of complexes. Directed site-specific mutagenesis was used to modify the heavy chain sequence

at residue 134. Mutant molecules were compared to the wild type molecule using several complementary approaches, including transfection of mammalian cells and characterization of the maturation rate and stability of the molecules by metabolic labeling.

## **Results and Discussion**

### **Identification of Cysteine 134 as Major Determinant of Qa-1<sup>b</sup> Stability**

During the initial efforts at Qa-1<sup>b</sup> complex generation discussed in chapter two, the profound instability of the resultant complex became apparent. Unlike MHC Ia complexes, which are ideally long lived, the biological role of Qa-1 is better served by an unstable molecule. The evolutionary advantage of this bimodal stability is obvious. Long lived MHC Ia complexes can indicate infection or transformation to CD8<sup>+</sup> effector T cells for an extended period of time, but the probability of such an encounter is greatly reduced by the small number of peripheral T cells specific for any given non-self peptide in the context of the presenting MHC Ia. NK cells, however, are innate effectors and therefore do not require a unique pathogen signal resulting from adaptive selection. The lack of receptor variation among these cells allows each individual cell to function nearly identically to other NK cells. This greatly increases the probability that a distressed cell will be recognized by NK receptors. As Qa-1 complexes are unstable, any of these MHC molecules on the surface of the cell must have been recently synthesized, and therefore provide a more recent indicator of MHC I biosynthesis within the cell.

Following the *in silico* identification of Cys134 as a potential determinant of Qa-1<sup>b</sup> instability, mutations were engineered in the soluble bacterial construct as well as the full-length molecule. Two different mutations were generated, one a conservative serine

substitution, and the other a glutamic acid, which is found in many murine Ia alleles at the same position (**Figure 3.1**). Bacterial expression of the mutant molecules was essentially indistinguishable from the wild type. Cell surface expression of the mutant molecules in mouse L(M)Tk<sup>-</sup> cells, however, suggested that there was a measurable difference. In both transient and stable expression experiments, the Cys134Ser (C134S) mutation enhanced cell surface expression compared to the wild type molecule (**Figure 3.2**).

This substitution was also engineered into a chimeric molecule already available in the lab. This construct was engineered by Adrian Davies to encode a tethered molecule which covalently links an N-terminal mouse  $\beta_2$ microglobulin open reading frame (ORF) to a leader-less Qa-1<sup>b</sup> heavy chain via a fifteen amino acid (Gly<sub>4</sub>Ser)<sub>3</sub> spacer. This molecule was used to generate Qa-1<sup>b</sup> knock-in mice in the  $\beta_2m^{-/-}$  background, an experimental approach that allowed dissection of immune recognition of Qa-1<sup>b</sup> in the absence of any other MHC I molecules which require  $\beta_2m$  [13]. Introduction of a serine substitution for the unpaired cysteine (also referred to as C134S for the sake of clarity, despite the altered numbering due to the N-terminal  $\beta_2m$  and linker sequences) in this molecule also enhances surface expression compared to wild type. It should be noted that surface expression of the mutant chimera is still significantly lower than even the wild type full length molecule in every cell line tested.

Three plausible explanations for enhanced surface expression can be considered. First, it is possible that the mutant molecule has lost the exquisite peptide selectivity characteristic of the wild type molecule [41]. This would allow newly synthesized molecules to display a larger repertoire of peptides and therefore transition to the surface in higher numbers. The second possibility is that the mutant has a longer half-life than the wild type, therefore any molecules which arrive at the surface persist longer, enhancing surface

staining. The third cause of increased surface staining may be increased maturation rate of the molecule. This third possibility would only enhance surface staining if the mutant molecule is at least as long-lived as the wild type. These three possibilities are not mutually exclusive, therefore the possibility that two or all three mechanisms occur simultaneously cannot be excluded simply based on surface staining.

The most obvious experimental approach to resolving these three plausible mechanisms is to quantify the relative ability to present QDM, the rates of egress from the endoplasmic reticulum and the mean lifetime of the mature molecule. The requirement for QDM can be determined by assessing the ability of the mutant to reach the surface of cells in the absence of endogenous QDM peptide. Since Qa-1<sup>b</sup>/QDM complexes are specifically recognized by the allogeneic CD8<sup>+</sup> T cell clone 5D2-T, standard CTL assays can be used to determine whether mutant molecules are still capable of presenting QDM. The rates of ER exit and total molecular turnover can be determined simultaneously by differential glycosidase sensitivity of metabolically labeled Qa-1<sup>b</sup> using pulse-chase analyses.

### **Expression of Qa-1<sup>b</sup> Protein in B78H1 Murine Cells**

Preliminary experiments were designed only to test the hypothesis that substitutions of other amino acids at the unpaired cysteine at position 134 would improve the stability of Qa-1 molecules. The initial experiments were performed in mouse L(M)Tk<sup>-</sup> cells, which are immortalized fibroblasts derived from C3H/An mice expressing the H2-<sup>k</sup> haplotype [79]. These cells express H2-D<sup>k</sup>, and therefore have QDM<sup>k</sup> (AMYPRTLLL), but are serendipitously null for Qa-1<sup>b</sup> expression as assessed by Western analysis and immunoprecipitation with the 6A8.6F10 monoclonal. The constitutive presence of QDM<sup>k</sup>, however, did not allow the peptide specificity of the mutant molecule to be readily assessed.

An ideal cell line would be QDM and Qa-1 null, while still maintaining Tapasin and TAP1/2 expression. Two additional characteristics which would be highly desirable in an experimental cell line are ease of stable transfection and high efficiency of sorting and subcloning.

The mouse B78H1 cell line is effectively null in MHC Ia expression [80] and is easily transfected and sorted. Initial transfection experiments of the constructs discussed herein were uniformly disappointing, as little surface expression could be detected by flow cytometry. Surprisingly, Western analysis of the cells indicated robust protein production, albeit at molecular weights suggestive of immature glycosylation. Based on previous experimental work performed in the lab using B78H1 cells, it was determined that Qa-1<sup>b</sup> surface expression is enhanced by shifting the cells to 25° C for 16 hours before analysis (**Figure 3.3**). The mechanistic details of this process have not been elucidated, but the result of the temperature shift is quite dramatic. Bulk transfectants were sorted twice sequentially to maximize protein expression, and the resultant clones were analyzed by metabolic labeling and pulse-chase analysis to quantify the kinetic parameters of these molecules.

Biochemical analysis of total enucleated lysates from temperature-shifted B78H1 cells pulsed with synthetic QDM peptide confirmed the observation that the C134S directed mutation increases the amount of maturely glycosylated protein relative to the wild type (**Figure 3.4**). By Western analysis, it is quite obvious that the introduction of this point mutation leads to the generation of diffuse, relatively retarded, mature protein which we propose is displayed on the plasma membrane based on live cell FACS analysis. It should be noted that the maturation of Qa-1<sup>b</sup> molecules is far from complete in this cell line and a significant amount of the high-mannose species can still be observed in lysates prepared from C134S mutants. Furthermore, and perhaps most interesting vis a vis the production

and maturation of Qa-1<sup>b</sup> pMHC complexes, the wild type chimeric construct encoding a single chain polypeptide with QDM,  $\beta_2m$  and Qa-1<sup>b</sup> is unexpectedly fully glycosylated at a much higher ratio than either wild type or C134S full length constructs. In fact, the majority of the protein species migrates as expected for terminally glycosylated species, while only a small fraction remains immature. These results were then confirmed by treatment of lysates with endoglycosidases.

Lysates prepared as in the previous experiment were divided into three aliquots and treated with Endoglycosidase H (EndoH), Peptide: N-glycosidase F (PngaseF), or left untreated and simultaneously analyzed by Western analysis (**Figure 3.5**). As would be expected, very little EndoH resistant protein can be observed in either the full length or  $\beta_2m_{(15)}$ Qa-1<sup>b</sup> wild type constructs. By comparison, the same proteins with the single C134S mutation generated notable quantities of EndoH-resistant species, albeit still a minority of the total observed Qa-1<sup>b</sup> species. The presence of predominantly fully matured QDM<sub>(15)</sub> $\beta_2m_{(20)}$ Qa-1<sup>b</sup> was confirmed by direct comparison of the untreated and EndoH treated lysates.

On the basis of the results of these experiments alone, it would be tempting to conclude that the mode of action for the single mutation at residue 134 has been conclusively determined to be the acceleration of the maturation velocity. It is in fact quite possible that this is the only mechanism at work in B78H1 cells, but this system fails to mimic the natural murine MHC synthetic pathway, as demonstrated by the temperature dependence of Qa-1<sup>b</sup> surface expression. One potential mechanistic explanation for the temperature dependence may be that the reduction in temperature alleviates the TAP1/2 dependence of Qa-1<sup>b</sup>. B78H1 cells do not transcribe the TAP2 gene product [81], therefore surface expressed pMHC do not arise via canonical means in this cell line. An equally likely



explanation is that the non-specific chaperone mediated refolding of heavy chain molecules is enhanced by this temperature shift due to a reduction in transcription or translation velocity of new molecules. Interestingly, a similar observation of temperature dependent maturation of Qa-1<sup>b</sup> was observed by Li et al. in tapasin<sup>-/-</sup> mice [4]. Additionally confounding straightforward interpretation of these observations, this cell line is completely deficient in endogenous sources of QDM peptide. The addition of synthetic peptide to the culture media likely bypasses the canonical ER maturation pathway. Due to the TAP<sup>-/-</sup> status of B78H1 and the absence of endogenous QDM, two additional experimental approaches were explored. First, maturation rates for natively expressed Qa-1<sup>b</sup> were determined in C57Bl/6 mice as well as the derivative H2-K/D null strain in the same background, which is also H2-L<sup>-/-</sup>.

### **Characterization of Qa-1<sup>b</sup> stability**

Pulse-chase analysis of Qa-1<sup>b</sup> was performed in freshly prepared splenocytes. As would be expected, the maturation of Qa-1<sup>b</sup> is severely hampered in the absence of any Ia leader in H-2K/D<sup>-/-</sup> mice, however the half-life of the immature molecules is increased to approximately 9.4 hours due to slower turnover in the ER (**Figure 3.6**). The wild type Qa-1<sup>b</sup> molecule in mice expressing H2-D<sup>b</sup> has a half-life of 69 minutes for all molecules, while half the molecules mature to an EndoH resistant state in 38 minutes. These experiments very nearly reproduce published observations from Peter Jensen's group [54], although those experiments used surface biotinylation to measure lifetimes. Due to the difficulty involved in genetically manipulating primary cells, we sought a more tractable experimental system.

We accomplished this goal by stably transfecting several of our constructs into the human B/T lymphoblastoid myeloma C1R cell line [82].

C1R cells are HLA-A,B,C null and express very low surface amounts of human HLA-G and F. They do, however, express the ER chaperones associated with Class Ia biogenesis as well as human  $\beta_2m$ , therefore they are nearly ideal cells for the analysis of our Qa-1<sup>b</sup> complexes. Furthermore, two control C1R clones, expressing wild type full length Qa-1<sup>b</sup> under the control of at least a portion of its natural promoter, already existed in the lab. One cell line is QDM-null, while the other has been co-transfected with H2-L<sup>d</sup>. These cell lines, named C1R G37 and C1R G37/L<sup>d</sup> were sorted for maximal surface expression of Qa-1<sup>b</sup> and were kindly provided by James Forman [83]. The name G37, an abbreviation for Gene37, denotes a deprecated appellation of Qa-1<sup>b</sup>. Unlike the B78H1 cells, C1R cells are capable of expressing Qa-1<sup>b</sup> complexes without any modification to their growth temperature. Additionally, the presence of an intact MHC I biogenesis machinery allows detailed investigation of the Qa-1<sup>b</sup> maturation kinetics in an environment which more closely resembles that found in normal mouse cells.

In order to generate additional stable cell lines of Qa-1<sup>b</sup> C134S or the chimeric constructs, with or without QDM present endogenously, C1R cells were first transfected with the pL<sup>d</sup>IH vector. This DNA encodes the full length H2-L<sup>d</sup> molecule, including the QDM-containing native leader sequence, and confers resistance to hygromycin via an Internal Ribosome Entry Site (IRES) on the same message as the MHC Ia molecule (**Figure 3.7a**). Stably transfected C1R/L<sup>d</sup> cells were sorted for the highest expressing 1%, and individual clones were analyzed by FACS. C1R/L<sup>d</sup> clone 6C7 was selected and transfected with the various Qa-1<sup>b</sup> constructs, as was the parental C1R line (**Figure 3.7b**). The ability to assess maturation of Qa-1 in cell lines differentiated only by the presence of endogenous

leader peptide would allow direct determination of the specificity of the mutant molecule for QDM.

While stable, sorted C1R cells were being generated, the maturation rate and half-life of the wild type and mutant full length molecules were determined in B78H1 cells. Prior to metabolic labeling, cells were augmented with 5  $\mu\text{M}$  synthetic QDM and shifted to 25°C. After metabolic labeling, cells were harvested at several time points and Qa-1<sup>b</sup> molecules were immunoprecipitated using 6A8.6F10-coupled resin. The immunoprecipitated <sup>35</sup>S labeled material was eluted by heating in SDS/DTT buffer and separated into three aliquots. For each time point, one aliquot was treated with PNGaseF to completely remove all glycosylation, another with EndoH, which only removes immature high mannose modifications found in the endoplasmic reticulum, and the last aliquot was left untreated. Samples were separated by SDS-PAGE and exposed to autoradiography film to allow quantitation of each species (**Figure 3.8**). It could not be determined from this experiment whether it is accelerated maturation or increased longevity of the surface molecule that leads to the enhanced surface expression of the C134S mutant as both processes are observed in B78H1 cells. Furthermore, the various biosynthetic defects in this cell line also strongly suggested that while this technical approach might prove useful, the choice of target cells is essential.

The same metabolic labeling approach, coupled with glycosidase treatment, was applied to several sorted C1R transfectants clones (e.g. **Figure 3.9**), as well as freshly explanted murine splenocytes. The murine splenocytes served as endogenous QDM controls for the wild type protein only, however we were able to additionally these data to determine that *lack* of egress from the ER leads to prolonged half -lives compared to surface expressed molecules. This is congruous with the notion that nascently synthesized MHC I

molecules are stabilized by chaperones until they egress the ER and proceed to the Golgi apparatus. These data from the experiments using B78H1 or C1R transfectants, as well as mouse splenocytes, are summarized in **Table 2**.

The most informative data were from C1R cells, which have an intact MHC I biogenesis pathway and  $\beta_2m$  expression, albeit from *Homo sapiens*. In the parental C1R line, which has no endogenous source of MHC Ia leader peptide, the mutant molecule does in fact convert to an EndoH resistant species more quickly ( $t_{1/2}$ =1.33 hours vs. 2.91 hours), but the C134S mutant also has a slightly higher turnover rate. Once QDM is present, however, the maturation rates are essentially identical, yet the half-life of the C134S mutant is nearly 4.9-fold longer. In C1R we do observe a small fraction of Qa-1<sup>b</sup> C134S molecules maturing in the absence of QDM, however a similar population is observed in H-2K/D<sup>-/-</sup> splenocytes. It is possible that the leader peptide of HLA-G supplies a sufficiently similar peptide (VMAPRTLFL) to QDM to allow a small fraction of Qa-1<sup>b</sup> molecules to mature. It cannot be determined from our experiments whether this population is always present, even in the presence of excess QDM, or if this is an artifact of the absence of cognate peptide. This population certainly cannot account for the dramatic difference in surface staining of Qa-1<sup>b</sup> between C1R and C1R/L<sup>d</sup> cells. The interpretation best supported by these observations is that the single point mutation increases the stability of the Qa-1<sup>b</sup> heavy chain once it has matured and exited the ER. The possibility that the point mutation accelerates the maturation of the complex is obviated by the fact that both wild type and C134S molecules mature with a nearly identical rate of ~36 minutes in C1R/L<sup>d</sup> cells.

This five-fold disparity in half-life is quite striking, considering that it is the result of a single atom change from sulfur to oxygen. Admittedly, this change does dramatically alter the chemical reactivity of the side chain at that position. However C134 was not predicted

to be able to form disulfide bridges due to its putative distance to other cysteine residues, and furthermore, the Bohr radii of the two atoms are not sufficiently different at 1.52 and 1.8 Å to suggest a dramatic alteration in the packing of nearby residues. Given that C134 is likely to remain unpaired, the most likely chemical difference between the sulfhydryl and the hydroxyl side-chain of a serine at the same position must be in the hydrophobic character of the interactions. Although cysteine sulfhydryls are often involved in nucleophilic attack (e.g. cysteine proteases such as papains[84]), this amino acid has a stronger hydrophobic character than serine. In fact, cysteine has been estimated to approximate the hydrophobicity of methionine, isoleucine or leucine when buried inside globular proteins [85]. These *in silico* calculations are derived from approximately 380 non-redundant published protein structures and exclude cystines as well as cysteines involved in metal coordination. Based on sequence alignment and homology modeling, C134 lies in the center of the  $\beta$ 6 strand with the sulfhydryl protruding away from the platform and along the edge of the peptide binding pocket which accommodates the leucine in position 7 of QDM.

Increased hydrophilicity in this pocket would not be likely to increase interactions with the  $\delta$ -methyl group of leucine. The most likely explanation for the enhanced stability of the heavy chain is that interatomic interactions among the pocket forming residues stabilize the side-chain accommodating pocket itself without disruption of the peptide specificity. The structure of the Qa-1<sup>b</sup>/QDM pMHC was recently determined by X-ray crystallography to a Bragg limiting resolution of 1.9Å[86]. Although the authors do not directly address the unpaired cysteine at position 134, the deposited structure provides an invaluable resource to further our understanding of this molecule, especially by comparison to murine MHC Ia molecules (**Figure 3.10**).

The binding of QDM within the peptide binding groove is largely mediated by 14 direct hydrogen bonds as well as eight additional bonds involving ordered water molecules. The coordination and burial of peptide Leu7 is primarily the result of five van der Waals interactions (Qa-1<sup>b</sup> residues Asn<sup>77</sup>, Glu<sup>116</sup>, Ile<sup>124</sup>, Trp<sup>133</sup>, and Glu<sup>152</sup>), as well as both one direct and one water mediated hydrogen bond to the P7 carbonyl. The hydrophobic pocket that surrounds the leucine side-chain also includes the sulfhydryl group of Cys134 (**Figure 3.11**). Given the atomic resolution structure solved by Zeng et alia, we can attempt a rational explanation for the stabilizing effect of a serine substitution for Cys134. If this sulfur atom were replaced by oxygen, it would only make one notable interatomic contact: with the  $\epsilon$ -nitrogen of Trp<sup>97</sup> at 3.5Å [87]. This interaction would further stabilize the orientation of the tryptophan indole side-chain providing a hydrophobic face along the side of the P7-binding pocket, as observed in the deposited structure.

Based on the maturation rate and half-life of the wild type and the C134S mutant in the C1R/L<sup>d</sup> cell line, we propose that this point mutation affects the stability of the pMHC trimer but not the peptide specificity. Although accelerated maturation of the protein is observed in B78H1 transfectants, the manifold MHC biogenesis defects in these cells do not support the hypothesis that egress velocity from the ER plays a major role in the disparity between the wild type and mutant Qa-1<sup>b</sup> molecule. The only remaining potential contributing factor is the loss of peptide selectivity, not definitively proven by the maturation rate of the C134S mutant in C1R cells. This possibility, which also addresses the biological significance of the work outlined here, was tested using two alloreactive mouse CD8<sup>+</sup> cytotoxic lines with distinct Qa-1<sup>b</sup> reactivity. These experiments are detailed in the subsequent chapter.

## **Materials and Methods**

### **Generation of Full Length cDNA Constructs**

Wild type and mutant DNA were cloned into either pCI-Neo (Promega Corporation) or a modified version of the related vector pCI-Pre, which does not have a selection marker but is reported to express higher levels of the message of interest relative to the parental pCI vector [88]. Both plasmids use the CMV promoter to generate the message of interest. Full length cDNA was augmented with an XhoI site 5' of the initiator methionine and a 3' XbaI site by PCR. The amplicon was digested and cloned directly into XhoI/XbaI cut vector and sequenced in its entirety to confirm preservation of the open reading frame. Mutations were introduced by the overlap PCR method. Briefly, two complementary oligonucleotides encoding the altered codon were designed centered over the desired position. Each fragment of the molecule was amplified with the appropriate 5' or 3' primer. The truncated PCR products were then gel purified and a second amplification using a mixture of the two initial products as targets and the outermost 5' and 3' primers resulted in an amplicon with the engineered mutation. In some cases the full length amplicon was initially cloned into the pCR2.1 vector directly following PCR, before being moved by restriction digestion into the final expression vector. In all cases the integrity of the entire ORF was confirmed by bidirectional sequencing.

### **Generation of Chimeric Constructs**

Constructs with a 15-mer spacer were amplified using a 5' XhoI  $\beta_2m$  primer and the XbaI 3' Qa-1<sup>b</sup> primer using pAD26.3 as a template. Mutations were introduced by using a unique BstXI restriction site 5' of Cys134 and the terminal XbaI site. Three part ligations of the XhoI/XbaI cut vector, the 5' fragment (XhoI/BstXI) and the 3' fragment containing the

confirmed mutation from wild type constructs, resulted in a chimeric molecule with a 15-mer spacer and the C134S missense mutation.

QDM-(G<sub>4</sub>S)<sub>3</sub>-β<sub>2</sub>m-(G<sub>4</sub>S)<sub>4</sub>-Qa-1<sup>b</sup> and β<sub>2</sub>m-(G<sub>4</sub>S)<sub>4</sub>-Qa-1<sup>b</sup> constructs were generated *ab initio* using an extended overlap PCR approach. Essentially, overlapping oligonucleotides which encoded the spacer segment and a small region of either β<sub>2</sub>m or Qa-1<sup>b</sup> were used to generate partial ORFs which were then purified, mixed in approximately equimolar concentrations and used as templates for full ORF amplification using the two outermost primers. In order to introduce the QDM sequence directly carboxy-terminal to the β<sub>2</sub>m signal sequence, the ORF 5' to the mature β<sub>2</sub>m sequence was synthesized by overlapping oligos. All amplicons were cloned into pCI-Neo or pCI-Pre following XhoI/XbaI digestion and gel purification. All sequences were confirmed by bidirectional sequencing.

### **Preparation of DNA and Transfections**

All DNA used in transfections was generated by a modified CsCl density gradient protocol. Briefly, crude nucleic acid prepared by alkaline lysis of saturated overnight DH5α (*recA/endA/hsd* mutant genotype) cultures was initially purified by precipitation of the majority of RNA and genomic DNA fragments using ammonium acetate at a final concentration of 2.7 M. The partially purified resultant plasmid DNA was then purified twice by self-forming CsCl equilibrium density centrifugation. Ethidium bromide was quantitatively removed by repeated extraction with 2-propanol saturated with 5 M NaCl. The DNA produced was in all cases found to have an OD<sub>260/280</sub> ratio of 1.81-1.85. For stable transfection, pCI based vectors were digested with XmnI, which cleaves once within the *bla* gene to linearize the plasmid. Following linearization, the DNA was extracted once by phenol:chloroform:isoamyl alcohol (25:24:1 by volume), three times with



Chlorform:isoamyl alcohol (24:1 v/v), and once with diethyl ether prior to ethanol precipitation. All DNA was quantified by spectroscopy at 260 and 280nm.

B78H1 were lifted by trypsinization, washed twice in serum containing media, and twice in 1XHBSS supplemented with 10 mM HEPES (pH 7.4). 400  $\mu$ l of  $1 \times 10^7$  cells/ml were transfected with 10  $\mu$ g of DNA by electroporation using 4 mm gap cuvettes and instrument settings of 250 V, 960  $\mu$ F. C1R cells were electroporated using the same instrument settings, however they were initially purified over a Ficoll-Paque cushion to remove dead cells. L(M)Tk<sup>-</sup> cells were electroporated at 400 V, 500  $\mu$ F. For stable clone selection, transfectants were allowed to recover 24-36 hours in complete media prior to the addition of 800  $\mu$ g/ml G418 or 100  $\mu$ g/ml Hygromycin B as appropriate.

### **Tissue Culture**

B78H1 and L(M)Tk<sup>-</sup> cells were grown in DMEM with 4.5 g/L glucose, supplemented with 10 mM HEPES 7.4, 10 mM L-glutamine and 10% (v/v) heat inactivated fetal calf serum. C1R cells were propagated in RPMI 1640 supplemented with 10 mM HEPES 7.4, 10 mM L-glutamine, and 10% (v/v) heat inactivated fetal calf serum. All three cell lines could be maintained on media with 5% serum to reduce proliferation with no observed difference in surface expression of transfected molecules. All cell lines were maintained in a humidified incubator at 37°C in the presence of 5% CO<sub>2</sub>. B78H1 cells used in experiments at reduced temperatures were grown and maintained as above. However 16 hours prior to analyses, sufficient numbers of cells for experiments were sealed in flasks with gas impermeable caps and transferred to Styrofoam containers at 25°C.

### **FACS Analysis and Preparative Sorting**

Surface expression of Qa-1<sup>b</sup> was monitored by staining with anti-Qa-1 monoclonal antibody 6A8.6F10 (BD Biosciences) in either purified or commercially biotinylated form.

Mouse Fcγ-specific fluorochrome-coupled secondary reagents were obtained from Jackson Labs. For analytical FACS assays,  $1 \times 10^6$  live cells per sample were incubated with 0.5 μg primary antibody for 30 minutes on ice, washed once in FACS buffer (1X PBS with 5% newborn calf serum, 0.02% (w/v) sodium azide, and 1 mM EDTA), then counterstained with 0.5 μg secondary, again for 30 minutes on ice. All analyses were performed on a FACSCalibur analyzer after the addition of 7-amino-actinomycin D (7-AAD). Sorting of cells was carried out on a Vantage sorter by R. Lee Blosser or Ada Tam, except for the initial sortings of the B78H1 clones, which were performed by Robert Wersto at the NIAID using a MoFlo instrument. For preparative sorting,  $5 \times 10^6$  cells were stained appropriately, resuspended in azide-free FACS buffer with 250 ng/ml 7-AAD and sorted into complete media augmented with 50 μg/ml each kanamycin, streptomycin, carbenicillin, and gentamicin. Antibiotics were removed following 14 days of uncontaminated culture. In cases where single cell cloning was performed, individual high expressing cells were sorted into 96-well plates at one cell per well. Bulk sorting was performed on all samples with the selected population representing the 1% highest Qa-1 expressing live cells as determined by the absence of 7-AAD staining. Typical bulk post-sort cultures began with 15-20,000 individual cells per clone. Post-sort analysis of select samples indicated over 80% viability.

### **Western Blot Analysis**

Live cells were collected by Ficoll-Paque or by gentle washing of adherent cell lines with HBSS prior to lifting with HBSS/5 mM EDTA. Cells were washed three times in 1X PBS to remove serum and phenol red, then lysed in RIPA buffer (50 mM Tris pH 7.4, 154 mM NaCl, 1 mM EDTA, 1% (v/v) NP-40, 0.5% (w/v) sodium deoxycholate, 0.1% (w/v) sodium dodecyl sulfate) with 10 U/ml Benzonase (Novagen) and 1X Sigma mammalian Protease Inhibitor Cocktail, at an approximate concentration of  $1 \times 10^7$  cells/ml. Nuclei and

insoluble material were removed by sequential centrifugation, first at 5,000xg, then 13,000xg. The clarified supernatant was assayed for protein content by bicinchoninic acid (Pierce) as recommended by the manufacturer. Commercial preparations of bovine serum albumin were used as standards following dilution in the lysis buffer. All samples were assayed in triplicate and absorption at 560 nm for each sample was used to determine the protein concentration of each sample. 5 µg of total protein was loaded on 4-12% NuPAGE Bis-Tris precast gels (Invitrogen) and separated using MOPS running buffer, prior to transfer to PVDF. In all cases anti-Qa-1 mAb 6A8.6F10 was used as a primary detection reagent at 250 ng/ml in 1X TBS/5% non-fat dry milk. As loading controls, identical blots were generated and probed with anti-β-actin mAb AC-74 (Sigma-Aldrich), used at 100-200 ng/ml. Appropriately exposed films, following ECL development (GE Healthcare), were digitized by scanning and relative band intensities were determined using ImageJ software ([rsbweb.nih.gov/ij/](http://rsbweb.nih.gov/ij/)).

### **Preparation of 6A8.6F10 and Pre-Clearing Resins**

1 gram of cyanogen bromide activated Sepharose 4B (Sigma Aldrich) was activated by washing with 400 ml 1 mM HCl, then equilibrated with 200 ml Coupling Buffer (100 mM NaHCO<sub>3</sub>, 500 mM NaCl, pH 8.3) in an acid washed sintered glass filter. 1 milligram of purified 6A8.6F10 was directly coupled to the activated resin in 10 ml Coupling Buffer for 16 hours at 4°C, followed by two washes in 20 column volumes Amine Blocking Buffer (50 mM ethanolamine, 150 mM NaCl, pH 8.3), and blocked in the same buffer for four hours at 4°C. The coupled resin was washed extensively in 1X TBS and stored in TBS + 0.005% (w/v) thimerosal as a preservative. Control resin was prepared by directly blocking activated and equilibrated resin. No difference in purity of final samples was observed when MOPC-21 IgG<sub>1b</sub> isotype control mAb was used in preparation of pre-clearing resin.

## Metabolic Labeling, Pulse-Chase Analysis

Cells were seeded at 50% confluency (B78H1/LMTk) or at  $5 \times 10^5$  cells/ml (C1R) 16 hours before pulse chase experiments. In the case of B78H1 cells, cells were simultaneously incubated with  $5 \mu\text{M}$  QDM where appropriate and placed at room temperature. Cells were harvested and washed extensively in HBSS to remove serum, then starved for 60 minutes in Cys<sup>-</sup>/Met<sup>-</sup> DMEM (Invitrogen) supplemented with 5% dialyzed calf serum,  $10 \text{ mM}$  HEPES pH 7.4 buffer, and  $10 \text{ mM}$  L-Glutamine. Cells were then washed twice in HBSS and counted prior to being resuspended at  $5 \times 10^6$  cells/ml in Cys<sup>-</sup>/Met<sup>-</sup> DMEM, 5% Dialyzed Calf Serum, and  $1 \text{ mCi/ml}$   $^{35}\text{S}$  Express Labeling Mix (Perkin Elmer) for 30 minutes. Labeling was stopped by the addition of 10 volumes cold complete media. Cells were washed twice more in ice cold media and cultured at  $37^\circ\text{C}$  for the indicated times at a density of  $1 \times 10^6$  cells/ml. At each time point, harvested cells were washed with ice cold 1X TBS before being lysed in 1 ml RIPA buffer supplemented with Benzonase and Sigma Protease Inhibitor Cocktail. Nuclei and other insoluble material were removed by centrifugation as already described, and the clarified supernatant was then pre-cleared with  $50 \mu\text{l}$  ethanolamine coupled resin. Following collection of all samples, the pre-cleared supernatant was then nutated 2-16 hours with  $20 \mu\text{l}$  6A8.6F10 resin at  $4^\circ$ . Beads were washed four times with RIPA buffer, with 10 minutes of nutation between each wash. The resin was collected by gentle centrifugation ( $2,000 \times g$ ) to prevent non-specific trapping of proteins within the pores of the resin. Fully washed beads were resuspended in  $50 \mu\text{l}$  denaturing buffer ( $0.5\%$  (w/v) SDS,  $40 \text{ mM}$  DTT) and captive proteins were released by heating samples to  $95^\circ\text{C}$  for 10 minutes. Enzymatic digest of samples with EndoH<sub>f</sub> and PNGase F (New England Biolabs) were carried out with 5 U enzyme per sample for 1 hour at  $37^\circ\text{C}$  according to the manufacturer's instructions and terminated by the addition of  $\frac{1}{4}$  volume 6X Laemmli buffer

and heating at 95°C for 5 minutes. All samples were analyzed on 4-12% NuPAGE Bis-Tris or 7% NuPAGE Tris Acetate gels with the appropriate running buffer. Gels were fixed for 1 hour in 10% (w/v) trichloroacetic acid/40% (v/v) methanol, washed in distilled H<sub>2</sub>O and dehydrated in three sequential 30 minute soaks of neat dimethyl sulfoxide prior to equilibration in PPO (2,5-diphenyloxazole, Sigma Aldrich) saturated DMSO. Excess PPO and DMSO were removed by washing in running H<sub>2</sub>O for 3 to 5 hours prior to drying the gels under vacuum. Dried gels were exposed to Kodak BioMax MR film without an intensifying screen for maximum resolution. Digitization and data processing were as with Western blots. The half-life of each molecule was determined by solving for the decay constant  $\lambda$  using the standard exponential decay equation  $A_t = A_0 e^{-\lambda t}$  where  $A_t$  is the quantity at time  $t$ , and  $A_0$  is the quantity at the starting point,  $t=0$ . Average decay constants and standard deviations were determined in Microsoft Excel by solving the equation  $\lambda = (-\ln(A_t/A_0))/t$ . Half-life was determined by using the average decay constant value in the equation  $t = -\ln(0.5)/\lambda$ .

### **Figure 3.1 Comparison of MHC Ia and Qa-1 sequences surrounding cysteine 134**

Multiple alignment of several murine Ia molecules with the human and rat homologues to Qa-1 alleles reveals that only the rodent proteins encode a cysteine at position 134, which corresponds to amino acid 135 in H2-K<sup>b</sup> (**A**). This residue, typically an aspartic or glutamic acid, is highlighted in the structure of K<sup>b</sup> (1KPV), along with surrounding residues and the canonical  $\alpha 2$  disulphide bond (**B**). Glutamine 135 is depicted in red and identified by the blue arrow, while surrounding residues are colored according to element type, cyan for carbon, red for oxygen, blue for nitrogen and sulfur in yellow. The unpaired cysteine in K<sup>b</sup> is also rendered.

A

	120	130	140	150	160	170
H2-Kb	HTIQVTS	GCEVGS	DGRLLRGY	QYAYDGC	DYIALNEDLKTWTAAD	MAALITKHKWEQA
H2-Db	HTLQQMS	GCDLGS	DWRLLRGY	LOFAYEGRDY	IALNEDLKTWTAAD	MAAQITRRKWEQS
H2-Ld	HTLQWMY	GCDVGS	DGRLLRGY	EQFAYDGC	DYIALNEDLKTWTAAD	MAAQITRRKWEQA
HLA-E	HTLQWMH	GCELGPD	RRFLRGY	EQFAYDGKDY	LTNEDLRSWTAVD	TAAQISEQKSNDA
RT-BM1	HTLQWMY	GCDVGP	DGHLLRGY	COEAYDGRDY	ISLNEDLRSWTATD	MASQASKIKSEEV
Qa-1a	HTLQWMY	GCDVGP	DGRLLRGY	COEAYDQQDY	ISLNEDLRSWTATD	FAAQISKHKSEMV
Qa-1b	HTLQWMY	GCDVGP	DGRLLRGY	COEAYDQQDY	ISLNEDLRSWTAND	IASQISKHKSEAV
Qa-1c	HTLQWMY	GCDMGP	DGRLLRGY	COEAYDQQDY	ISLNEDLRSWTAND	IASQISKHKSEAV
Qa-1d	HTLQWMY	GCDVGP	DGRLLRGY	COEAYDQQDY	ISLNEDLRSWTAND	IASQISKHKSEAI



B

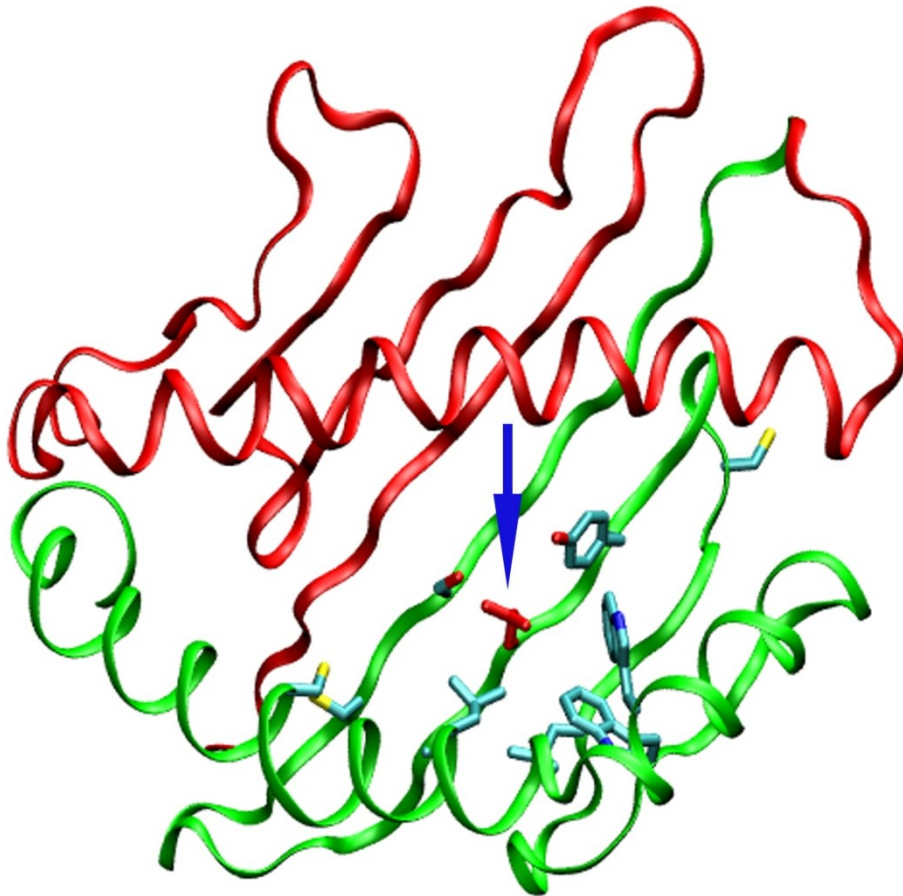


### Figure 3.2 Surface expression of Qa-1<sup>b</sup> wild type and C134 mutants in L cells

The murine fibroblast cell line L(M)Tk<sup>-</sup> was transiently transfected with CMV-driven expression plasmids encoding wild type or mutant versions of either full-length or  $\beta_2m$ -(G<sub>4</sub>S)<sub>3</sub>-Qa-1<sup>b</sup> single chain chimeras. A CMV-driven Green Fluorescent Protein (GFP) construct was used to assess transfection efficiency. Mutation of cysteine 134 to serine resulted in a slight yet reproducible increase in mean surface expression of both constructs. Mutation of the same residue to glutamic acid, the most common amino acid at this position in murine MHC Ia molecules, reduced surface expression compared to wild type. The mean fluorescence intensity for each sample is indicated in the panel.

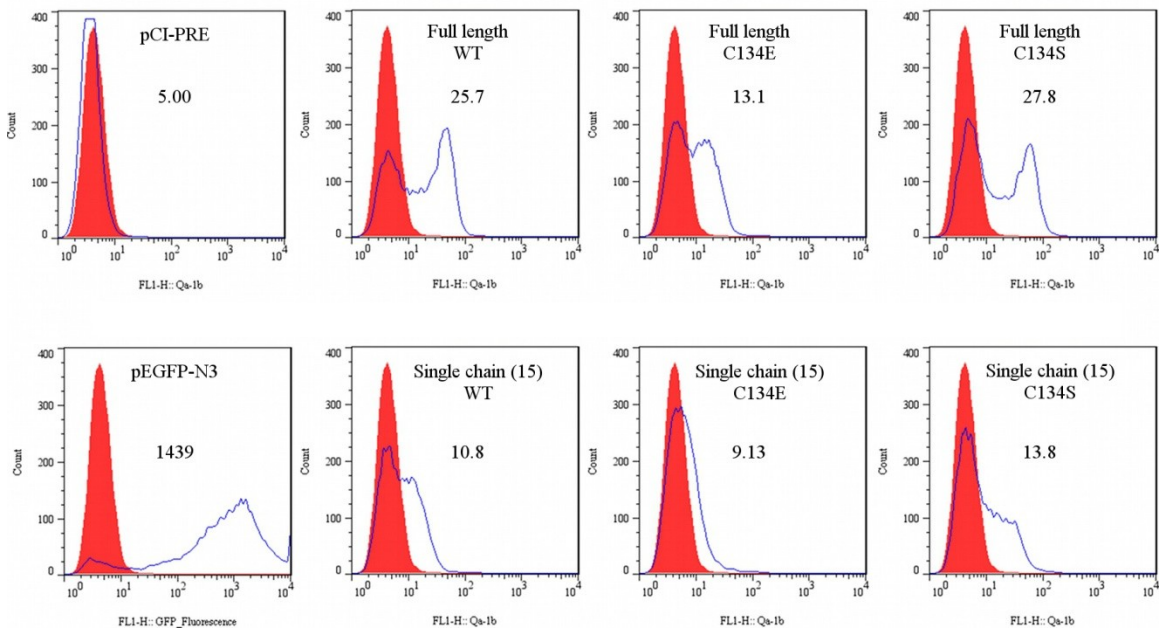




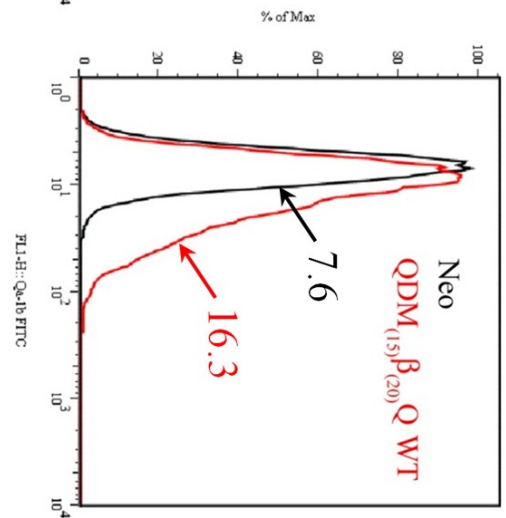
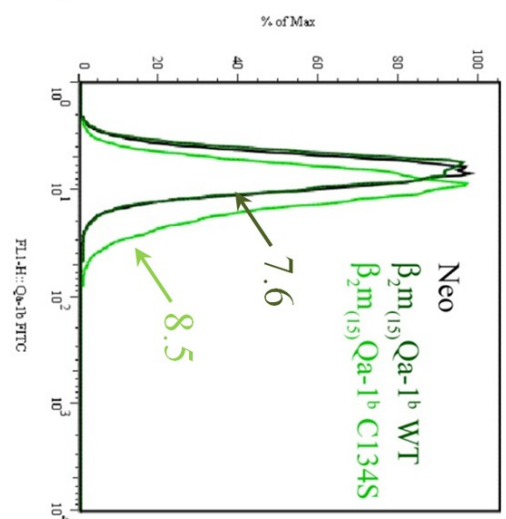
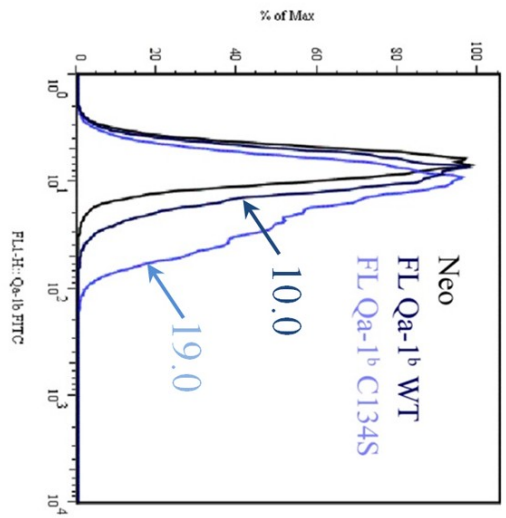
### **Figure 3.3 Temperature dependence of Qa-1 surface expression**

Stably transfected B78H1 cells were assayed by FACS either directly from culture at 37° C

(**A**) or incubated for 16 hours at 25° C (**B**) prior to analysis. The mean fluorescence intensity

is shown in each panel.

A. 37°C



B. 25°C

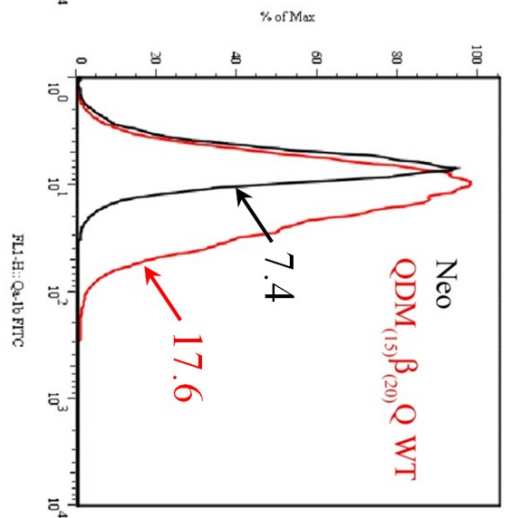
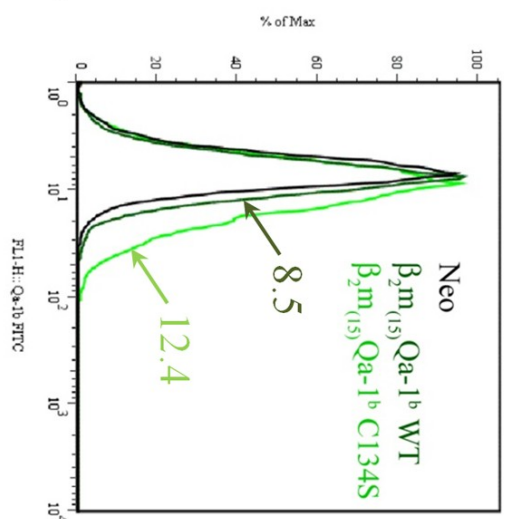
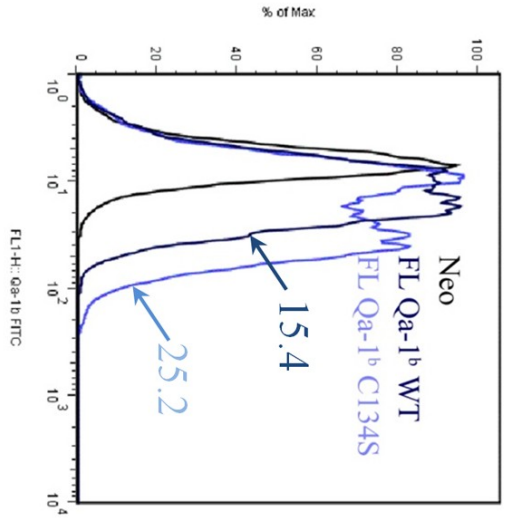


**Figure 3.4 Stable expression of Qa-1<sup>b</sup> constructs in B78H1 cells**

Stably transfected and sorted B78H1 cells were analyzed for Qa-1<sup>b</sup> expression by Western analysis of total protein lysate. More rapidly migrating, immature high mannose species are marked with a red arrow. For both the full length and the  $\beta_2m-(G_4S)_3$ -Qa-1<sup>b</sup> chimeras, little fully glycosylated, mature protein (blue arrows) can be observed unless C134 is mutated to serine. By contrast, the majority of the QDM- $(G_4S)_3$ - $\beta_2m-(G_4S)_4$ -Qa-1<sup>b</sup> chimera is fully mature.

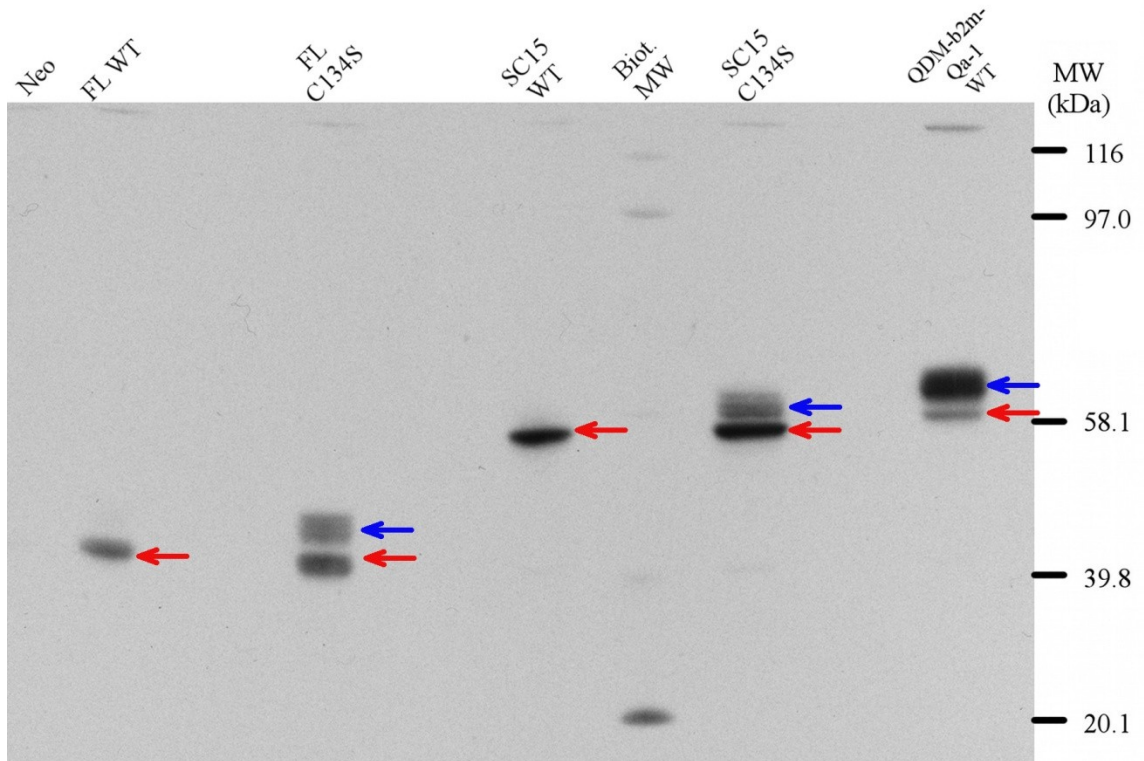


### **Figure 3.5 Relative Maturation of B78HI Expressed Qa-1<sup>b</sup> Constructs**

B78H1 transfectants were temperature shifted and pulsed with QDM peptide prior to preparation of post-nuclear lysates. Treatment with endoglycosidases and comparison with untreated sample facilitates identification of mature protein. By Western analysis, in both the full length and single chain chimeras, the C134S mutation enhances the amount of mature protein compared to wild type. Surprisingly, the vast majority of the QDM-containing chimera is fully glycosylated, despite the presence of the native unpaired cysteine in this construct.

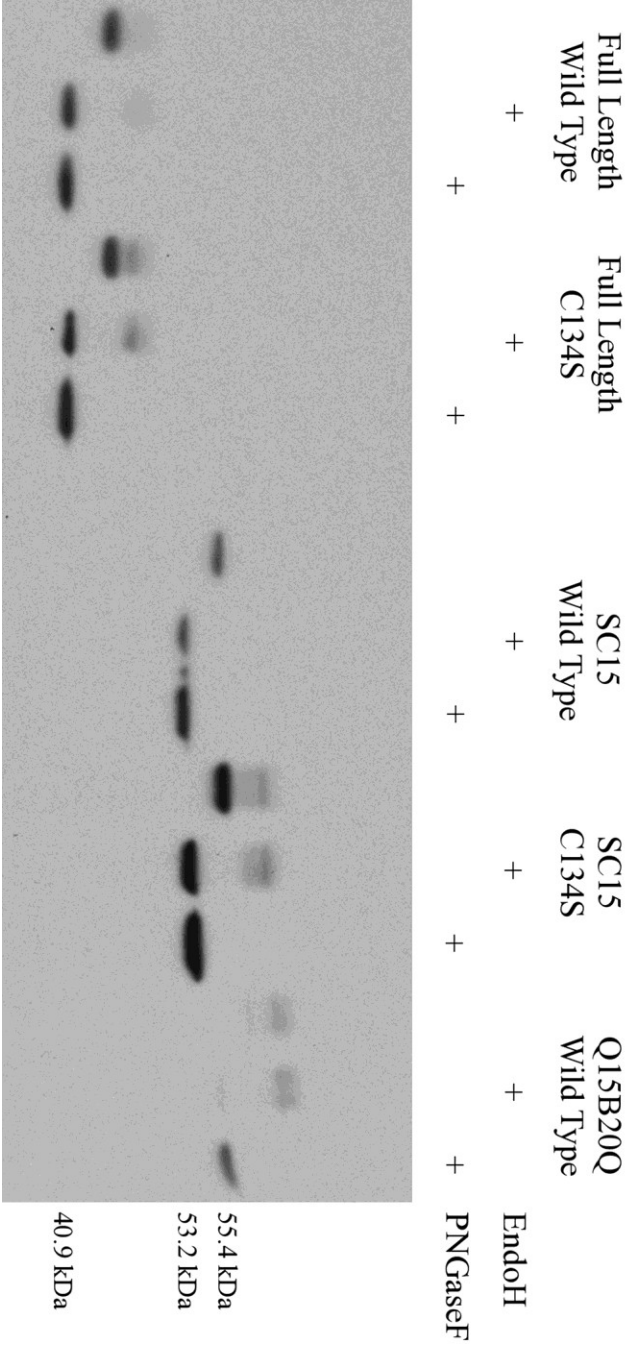


### **Figure 3.6 Qa-1<sup>b</sup> maturation in C57Bl/6 and H2-K/D<sup>-/-</sup> splenocytes**

The maturation velocity and half-life of natively translated Qa-1<sup>b</sup> was measured in *b* haplotype mice lacking H2-L and a directed congenic strain lacking all MHC Ia. The approximate half-life of Qa-1<sup>b</sup> in wild type splenocytes is 38 and 69 minutes for the EndoH sensitive and resistant species, respectively as determined by densitometry. In splenocytes from mice lacking all MHC Ia molecules, the half-life is increased to 279 and 292 minutes (EndoH sensitive and resistant) due to slower turnover of molecules retained in the ER. Although the latter mice lack an endogenous source of QDM, a small fraction of Qa-1<sup>b</sup> molecules do acquire peptides of sufficient affinity to allow egress, maturation, and subsequent presentation on the surface. Due to the low level of expression driven by the native murine Qa-1 promoter, reduced chase times had to be employed compared to experimental stable transfectants which express superphysiological levels of Qa-1<sup>b</sup> under the control of a viral promoter.

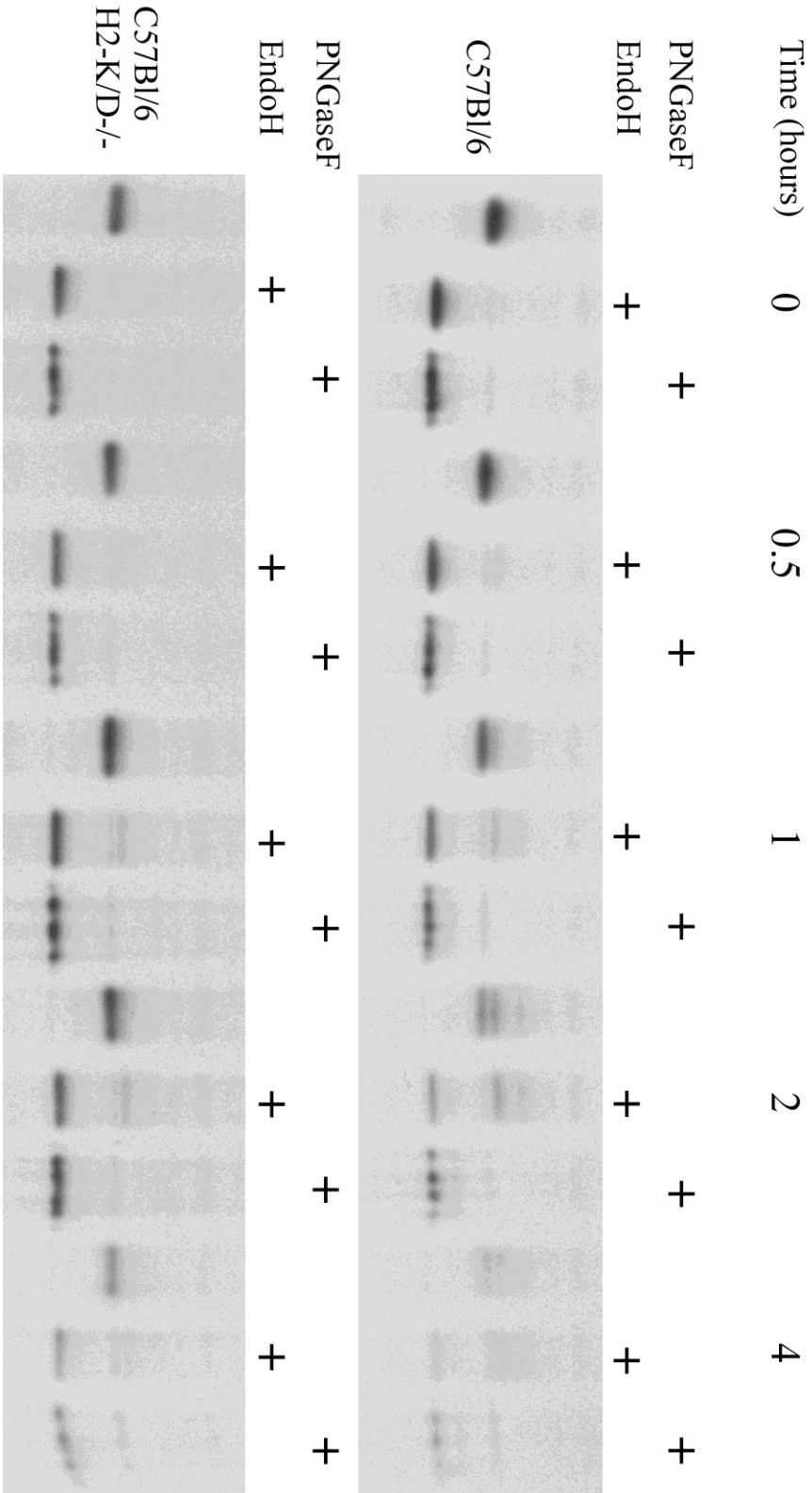


### **Figure 3.7 Co-expression of H2-L<sup>d</sup> as a source of QDM in C1R cells**

C1R cells were stably transfected with an H2-L<sup>d</sup> expression vector (**A**) and single cell cloned to generate a derivative cell line with uniform H2-L<sup>d</sup> surface expression. Clone 6C7 or the parental line were then transfected with full length and chimeric wild type and mutant Qa-1<sup>b</sup> constructs using a plasmid conferring neomycin resistance. Pooled neomycin resistant cells were analyzed for surface expression of both H2-L<sup>d</sup> and Qa-1<sup>b</sup> (**B**). Qa-1<sup>b</sup> transfectants display uniform levels of H2-L<sup>d</sup> expression in each doubly transfected cell line. The Qa-1<sup>b</sup> surface expression in the pool of neomycin resistant cells is highly variable. C1R/L<sup>d</sup> lines are indicated with dashed traces, while the parental C1R transfectants have solid lines.



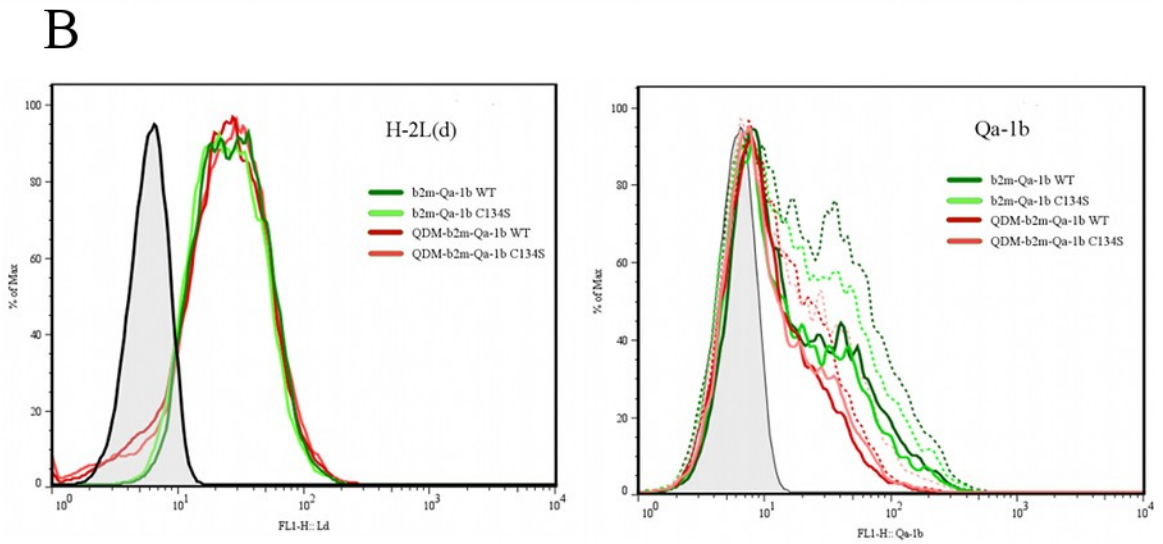
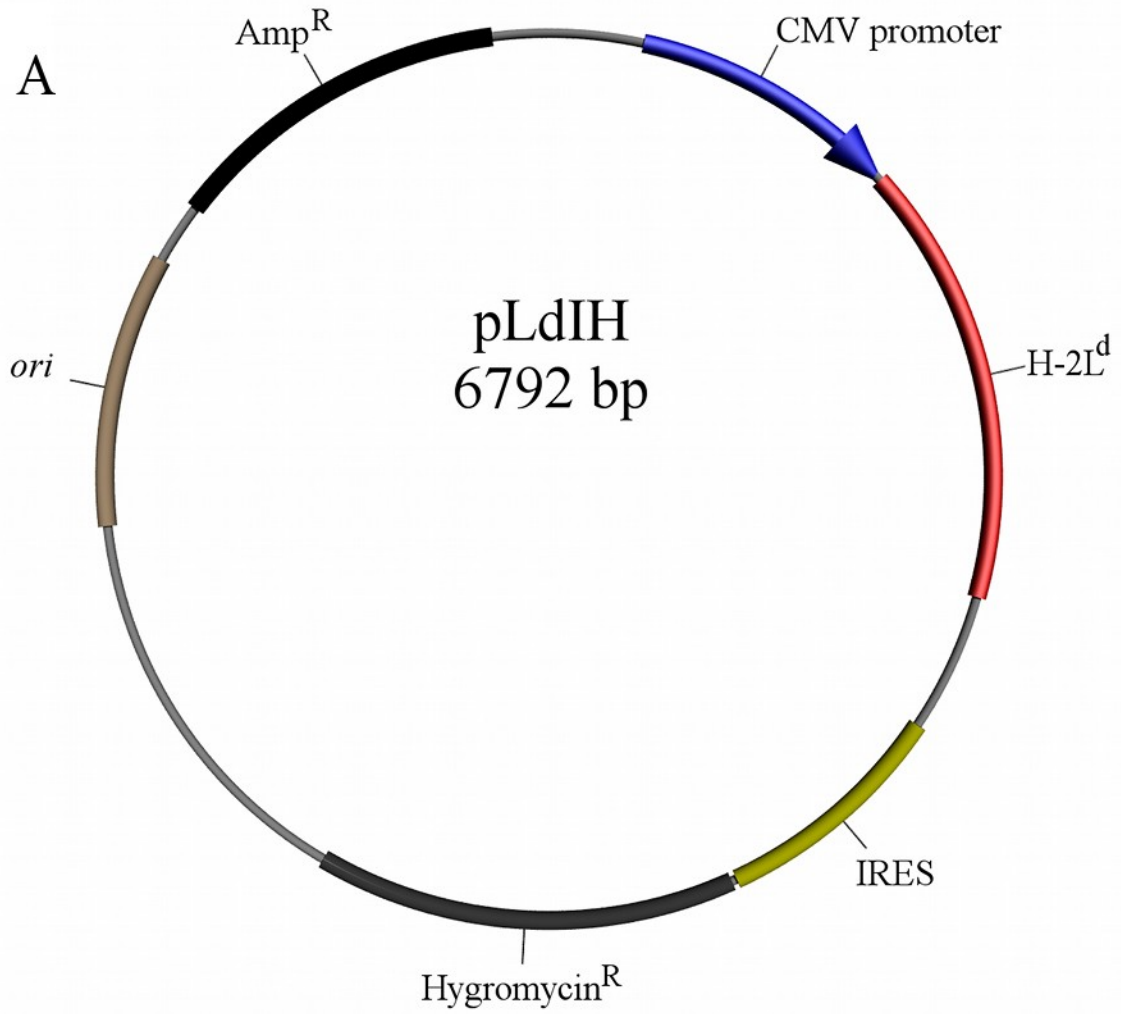
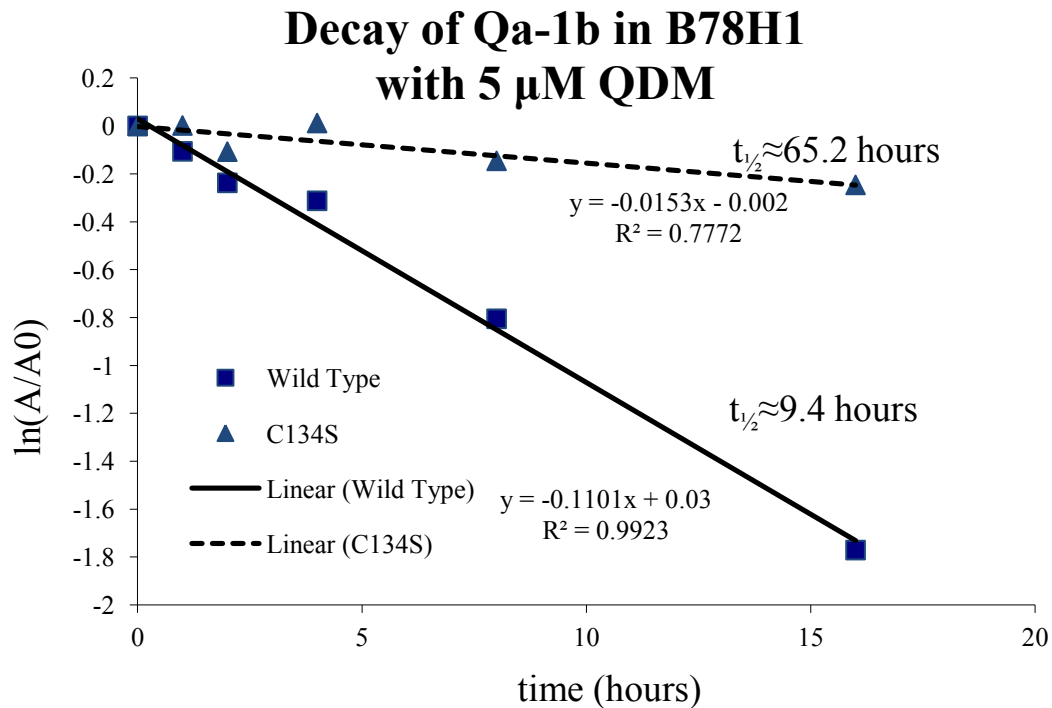


### Figure 3.8 Maturation and turnover of Qa-1<sup>b</sup> in B78H1 cells

B78H1 cells transfected with either full length Qa-1<sup>b</sup> or the C134S mutant were metabolically labeled with <sup>35</sup>S cysteine/methionine for 30 minutes then chased in complete media for 0,1, 2, 4, 8 or 16 hours at 25°C. Endoglycosidase treated samples were analyzed by autoradiography and densitometry. Half the wild type molecule converted to an EndoH resistant species in 9.2 hours. However, the C134S mutant proceeded through the maturation pathway 2.5 times faster (3.7 hours). The more rapidly maturing molecule also persisted approximately 7 times longer than the wild type, which turned decays with a half-life of 9.4 hours. The wild type molecule does not efficiently exit the ER and therefore remains in the immature high mannose form. By contrast, the mutant rapidly egresses to the cell surface and persists for an extended period of time. Due to it's surprising longevity, the half-life of the full length C134S molecule had to be calculated by regression.



### **3.9 Maturation and stability of Qa-1<sup>b</sup> in C1R cells**

Two stable transfectants of Qa-1<sup>b</sup> in C1R cells were assessed by pulse-chase metabolic labeling and endoglycosidase treatment. Only a very small fraction of the Qa-1<sup>b</sup> molecules mature into an EndoH resistant species in cells lacking the cognate peptide. These cell lines which only differ in the expression of H-2L<sup>d</sup> exemplify the requirement for QDM peptide.

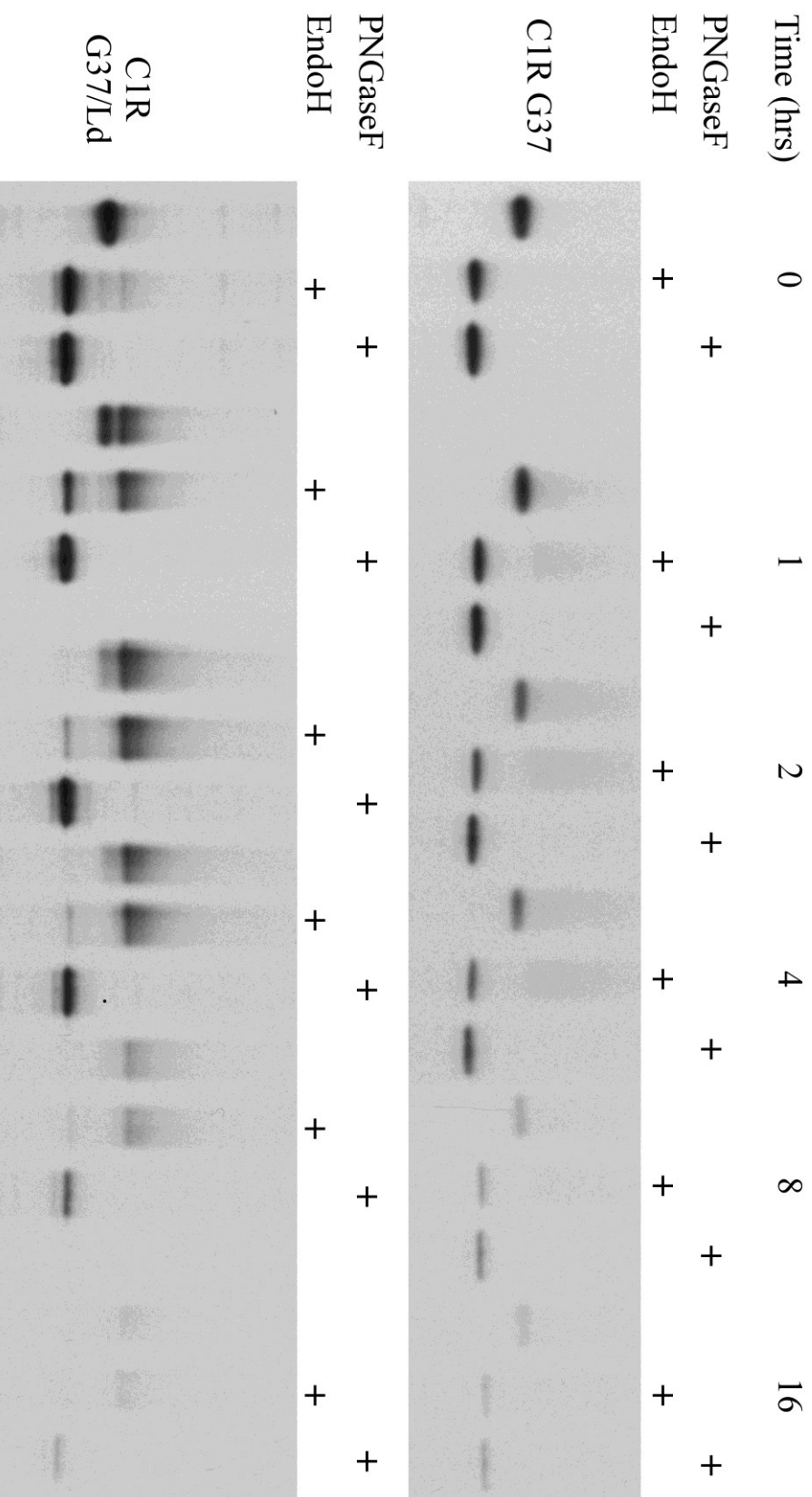


### Figure 3.10 Comparison of the Qa-1<sup>b</sup> and H-2K<sup>b</sup> structures

The deposited structures of Qa-1<sup>b</sup>/QDM (PDB ID 3VJ6) and H-2K<sup>b</sup>/HSV glycoprotein B peptide (PDB ID 1RJY) were compared. The atomic resolution structures were re-oriented to minimize differences between heavy chain backbone atoms using STAMP [89] and rendered using the VMD software package. The  $\alpha 1$  and  $\alpha 2$  domains were rendered as red and green cartoons, respectively, while all heavy chain protein atoms within 5Å of the peptide were rendered as a diffuse purple mesh. The peptides in each structure are rendered as licorice with black carbon atoms (panels **A** and **B**). In the truncated edge-on view, all interacting side-chains from the MHC molecule are rendered as licorice sticks and all carbon atoms are colored cyan. Finally, to demonstrate the disparity between the solvent exposed surfaces of the peptides bound to each MHC I molecule, the entire molecular envelope was rendered as a solid gray surface surrounding the peptide molecular surface colored according to atom type. The QDM peptide, although it also bound in an extended conformation within the groove, is much less accessible to either NK or TCR  $\alpha\beta$  receptors.

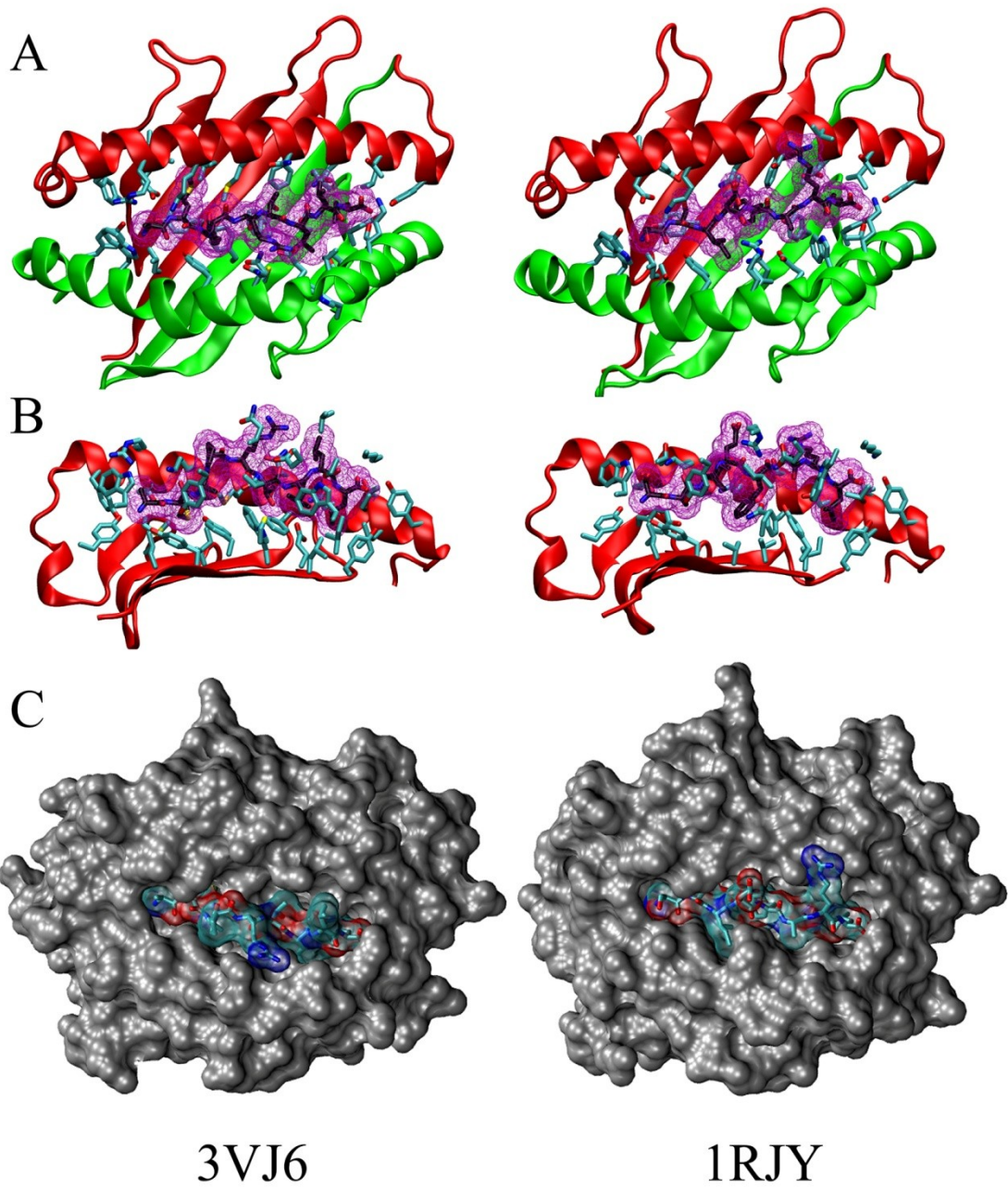


**Figure 3.11 Stereo representation of the Qa-1<sup>b</sup> P7 peptide binding cleft**

The peptide binding cleft of Qa-1<sup>b</sup> and the P7 peptide leucine are rendered in side-by-side stereo. The molecular envelope of the protein is shown as a transparent surface over the cartoon rendering of the  $\alpha 1$  (red) and  $\alpha 2$  (green) heavy chain domains, with the bound peptide displayed as a licorice model with carbon atoms colored in black. Heavy chain residues located within 3.5Å of the peptide are also rendered as licorice bonds, but with cyan carbon atoms. Cysteine 134 lines an edge of the deep peptide pocket which is only partially filled by the side-chain of QDM P7 leucine. The sulfhydryl moiety points directly away from the  $\beta$ -strand platform.

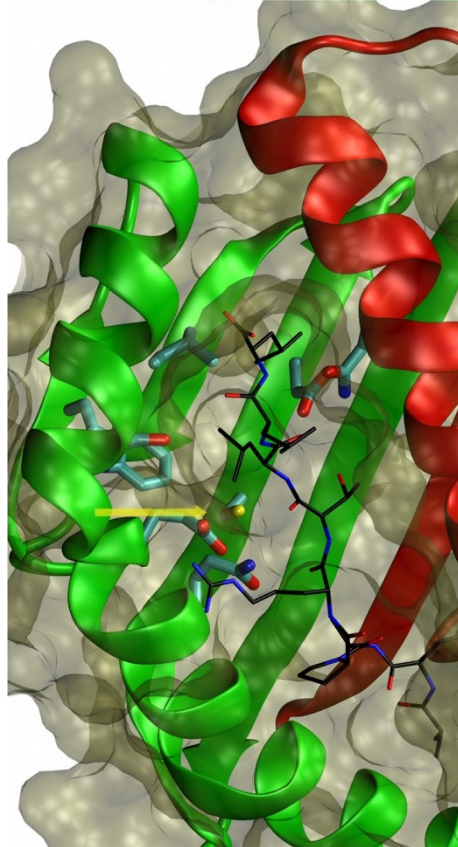
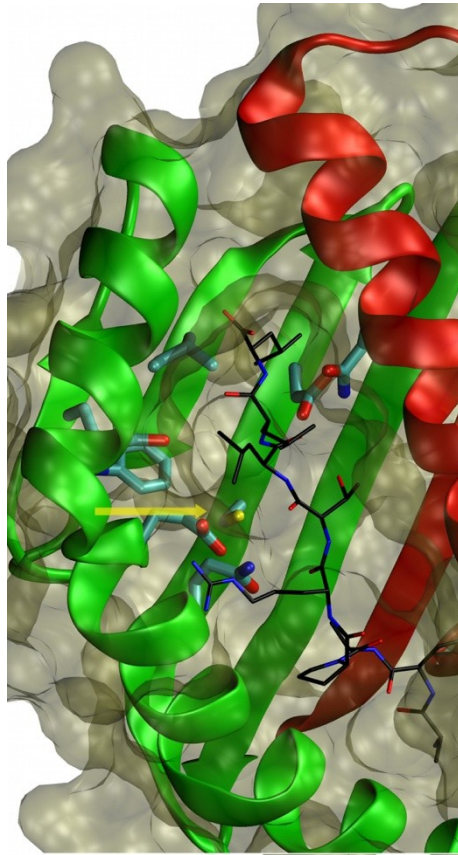




**Table 2. Maturation and Half-Life of Qa-1<sup>b</sup> is enhanced by the C134S mutation**

Analysis of several pulse chase experiments reveals the distinct difference between the wild type Qa-1<sup>b</sup> molecule and the C134S point mutant. In the absence of the C134S mutation, the rate limiting factor affecting both the maturation and turnover of Qa-1<sup>b</sup> is the availability of the QDM peptide. In the absence of QDM, the majority of Qa-1<sup>b</sup> molecules are retained in the ER and turn over more slowly than molecules which fully mature and are expressed on the cell surface.

	Maturation <sup>1</sup> (hours)	Half-Life (hours)
<b>Murine splenocytes</b>		
C57BL/6	0.6	1.2
H2-K/D-/-	4.7	4.9
<b>B78H1 (25°C)</b>		
FL WT	9.2	9.4
FL C134S	3.7	65.2 <sup>2</sup>
<b>C1R</b>		
G37	6.6	8.4
G37/L <sup>d</sup>	2.7	9.0
FL WT	2.9	7.7
FL WT/Ld	0.6	2.3
FL C134S	1.3	6.0
FL C134S/Ld	0.6	11.2
<b>Previously Published Results<sup>3</sup></b>		
C57BL/6	n/a	2.58 <sup>4</sup>
T2 cells	n/a	0.77 <sup>4</sup>
J1 cells	n/a	1.58 <sup>4</sup>
<i>In vitro</i>	n/a	1.62 <sup>5</sup>

<sup>1</sup>Time to loss of 50% of the EndoH sensitive species.

<sup>2</sup>Extrapolated, but not observed during 16 hour chase.

<sup>3</sup>From Kambayashi *et al.* [54].

<sup>4</sup>Measured by Brefeldin A blockade of ER egress and FACS analysis.

<sup>5</sup>Measured by indirect ELISA of biotinylated-QDM complexes

## **Chapter 4**

### **Biological Significance of the C134S Mutation**

## **Introduction**

Following the identification of Cys134 as a determinant of Qa-1<sup>b</sup>/QDM instability, we wondered if the single substitution of serine for this unpaired cysteine would also have an effect on the recognition of the mutant pMHC by immune receptors. As Qa-1 molecules function in bridging the innate and adaptive immune systems, they play a critical role in central immunity. Two parallel approaches were used to quantitatively measure the effects of a serine substitution for the unpaired cysteine at position 134. The first experimental approach was to determine the altered maturation rate and half-life of the mutant molecules compared to the wild type Qa-1<sup>b</sup> constructs using metabolic labeling of transfected cells. The second series of experiments, detailed here, were designed to ascertain whether the mutant molecule is recognized similarly to the wild type molecule by cytotoxic T cell receptors and the lectin-like NKG2/CD94 receptors. It was proposed that these experiments would address, in as quantifiable a manner as possible, the disparity between the wild type and the single amino acid substitution mutant as it affects immunological surveillance mechanisms.

## **Biological Significance of the C134S Mutation**

The first quantitative approach to discern any differences between the wild type and mutant molecules was to use two CD8<sup>+</sup> alloreactive CTL clones. These two clones, designated 39.1D7X and 5D2-T, were generated in the Qa-1<sup>a</sup> background and represent two distinct modes of Qa-1<sup>b</sup> mediated recognition [90]. The first clone, 39.1D7X, recognizes Qa-1<sup>b</sup> pMHC and does not specifically require QDM as the bound peptide, while clone 5D2-T is restricted to both Qa-1<sup>b</sup> and the QDM peptide (or the QDM<sup>k</sup> variant) for effective targeting [91]. By using these two CTL clones, we were confident that both gross structural

changes as well as subtle perturbations in the presentation of the peptide could be deduced. Furthermore, the biological significance of chimeric constructs with the extended tether between  $\beta_2m$  and Qa-1<sup>b</sup>, as well as the trimeric construct, which includes QDM in cis, could also be assessed.

## Results and Discussion

CTL assays were essentially performed as first described in 1968 by Brunner et al. [92], loading target cells with <sup>51</sup>Cr (as sodium chromate) and assessing specific lysis at several different effector to target ratios. The initial experiments were designed to evaluate any differences between the surface expressed wild type and C134S mutant. C1R transfectants, including the G37 and G37/L<sup>d</sup> lines, were used as targets in 39.1D7X CTL assays. Consistent with the previously described QDM-independent alloreactivity of this CD8<sup>+</sup> clone, all targets with the exception of the empty vector control were lysed in an Effector:Target ratio dependent manner (**Figure 4.1 A**). In addition to the full-length constructs, both chimeras fusing either just  $\beta_2m$ , or both QDM and  $\beta_2m$ , to the Qa-1<sup>b</sup> heavy chain proved to be suitable targets for 39.1D7X cells. Unexpectedly, however, in all cases the C134S mutation resulted in a puzzling reduction in specific lysis compared to the same wild type construct. The addition of QDM by using H2-L<sup>d</sup> co-transfected targets (**Figure 4.1 B**) further diminished the specific lysis of target cells, although no similar reduction was seen for the G37 and G37/L<sup>d</sup> control cell lines.. This was an unexpected outcome, as the surface expression levels as assessed by 6A8.6F10 staining correlate nearly inversely with the CTL activity observed here. The highest surface expressing constructs with the longest half-lives surprisingly made poorer targets for the 39.1D7X effector cells.

Despite this incongruity, it was significantly more interesting to note that all the constructs used up to this point, including those with the C134S mutation, and more importantly those with Gly<sub>4</sub>Ser linkers, did indeed act as ligands for the 39.1D7X TCR. This was an important validation of the overall conservation of the MHC fold despite the various genetic manipulations of Qa-1<sup>b</sup>, therefore all of the constructs were further characterized for the ability to present the QDM peptide using the 5D2-T alloreactive CD8<sup>+</sup> clone. These experiments, we hoped, would either confirm or refute the hypothesis that the mutant molecule presents QDM in a manner indistinguishable from the wild type. Again using standard <sup>51</sup>Cr release assays, all of the cell lines generated were assessed as targets. The rationale behind using all of the cell lines was that no individual line represented an adequate mimic for the *in vivo* expression of Qa-1<sup>b</sup>/QDM complexes for various reasons.

The first set of transfectants generated and characterized biochemically were in the B78H1 cell line, which as previously described lacks critical components of the MHC I biogenesis pathway. Although transfectants generated in this line were extensively characterized by Western analysis and metabolic labeling, we had significant questions regarding the biological significance of these molecules. Using B78H1 target cells and 5D2-T effector T cells, we confirmed that in fact the QDM<sub>15</sub>β<sub>2</sub>m<sub>20</sub>Qa-1<sup>b</sup> construct is well folded and presents the covalently tethered peptide to TCRs. In the absence of QDM peptide added to the culture media, only the QDM<sub>15</sub>β<sub>20</sub>Qa-1<sup>b</sup> construct was effectively lysed (**Figure 4.2A**). As would be expected using these alloreactive T cells, there was little specific lysis observed in the other transfectants, regardless of the presence of a cysteine or serine at position 134. Upon addition of 5μM synthetic QDM peptide to the targets, all Qa-1<sup>b</sup> constructs were recognized and lysed in a ratio dependent manner (**Figure 4.2B**). Unlike the 39.1D7X clone, this peptide and MHC restricted clone did lyse C134S mutant expressing

targets more effectively than the wild type counterparts. Furthermore, the addition of QDM peptide did not significantly alter the specific lysis of the single chain QDM<sub>15</sub>β<sub>20</sub>Qa-1<sup>b</sup> chimera targets, although there was a slight increase in the highest Effector:Target ratio.

Having produced a large number of single cell cloned lines from the C1R lineage, we proceeded to test 5D2-T alloreactivity to both C1R and C1R/H2-L<sup>d</sup> targets. We had proposed that these cells were an ideal expression system to test Qa-1 biogenesis while still allowing regulated production of biogenic QDM peptide. As was observed in the B78H1 transfected clones, only the chimeric construct which include QDM could be effectively targeted by these CTL clones. Somewhat surprisingly, there was a modest but measurable response to the full length C134S mutant as well (**Figure 4.3A**), despite the absence of any QDM. C1R cells do express a small quantity of the human MHC Ib genes HLA-F and HLA-G. While the HLA-F leader peptide does not include a QDM-like sequence, the HLA-G leader does encode VMAPRTLFL in residues 3-11. It is likely that this highly similar peptide is therefore responsible for the specific lysis of the full length C134S mutant, as well as its accelerated maturation as assessed in the metabolic labeling experiments described earlier.

If, however, H2-L<sup>d</sup> is co-expressed with the same Qa-1<sup>b</sup> constructs as a source of leader peptide, the full length and Q<sub>15</sub>β<sub>20</sub>Qa-1<sup>b</sup> chimeras are lysed robustly. Noticeably, the β<sub>20</sub>Qa-1<sup>b</sup> single chain constructs were not able to elicit a robust CTL response (**Figure 4.3B**). This was somewhat surprising, given their expression levels. Further confounding the analysis of this data was the reproducible disparity between the wild type and C134S mutant molecules when QDM is present. We observed once again that the more rapidly maturing, longer half-lived molecule was less effectively targeted by an alloreactive clone. In fact, the single point mutation markedly reduced the lysis of target cells in the presence of

QDM peptide. Given that this observation was reproducible, we wondered if the mutant molecule would also perform less well in CTL assays performed in mouse L(M)Tk<sup>-</sup> cells, which constitutively express QDM<sup>k</sup> but no Qa-1 molecules.

We proceeded to test both the full length Qa-1<sup>b</sup> protein and the Q<sub>15</sub>β<sub>20</sub>Qa-1<sup>b</sup> chimeras with or without the C134S substitution in these cells. Once again, the point mutation led to a decrease in specific lysis, although the difference was much more pronounced in the full length transfectants than those expressing the chimeras (**Figure 4.4A**). Although Lowen *et al.* [91] had reported that 5D2-T could target Qa-1<sup>b+</sup> cells from either QDM or QDM<sup>k</sup> backgrounds, we proceed to test whether the difference between AMVPRTLL (QDM<sup>b</sup>) and AMAPRTLLL could account for the observed differences. The same target cells were pre-incubated for 16 hours with synthetic QDM in their growth media at a concentration of 5 μM. The cells were then washed and used in a CTL assay with 5D2-T effector cells (**Figure 4.4B**). Exogenous QDM, in addition to endogenous QDM<sup>k</sup> peptide relieved what we were beginning to consider C134S suppression of cytotoxicity. The difference between the Q<sub>15</sub>β<sub>20</sub>Qa-1<sup>b</sup> chimeras was diminished in these experiments. In considering possible mechanisms which might explain why higher surface expression levels might cause a reduction in the effective CTL response, we turned our attention to the natural ligands of Qa-1 molecules, the heterodimeric CD94/NKG2 receptors.

While it is obvious that natural killer cells express these receptors, they are also found on a subset of canonical CD8<sup>+</sup> cytotoxic lymphocytes in mice [93-95]. The subset of CD8<sup>+</sup> cells which acquire NKR expression following TCR rearrangement retain the ability to express these receptors in a clonal fashion, although expression is upregulated following antigen challenge. We therefore tested our alloreactive clones for expression of CD94/NKG2A, an inhibitory receptor that could diminish but not ablate activation of CTL



via the TCR. Both T cell clones were harvested ten days after stimulation, purified by isopycnic gradient centrifugation, and immunophenotyped using two commercially available antibodies (**Figure 4.5**). Both clones were unambiguously positive for expression of both CD94 and NKG2A/C/E. The 39.1D7X clone exhibited a cryptic bimodal distribution of both receptor chains which may be the result of either insufficient rest after stimulation or lack of clonality. The only commercially available reagent, rat monoclonal antibody 20D5, that can be used to detect mouse NKG2A also exhibits cross-reactivity with the highly similar NKG2C and NKG2E ectodomains. Serendipitously this antibody has a modest blocking activity against these receptors. We therefore chose it to validate the hypothesis that increased surface expression of Qa-1<sup>b</sup>/QDM complexes blunted an alloreactive response by engaging the ITIM-containing CD94/NKG2A receptors.

Due to the cost of the commercial antibody, a limited CTL assay was performed using both 39.1D7X and 5D2-T effector T cells and C1R cells transfected with both wild type and C134S mutant Q<sub>15</sub>β<sub>20</sub>Qa-1<sup>b</sup> chimeras. An isotype control rat monoclonal antibody was also used in these CTL assays at identical final concentrations of 10 and 30 μg/ml. Both T cell clones were pre-incubated with the appropriate antibody beginning immediately after they were purified by isopycnic sedimentation at twice the indicated concentrations. A modest enhancement of specific lysis is observed in the presence of NKG2A/C/E blockade, although this effect is more pronounced at 10 μg/ml than at 30 μg/ml (**Figure 4.6**). In all cases the C134S mutant chimera is less effectively lysed than the wild type, which is incongruous with its slightly elevated relative surface expression. The fact that increased concentrations of both 20D5 and the control monoclonal antibody resulted in reduced specific lysis is also inexplicable. Even if only pair matched 20D5 and control lysis results are compared, the enhancement in lytic activity is still quite modest. Although well beyond

the scope of this work, the contribution of NK receptors to anti-Qa-1 restricted alloreactivity required further elucidation. This would best be explored by generating new alloreactive clones in either a CD94<sup>-/-</sup> background [96] or selective ablation of NKG2 gene expression.

In the work presented here, a modal explanation has been provided for at least one mechanism leading to the inherent instability of surface expressed Qa-1 molecules. Despite the obvious advantages of pMHC Ia complexes already described here, the innate surveillance of Qa-1/QDM complexes by NK cells must instead rely on transiently stable ligands which are continuously replaced by *de novo* synthesis and surface expression. The ephemeral nature of Qa-1 complexes inherently leads to a continuously refreshed but temporally limited interrogation of MHC Ia synthesis within each cell, essentially a moving window of opportunity. As there is no adaptive mechanism for the generation of NKs, any individual cell in the periphery can adequately survey MHC Ia production and respond appropriately to the loss of Qa-1/QDM complexes. This is in direct contrast to the low probability occurrence of stochastic encounters between a highly diverse pool of CD8<sup>+</sup> CTL and agonist peptides in the context of an appropriate MHC Ia. The probability of the productive encounter of CTL and agonists are significantly enhanced through several mechanisms, e.g. clonal expansion, antigen presenting cell migration to lymphatic tissues, and certainly the secretion of cytokines and chemokines to recruit both professional APC and effector cells to the site of antigen encounter. No similar mechanisms are required when the effector cells are somatically encoded and equally capable of mounting a cytotoxic response.

While it was not possible to elucidate the atomic structure of Qa-1<sup>b</sup>/QDM complexes during these studies, we were able to identify at least one conserved difference

between Qa-1 molecules and other MHC Ia proteins which contributes directly to destabilizing the pMHC surface complexes. The presence of a cysteine residue at position 134 results in the accelerated turn over of Qa-1. This instability can be greatly ameliorated by the semi-conservative substitution of a similar, but more polar and hydrophilic serine. Several mammalian cell lines, each with unique attributes beneficial to these studies, were transfected with various Qa-1<sup>b</sup> constructs and queried to determine the maturation rate, stability and gross structure of the resulting proteins. In all cases, the substitution of serine at residue 134 led to increased surface expression of Qa-1<sup>b</sup> molecules. The maturation of both wild type and mutant molecules is largely dependent on the presence of Qa-1's cognate peptide, QDM, which is derived from the leader peptide of several MHC Ia molecules. Although Qa-1 molecules generated in the absence of QDM have longer half-lives, they are largely retained within the endoplasmic reticulum and are degraded within that organelle. Our proposed model is therefore that Qa-1, perhaps as well as the related rat molecule RT-BM1, are destabilized by the presence of an unpaired cysteine at a position likely to place the sulfhydryl moiety along a deep pocket accommodating the cognate peptide's P2 residue. No similar destabilizing mechanism can be proposed for the human functional homologue of Qa-1, HLA-E. Whether HLA-E/human leader peptide complexes are inherently unstable has not been directly tested, although extensive characterization of the two extant alleles of the human molecule have been performed, including relative surface expression studies and thermal denaturation of *in vitro* assembled pMHC [97]. A more complete understanding of NK surveillance of MHC Ia synthesis would emerge from the application of the biochemical approaches described within our work to both the rat RT-BM1 molecule as well as human HLA-E.



## Materials and Methods

### Growth and Maintenance of CD8<sup>+</sup> T Cells

The CTL lines 5D2-T and 39.1D7X were expanded every ten to fourteen days using irradiated (1500 rads) C57BL6 splenocytes. Following each stimulation period, live T cells were enriched by Lympholyte M (Cedar Lane Laboratories) cushion gradient centrifugation and used immediately in experiments or returned to culture with freshly prepared feeder cells. T cells were grown in RPMI 1640 supplemented with 10 g/L  $\alpha$ -methyl-D-mannopyranoside, 10 mM L-glutamine, 10 mM HEPES, pH 7.4, sodium pyruvate, MEM essential amino acids, MEM non-essential amino acids,  $\beta$ -mercaptoethanol, penicillin/streptomycin/amphotericin B, and 10% (v/v) T-Stim rat splenocyte concanavalin A treated supplement (BD Biosciences).

### <sup>51</sup>Cr release Cytotoxic Lymphocyte Assays

Target cells growing in mid-log phase or fresh splenocytes were harvested and live cells were purified by either Lympholyte M or Ficoll-Paque (GE Healthcare) cushion gradient centrifugation as appropriate. Cells were washed extensively with HBSS to remove any extracellular protein and  $1 \times 10^6$  target cells were resuspended in 100  $\mu$ l additive-free RPMI 1640 supplemented with 10  $\mu$ l fetal calf serum. 0.5-1 mCi [<sup>51</sup>Cr] sodium chromate (Perkin Elmer) was added and cells were incubated for one hour at 37° C to load targets. Excess label was then removed by three washes with complete RPMI 1640 media and the targets were diluted to a final concentration of 100,000 cells per milliliter. 5000 target cells and an appropriate number of effector T cells were mixed in V-bottom 96-well plates and centrifuged at 800xg for 5 minutes prior to being placed at 37° C. Spontaneous <sup>51</sup>Cr release was determined for each target by substitution of media for the T cells, and total release was

determined by adding SDS to a final concentration of 0.5% (w/v). All CTL experiments were conducted in triplicate. After four hours, the plates were again centrifuged and either 50% or 75% of each supernatant was carefully removed and directly quantified by an LKB 1284 Gamma counter. Data were processed in Microsoft Excel to determine percent specific lysis according to the formula:

$$\%specific\ lysis = \left( \frac{Experimental - Spontaneous}{Total - Spontaneous} \right)$$

### **CD94/NKG2(A/C/E) Blocking Experiments**

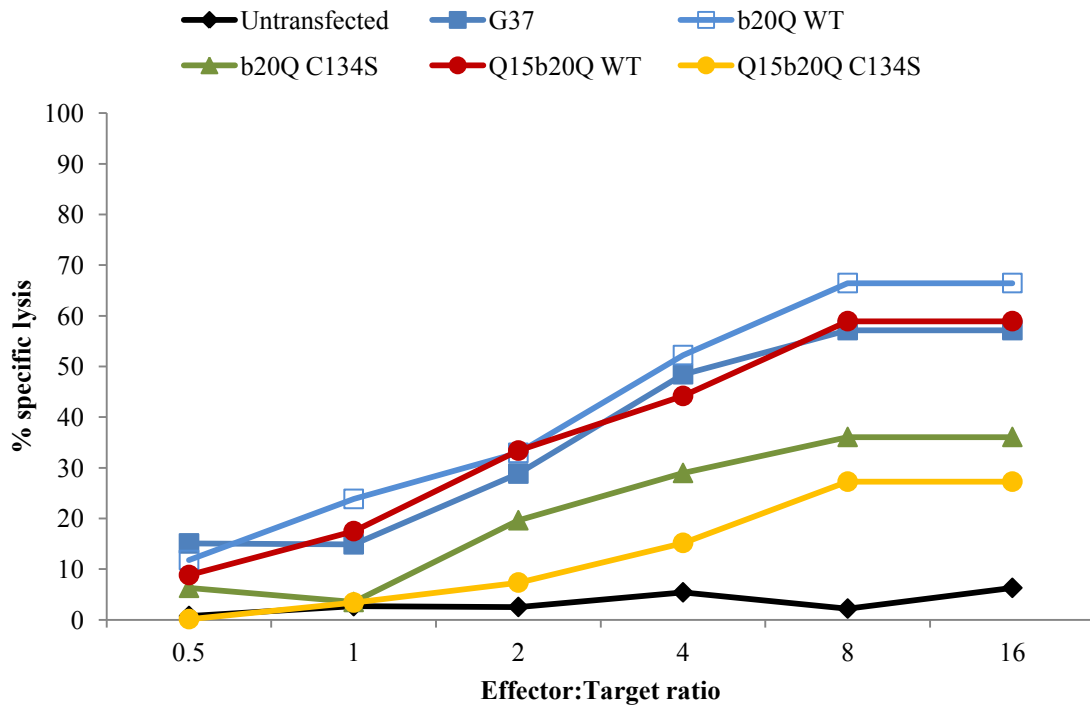
CTL assays were performed as previously described, with the exception of resuspending the effector T cells in media containing either the NKG2(A/C/E) blocking rat monoclonal 20d5 (BD Biosciences) or an isotype control rat monoclonal at 20 or 60 µg/ml. Addition of the effector cells to targets effectively diluted the monoclonal antibodies to final concentrations of 10 and 30 µg/ml, respectively. Prior to use in the CTL assays, each commercial monoclonal preparation was concentrated and buffer exchanged to PBS using a 30 kDa molecular weight cut-off Amicon microcentrifuge concentrator to quantitatively remove all sodium azide from the preparation. The resulting product was quantified by BCA assay (Pierce Biotechnology).

### Figure 4.1 39.1D7X Cytotoxic Lysis of C1R Transfectants

The alloreactive CD8<sup>+</sup> T cell clone 39.1D7X was used to assess differences between surface expressed wild type and C134S mutant Qa-1<sup>b</sup> transfected C1R cells. <sup>51</sup>Cr loaded target cells were incubated with the effector T cells at the indicated ratios in triplicate. As expected all cells expressing the wild type constructs were lysed in a dose dependent manner.

Introduction of the point mutation C134S in all cases resulted in lower specific lysis, despite enhanced surface expression and longer half-life. Furthermore, chimeric constructs which encode either  $\beta_2m$  or QDM and  $\beta_2m$  fused to the Qa-1<sup>b</sup> heavy chain using (Gly<sub>4</sub>Ser)<sub>n</sub> spacers were also efficiently recognized as targets. Unexpectedly, specific lysis appeared to correlate inversely with surface expression of Qa-1<sup>b</sup> molecules, particularly when QDM was expressed in trans by co-transfection with the H2-L<sup>d</sup> MHC Ia molecule (**B**). This suppression was most notable in the QDM- $\beta_2m$ -Qa-1<sup>b</sup> constructs.

## A 39.1D7X Cytotoxic Lysis of C1R Cells



## B 39.1D7X Cytotoxic Lysis of C1R/L<sup>d</sup> Cells

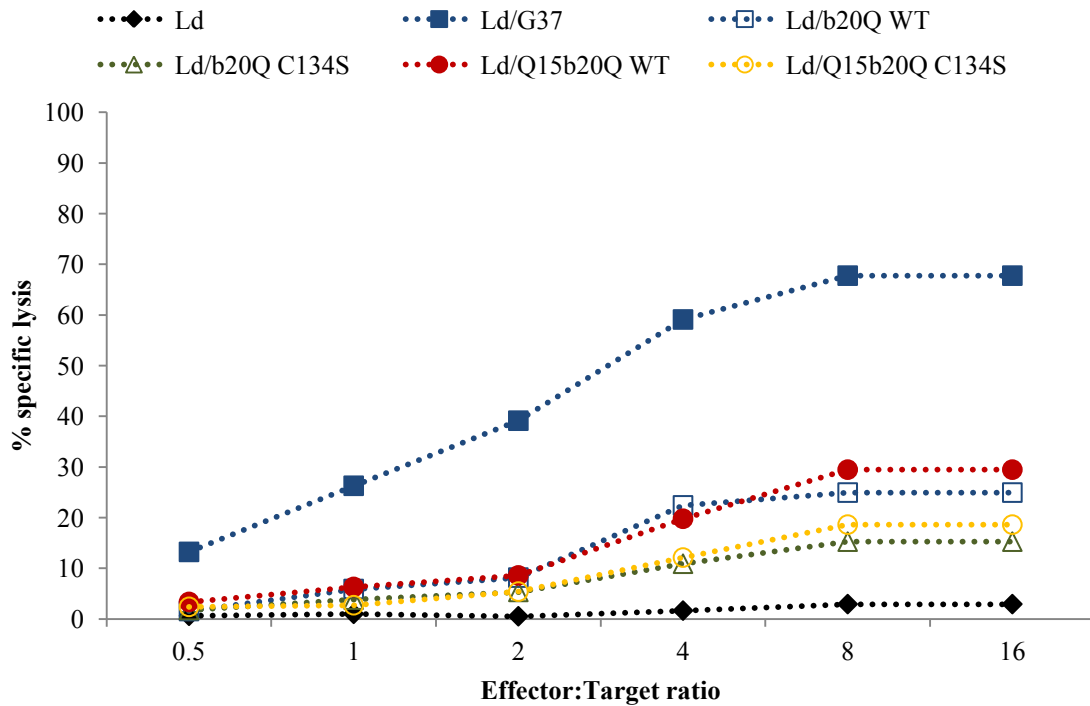




### Figure 4.2 5D2-T Cytotoxic Lysis of B78H1 Transfectants

B78H1 cells transfected with various Qa-1<sup>b</sup> constructs, or empty vector, were used as targets in a standard 4 hour <sup>51</sup>Cr release assay. The QDM/Qa-1<sup>b</sup> restricted alloreactive clone 5D2-T demonstrated a dose-dependent cytotoxic activity against Qa-1<sup>b</sup> transfected targets only when exogenous QDM was present (**B**), except in the case of the chimeric QDM<sub>15</sub>β<sub>2m20</sub>Qa-1<sup>b</sup> construct (**A**). Furthermore, the introduction of the C134S point mutation did not reduce the CTL response, but instead significantly enhanced it only in the presence of QDM peptide. This is strong evidence that the increased number of molecules on the surface of these cells are indeed well folded and present the cognate peptide. In order to maximize surface expression of Qa-1<sup>b</sup> proteins, target cells were shifted to 25°C with or without the addition of QDM peptide for 16 hours prior to radioactive chromium loading.

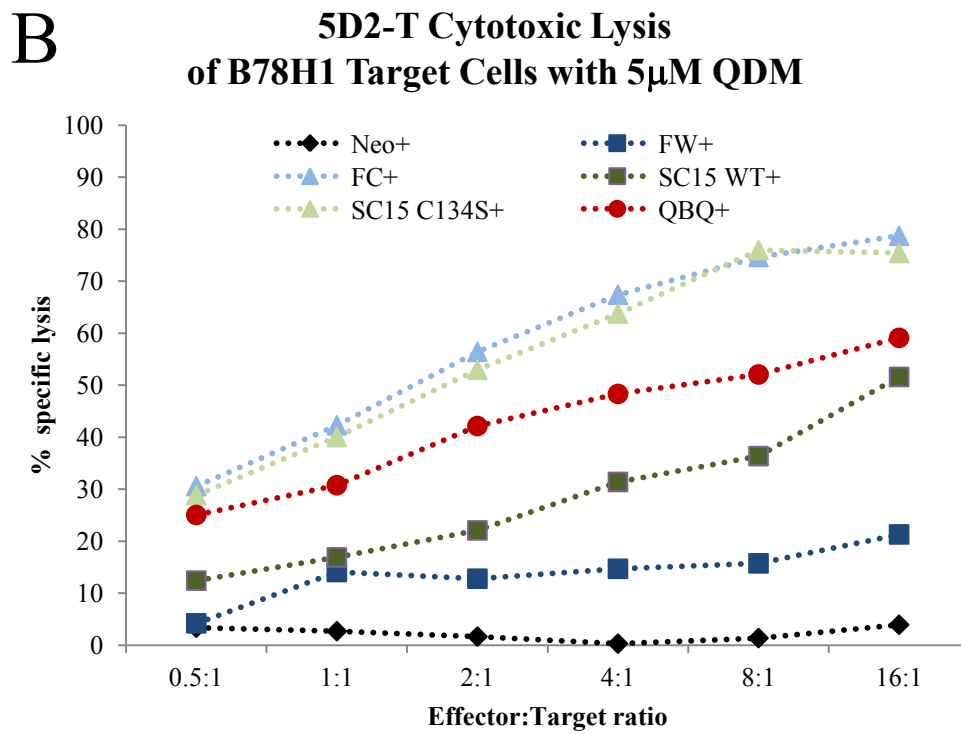
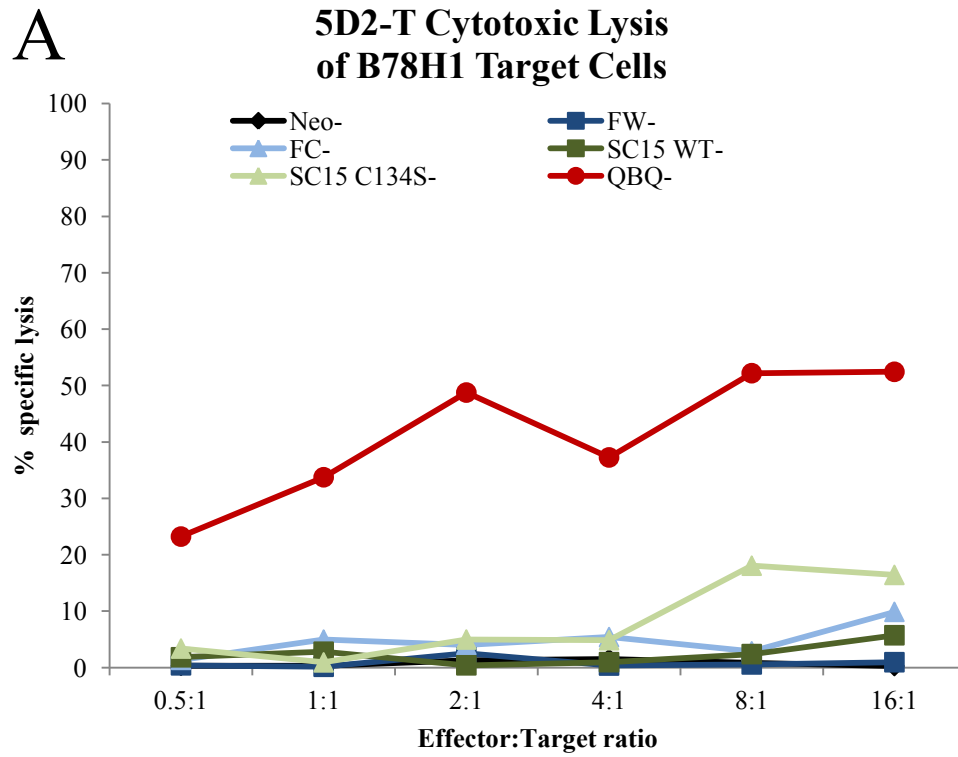


### Figure 4.3 5D2-T Cytotoxic Lysis of C1R and C1R/L<sup>d</sup> Transfectants

Human HLA-A/B null C1R cells transfected with several Qa-1<sup>b</sup> constructs with or without the additional co-expression of H2-L<sup>d</sup> were used as targets in a <sup>51</sup>Cr release assay. 5D2-T CD8<sup>+</sup> T cells effectively lyse chimeric QDM<sub>15</sub>β<sub>2</sub>m<sub>20</sub>Qa-1<sup>b</sup> expressing C1R cells (**A**) in the absence of co-expressed H2-L<sup>d</sup>, which provides the QDM peptide in trans(**B**). There is slight specific lysis of Qa-1<sup>b</sup> C134S target cells, however it is only marginally more effective than the lysis seen in wild type Qa-1<sup>b</sup> or β<sub>2</sub>m<sub>15</sub>Qa-1<sup>b</sup> constructs with or without the C134S mutation. Not surprisingly, the presence of H2-L<sup>d</sup> permits specific targeting of all Qa-1<sup>b</sup> transfected cell lines, although the β<sub>2</sub>m<sub>15</sub>Qa-1<sup>b</sup> chimeras were poor targets with or without QDM present. Additionally, in the presence of QDM in trans, all C134S mutants proved to be slightly poorer targets than their wild type counterparts, despite robust surface expression and prolonged half-lives.

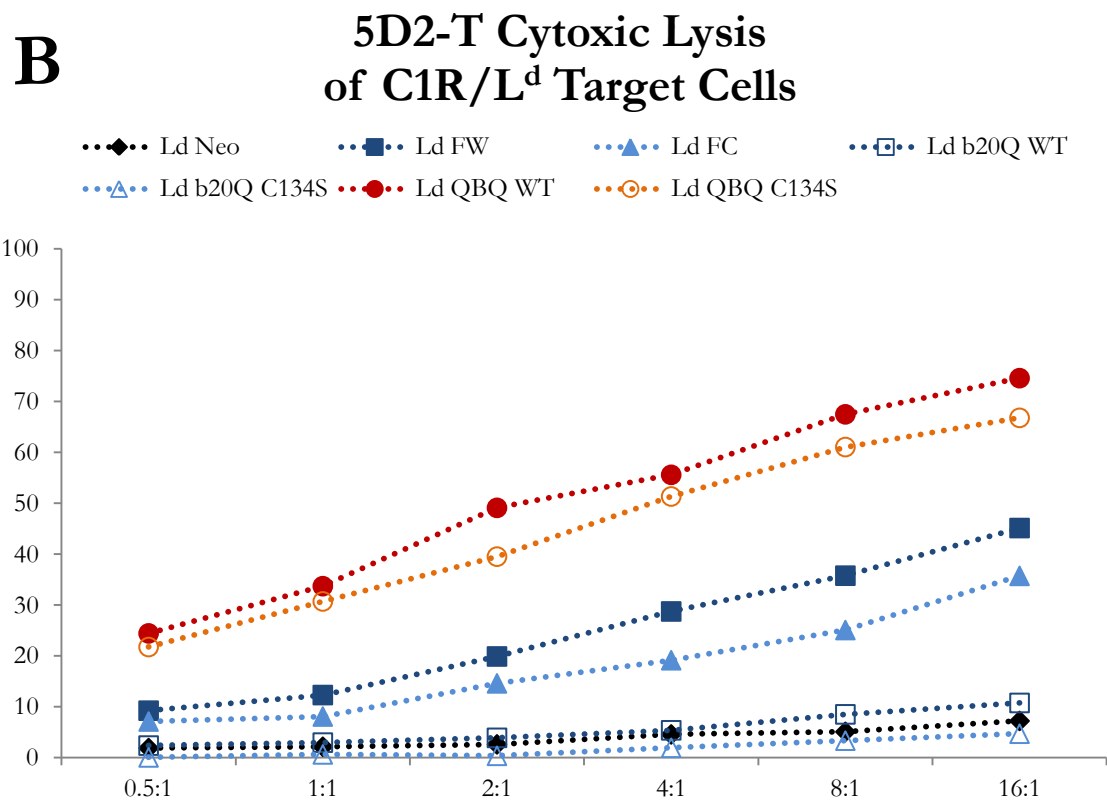
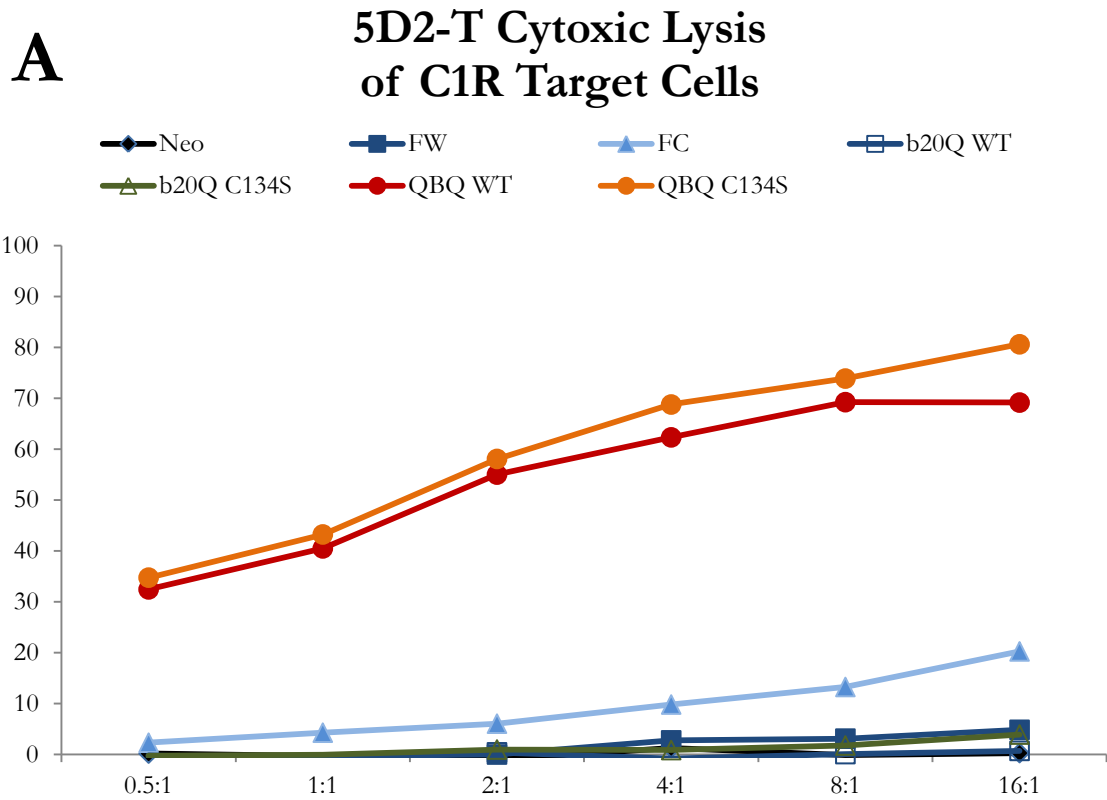


#### **Figure 4.4 5D2-T Cytotoxic Lysis of L(M)Tk<sup>-/-</sup> Transfectants**

Mouse fibroblast cell line L(M)Tk<sup>-/-</sup> were stably transfected with various CMV-promoter driven constructs of Qa-1<sup>b</sup> or an empty vector. Following single cell cloning by preparative FACS, cells were loaded with <sup>51</sup>Cr and used as targets in a cytotoxic release assay using the Qa-1<sup>b</sup>/QDM specific CD8<sup>+</sup> allotypic clone 5D2-T. While the parental cell line is Qa-1<sup>b</sup>-null, other class Ia and Ib MHC are expressed on the cell surface and the cell line generates endogenous QDM peptide derived from the leader sequence of Ia proteins. While all Qa-1<sup>b</sup> transfected clonal targets can be recognized by the 5D2-T effector cells, the addition of exogenous synthetic QDM enhanced target lysis for all constructs except the full-length wild type. Surprisingly, in the absence of exogenous peptide, when QDM is likely to be a limiting factor, the full-length C134S mutant proved to be a very poor target for 5D2-T effector cells.

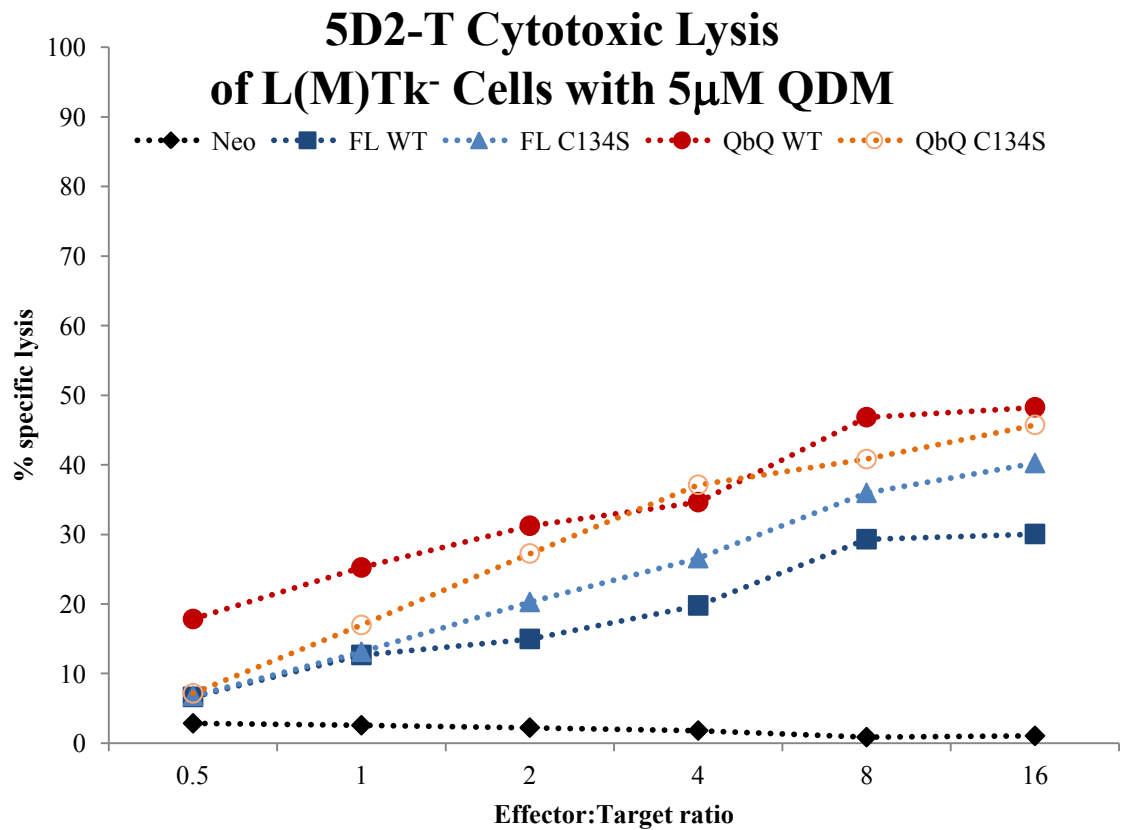
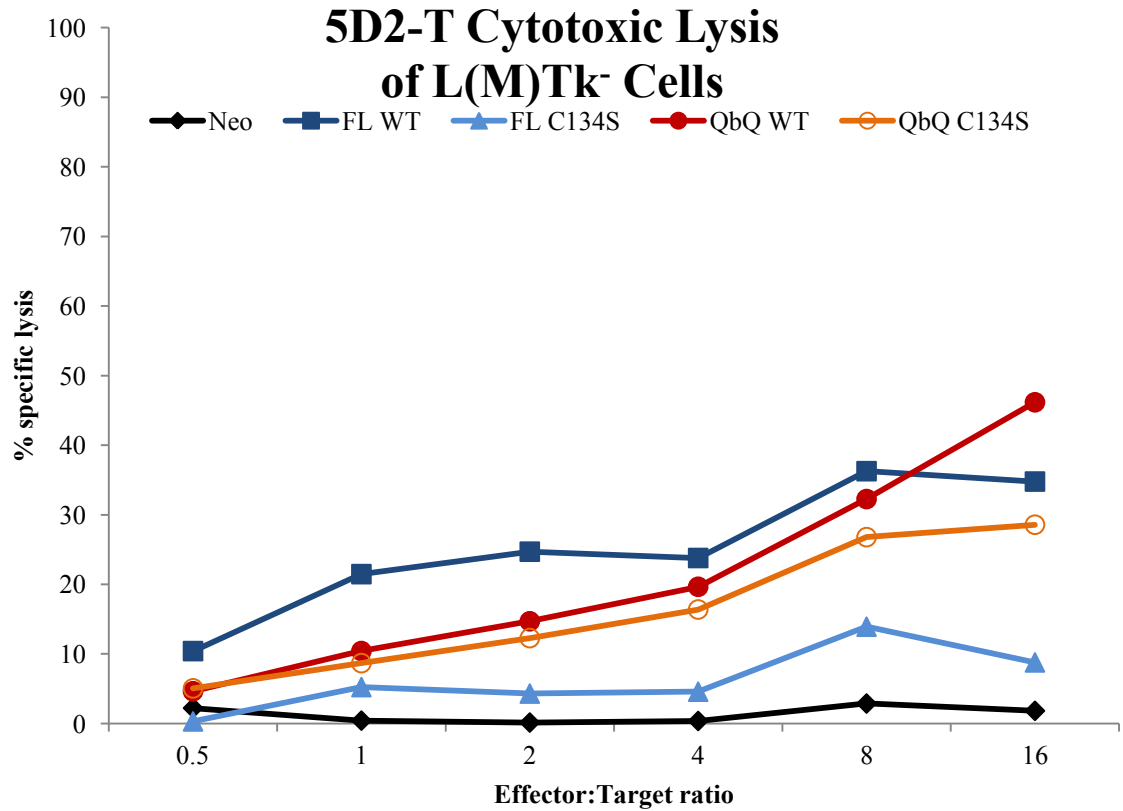


### Figure 4.5 CD94 and NKG2A/C/E expression by CTL clones

Alloreactive clones 5D2-T and 39.1D7X were analyzed by FACS for expression of CD94 and NKG2 receptors. Both clones express significant levels of the receptors specific for Qa-1 MHC. Surprisingly, clone 39.1D7X expresses both components of the heterodimeric receptor in a bimodal fashion. The 5D2-T clone, however, expresses a lower, but uniform quantity of each chain.

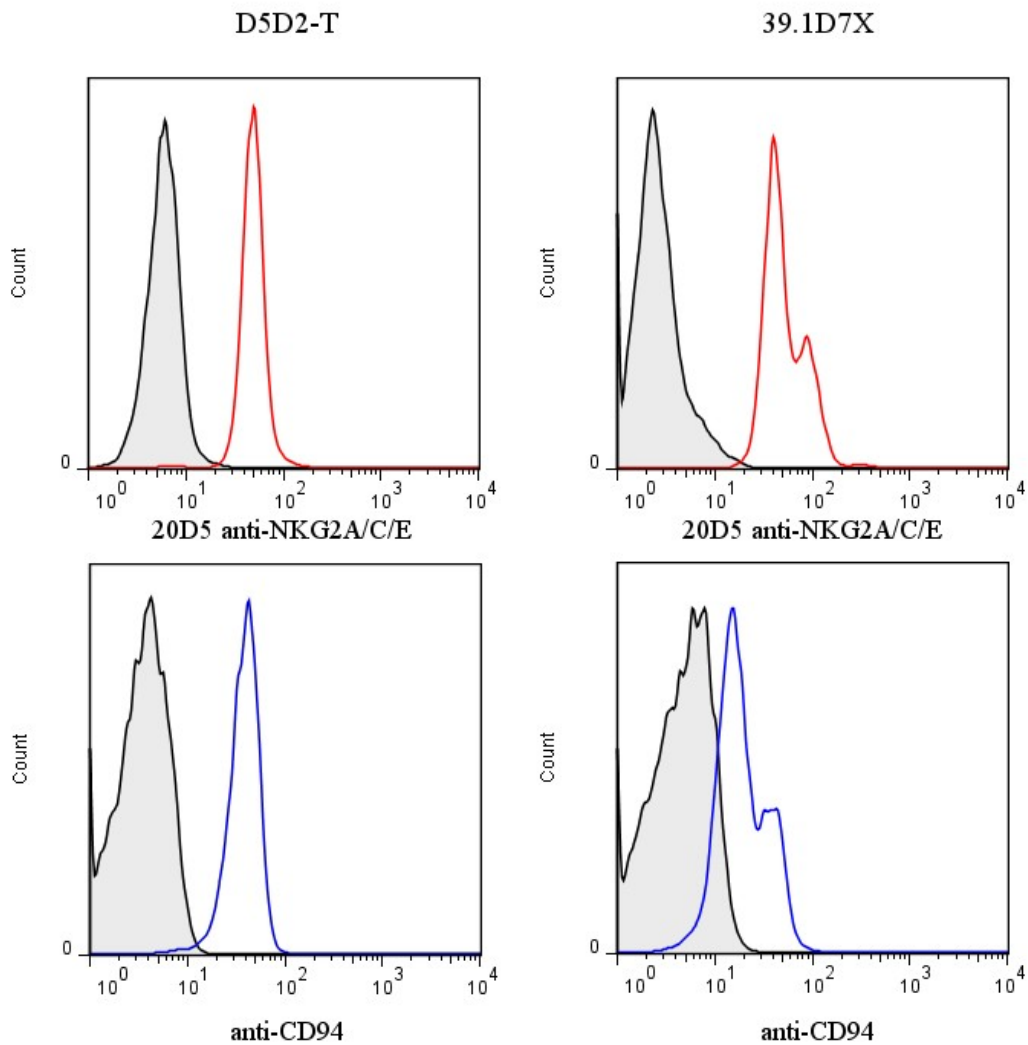
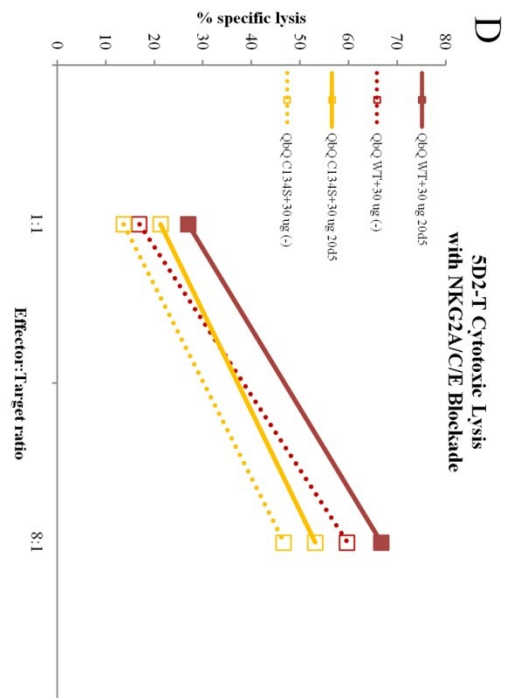
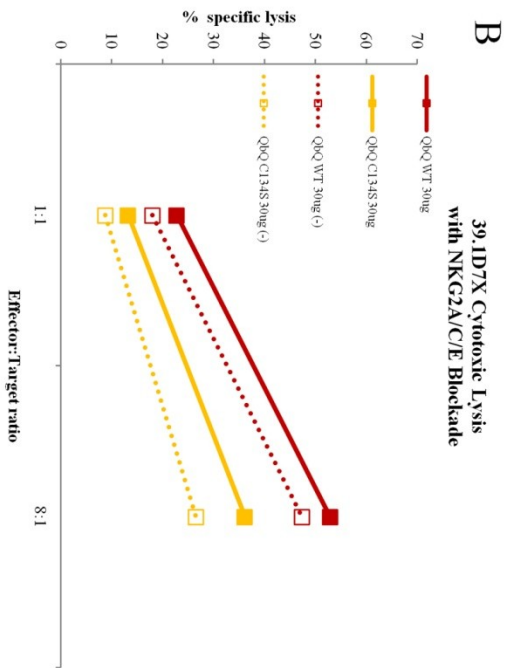
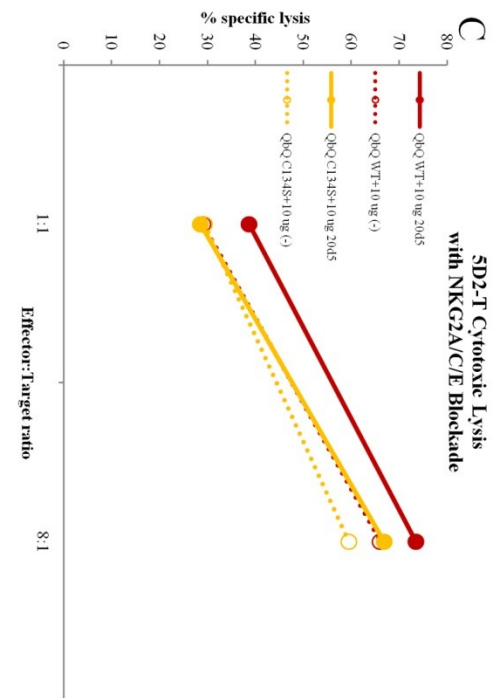
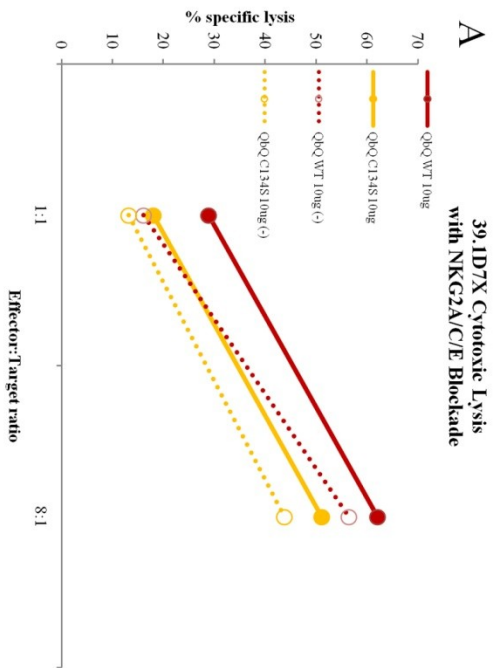


**Figure 4.6 CTL activity is enhanced by NKG2A/C/E blockade**

C1R cells expressing single chain chimeras of QDM<sub>15</sub>β<sub>2</sub>m<sub>20</sub>-Qa-1<sup>b</sup> were used as targets in a cytotoxic lysis assay in the presence of 10 or 30 μg/ml of the rat monoclonal antibody 20d5. This antibody blocks, but is not an agonist of heterodimeric CD94/NKG2A/C/E receptors. Qa-1<sup>b</sup> alloreactive T cell clones 39.1D7X (panels **A** and **B**) and 5D2-T (panels **C** and **D**) both display enhanced killing in the presence of the blocking antibody, compared to equimolar amounts of an isotype control. The presence of the C134S point mutation in each cell line results in higher surface levels of Qa-1<sup>b</sup> molecules, but leads to reduced specific lysis.





## References

1. Klein, J., A. Sato, and N. Nikolaidis, *MHC, TSP, and the origin of species: from immunogenetics to evolutionary genetics*. *Annu Rev Genet*, 2007. **41**: p. 281-304.
2. Sato, A., et al., *Class I mhc genes of cichlid fishes: identification, expression, and polymorphism*. *Immunogenetics*, 1997. **46**(1): p. 63-72.
3. Ohtsuka, M., et al., *Major histocompatibility complex (Mhc) class Ib gene duplications, organization and expression patterns in mouse strain C57BL/6*. *BMC Genomics*, 2008. **9**: p. 178.
4. Li, L., et al., *Differential requirement for tapasin in the presentation of leader- and insulin-derived peptide antigens to Qa-1b-restricted CTLs*. *J Immunol*, 2004. **173**(6): p. 3707-15.
5. Mempel, M., et al., *Natural killer T cells restricted by the monomorphic MHC class 1b CD1d1 molecules behave like inflammatory cells*. *J Immunol*, 2002. **168**(1): p. 365-71.
6. West, A.P., Jr. and P.J. Bjorkman, *Crystal structure and immunoglobulin G binding properties of the human major histocompatibility complex-related Fc receptor(γ)*. *Biochemistry*, 2000. **39**(32): p. 9698-708.
7. Delker, S.L., et al., *Crystallographic studies of ligand binding by Zn-alpha2-glycoprotein*. *J Struct Biol*, 2004. **148**(2): p. 205-13.
8. Lebron, J.A., et al., *Crystal structure of the hemochromatosis protein HFE and characterization of its interaction with transferrin receptor*. *Cell*, 1998. **93**(1): p. 111-23.
9. Krangel, M.S., et al., *Enforcing order within a complex locus: current perspectives on the control of V(D)J recombination at the murine T-cell receptor alpha/delta locus*. *Immunol Rev*, 2004. **200**: p. 224-32.
10. Colf, L.A., et al., *How a single T cell receptor recognizes both self and foreign MHC*. *Cell*, 2007. **129**(1): p. 135-46.
11. Wucherpfennig, K.W., et al., *Polyspecificity of T cell and B cell receptor recognition*. *Semin Immunol*, 2007. **19**(4): p. 216-24.
12. Sullivan, B.A., et al., *Homeostatic proliferation of a Qa-1b-restricted T cell: a distinction between the ligands required for positive selection and for proliferation in lymphopenic hosts*. *J Immunol*, 2004. **173**(10): p. 6065-71.
13. Davies, A., et al., *Infection-induced expansion of a MHC Class Ib-dependent intestinal intraepithelial gammadelta T cell subset*. *J Immunol*, 2004. **172**(11): p. 6828-37.
14. Soloski, M.J., et al., *Host immune response to intracellular bacteria: A role for MHC-linked class-Ib antigen-presenting molecules*. *Proc Soc Exp Biol Med*, 2000. **224**(4): p. 231-9.

15. Vance, R.E., et al., *Mouse CD94/NKG2A is a natural killer cell receptor for the nonclassical major histocompatibility complex (MHC) class I molecule Qa-1(b)*. J Exp Med, 1998. **188**(10): p. 1841-8.
16. Vance, R.E., A.M. Jamieson, and D.H. Raulet, *Recognition of the class Ib molecule Qa-1(b) by putative activating receptors CD94/NKG2C and CD94/NKG2E on mouse natural killer cells*. J Exp Med, 1999. **190**(12): p. 1801-12.
17. Deng, L. and R.A. Mariuzza, *Structural basis for recognition of MHC and MHC-like ligands by natural killer cell receptors*. Semin Immunol, 2006. **18**(3): p. 159-66.
18. Smyth, M.J., et al., *Activation of NK cell cytotoxicity*. Mol Immunol, 2005. **42**(4): p. 501-10.
19. Antoniou, A.N. and S.J. Powis, *Pathogen evasion strategies for the major histocompatibility complex class I assembly pathway*. Immunology, 2008. **124**(1): p. 1-12.
20. Dierssen, J.W., et al., *High-resolution analysis of HLA class I alterations in colorectal cancer*. BMC Cancer, 2006. **6**: p. 233.
21. Trowsdale, J. and P. Parham, *Mini-review: defense strategies and immunity-related genes*. Eur J Immunol, 2004. **34**(1): p. 7-17.
22. Biassoni, R., et al., *Human natural killer cell receptors: insights into their molecular function and structure*. J Cell Mol Med, 2003. **7**(4): p. 376-87.
23. Dimasi, N. and R. Biassoni, *Structural and functional aspects of the Ly49 natural killer cell receptors*. Immunol Cell Biol, 2005. **83**(1): p. 1-8.
24. Dimasi, N., L. Moretta, and R. Biassoni, *Structure of the Ly49 family of natural killer (NK) cell receptors and their interaction with MHC class I molecules*. Immunol Res, 2004. **30**(1): p. 95-104.
25. Dam, J., et al., *Variable MHC class I engagement by Ly49 natural killer cell receptors demonstrated by the crystal structure of Ly49C bound to H-2K(b)*. Nat Immunol, 2003. **4**(12): p. 1213-22.
26. Dimasi, N., et al., *Crystal structure of the Ly49I natural killer cell receptor reveals variability in dimerization mode within the Ly49 family*. J Mol Biol, 2002. **320**(3): p. 573-85.
27. Tormo, J., et al., *Crystal structure of a lectin-like natural killer cell receptor bound to its MHC class I ligand*. Nature, 1999. **402**(6762): p. 623-31.
28. Lee, N., et al., *HLA-E is a major ligand for the natural killer inhibitory receptor CD94/NKG2A*. Proc Natl Acad Sci U S A, 1998. **95**(9): p. 5199-204.
29. Lopez-Botet, M., et al., *The CD94/NKG2 C-type lectin receptor complex*. Curr Top Microbiol Immunol, 1998. **230**: p. 41-52.

30. Lopez-Botet, M., et al., *Structure and function of the CD94 C-type lectin receptor complex involved in recognition of HLA class I molecules*. Immunol Rev, 1997. **155**: p. 165-74.
31. Perez-Villar, J.J., et al., *Biochemical and serologic evidence for the existence of functionally distinct forms of the CD94 NK cell receptor*. J Immunol, 1996. **157**(12): p. 5367-74.
32. Perez-Villar, J.J., et al., *The CD94/NKG2-A inhibitory receptor complex is involved in natural killer cell-mediated recognition of cells expressing HLA-G1*. J Immunol, 1997. **158**(12): p. 5736-43.
33. Wolan, D.W., et al., *Crystal structure of the murine NK cell-activating receptor NKG2D at 1.95 Å*. Nat Immunol, 2001. **2**(3): p. 248-54.
34. Petrie, E.J., et al., *CD94-NKG2A recognition of human leukocyte antigen (HLA)-E bound to an HLA class I leader sequence*. J Exp Med, 2008. **205**(3): p. 725-35.
35. Aldrich, C.J., J.R. Rodgers, and R.R. Rich, *Regulation of Qa-1 expression and determinant modification by an H-2D-linked gene, Qdm*. Immunogenetics, 1988. **28**(5): p. 334-44.
36. Kaiser, B.K., et al., *Structural basis for NKG2A/CD94 recognition of HLA-E*. Proc Natl Acad Sci U S A, 2008. **105**(18): p. 6696-701.
37. Lefranc, M.P., et al., *IMGT, the international ImMunoGeneTics database*. Nucleic Acids Res, 1999. **27**(1): p. 209-12.
38. Lefranc, M.P., *IMGT, the international ImMunoGeneTics database*. Nucleic Acids Res, 2003. **31**(1): p. 307-10.
39. Maglott, D., et al., *Entrez Gene: gene-centered information at NCBI*. Nucleic Acids Res, 2007. **35**(Database issue): p. D26-31.
40. Davies, A., et al., *A peptide from heat shock protein 60 is the dominant peptide bound to Qa-1 in the absence of the MHC class Ia leader sequence peptide Qdm*. J Immunol, 2003. **170**(10): p. 5027-33.
41. DeCloux, A., et al., *Dominance of a single peptide bound to the class I(B) molecule, Qa-1b*. J Immunol, 1997. **158**(5): p. 2183-91.
42. Braud, V., E.Y. Jones, and A. McMichael, *The human major histocompatibility complex class Ib molecule HLA-E binds signal sequence-derived peptides with primary anchor residues at positions 2 and 9*. Eur J Immunol, 1997. **27**(5): p. 1164-9.
43. Wooden, S.L., et al., *Cutting edge: HLA-E binds a peptide derived from the ATP-binding cassette transporter multidrug resistance-associated protein 7 and inhibits NK cell-mediated lysis*. J Immunol, 2005. **175**(3): p. 1383-7.
44. O'Callaghan, C.A., et al., *Structural features impose tight peptide binding specificity in the nonclassical MHC molecule HLA-E*. Mol Cell, 1998. **1**(4): p. 531-41.

45. Ulbrecht, M., et al., *Cell surface expression of HLA-E: interaction with human beta2-microglobulin and allelic differences*. Eur J Immunol, 1999. **29**(2): p. 537-47.
46. Bjorkman, P.J., J.L. Strominger, and D.C. Wiley, *Crystallization and X-ray diffraction studies on the histocompatibility antigens HLA-A2 and HLA-A28 from human cell membranes*. J Mol Biol, 1985. **186**(1): p. 205-10.
47. Sanchez, L.M., C. Lopez-Otin, and P.J. Bjorkman, *Biochemical characterization and crystallization of human Zn-alpha2-glycoprotein, a soluble class I major histocompatibility complex homolog*. Proc Natl Acad Sci U S A, 1997. **94**(9): p. 4626-30.
48. Fremont, D.H., et al., *Crystal structures of two viral peptides in complex with murine MHC class I H-2Kb*. Science, 1992. **257**(5072): p. 919-27.
49. Altman, J.D., et al., *Phenotypic analysis of antigen-specific T lymphocytes*. Science, 1996. **274**(5284): p. 94-6.
50. He, X., et al., *Promiscuous antigen presentation by the nonclassical MHC Ib Qa-2 is enabled by a shallow, hydrophobic groove and self-stabilized peptide conformation*. Structure, 2001. **9**(12): p. 1213-24.
51. Madden, D.R., D.N. Garboczi, and D.C. Wiley, *The antigenic identity of peptide-MHC complexes: a comparison of the conformations of five viral peptides presented by HLA-A2*. Cell, 1993. **75**(4): p. 693-708.
52. Collins, E.J., D.N. Garboczi, and D.C. Wiley, *Three-dimensional structure of a peptide extending from one end of a class I MHC binding site*. Nature, 1994. **371**(6498): p. 626-9.
53. Carrington, J.C., et al., *Internal cleavage and trans-proteolytic activities of the VPg-proteinase (NIa) of tobacco etch potyvirus in vivo*. J Virol, 1993. **67**(12): p. 6995-7000.
54. Kambayashi, T., et al., *The nonclassical MHC class I molecule Qa-1 forms unstable peptide complexes*. J Immunol, 2004. **172**(3): p. 1661-9.
55. Kurucz, I., et al., *Correct disulfide pairing and efficient refolding of detergent-solubilized single-chain Fv proteins from bacterial inclusion bodies*. Mol Immunol, 1995. **32**(17-18): p. 1443-52.
56. Tan, S., *A modular polycistronic expression system for overexpressing protein complexes in Escherichia coli*. Protein Expr Purif, 2001. **21**(1): p. 224-34.
57. Tan, S., R.C. Kern, and W. Selleck, *The pST44 polycistronic expression system for producing protein complexes in Escherichia coli*. Protein Expr Purif, 2005. **40**(2): p. 385-95.
58. Manting, E.H. and A.J. Driessen, *Escherichia coli translocase: the unravelling of a molecular machine*. Mol Microbiol, 2000. **37**(2): p. 226-38.

59. Cretney, E., K. Takeda, and M.J. Smyth, *Cancer: novel therapeutic strategies that exploit the TNF-related apoptosis-inducing ligand (TRAIL)/TRAIL receptor pathway*. Int J Biochem Cell Biol, 2007. **39**(2): p. 280-6.
60. Speir, J.A., et al., *Structural basis of 2C TCR allorecognition of H-2Ld peptide complexes*. Immunity, 1998. **8**(5): p. 553-62.
61. Fremont, D.H., et al., *Crystal structure of an H-2Kb-ovalbumin peptide complex reveals the interplay of primary and secondary anchor positions in the major histocompatibility complex binding groove*. Proc Natl Acad Sci U S A, 1995. **92**(7): p. 2479-83.
62. Hoare, H.L., et al., *Subtle changes in peptide conformation profoundly affect recognition of the non-classical MHC class I molecule HLA-E by the CD94-NKG2 natural killer cell receptors*. J Mol Biol, 2008. **377**(5): p. 1297-303.
63. Zijlstra, M., et al., *Beta 2-microglobulin deficient mice lack CD4-8+ cytolytic T cells*. Nature, 1990. **344**(6268): p. 742-6.
64. Gras, S., et al., *T-cell receptor bias and immunity*. Curr Opin Immunol, 2008. **20**(1): p. 119-25.
65. Lybarger, L., et al., *Enhanced immune presentation of a single-chain major histocompatibility complex class I molecule engineered to optimize linkage of a C-terminally extended peptide*. J Biol Chem, 2003. **278**(29): p. 27105-11.
66. Chen, W. and P. Stanley, *Five Lec1 CHO cell mutants have distinct Mgat1 gene mutations that encode truncated N-acetylglucosaminyltransferase I*. Glycobiology, 2003. **13**(1): p. 43-50.
67. Leahy, D.J., et al., *A mammalian expression vector for expression and purification of secreted proteins for structural studies*. Protein Expr Purif, 2000. **20**(3): p. 500-6.
68. Aricescu, A.R., W. Lu, and E.Y. Jones, *A time- and cost-efficient system for high-level protein production in mammalian cells*. Acta Crystallogr D Biol Crystallogr, 2006. **62**(Pt 10): p. 1243-50.
69. Bendtsen, J.D., et al., *Improved prediction of signal peptides: SignalP 3.0*. J Mol Biol, 2004. **340**(4): p. 783-95.
70. Nielsen, H. and A. Krogh, *Prediction of signal peptides and signal anchors by a hidden Markov model*. Proc Int Conf Intell Syst Mol Biol, 1998. **6**: p. 122-30.
71. Geisbrecht, B.V., S. Bouyain, and M. Pop, *An optimized system for expression and purification of secreted bacterial proteins*. Protein Expr Purif, 2006. **46**(1): p. 23-32.
72. Busch, D.H., I. Pilip, and E.G. Pamer, *Evolution of a complex T cell receptor repertoire during primary and recall bacterial infection*. J Exp Med, 1998. **188**(1): p. 61-70.
73. Busch, D.H., et al., *Coordinate regulation of complex T cell populations responding to bacterial infection*. Immunity, 1998. **8**(3): p. 353-62.

74. Sato, A. and N. Okamoto, *Characterization of the cell-mediated cytotoxic responses of isogenic ginbuna crucian carp induced by oral immunisation with hapten-modified cellular antigens*. Fish Shellfish Immunol, 2008. **24**(6): p. 684-92.
75. Fulton, Z., et al., *Expression, purification, crystallization and preliminary X-ray characterization of a putative glycosyltransferase of the GT-A fold found in mycobacteria*. Acta Crystallogr Sect F Struct Biol Cryst Commun, 2008. **64**(Pt 5): p. 428-31.
76. Godfrey, D.I., J. Rossjohn, and J. McCluskey, *The fidelity, occasional promiscuity, and versatility of T cell receptor recognition*. Immunity, 2008. **28**(3): p. 304-14.
77. Rossjohn, J., et al., *Human theta class glutathione transferase: the crystal structure reveals a sulfate-binding pocket within a buried active site*. Structure, 1998. **6**(3): p. 309-22.
78. Altschul, S.F., et al., *Basic local alignment search tool*. J Mol Biol, 1990. **215**(3): p. 403-10.
79. Kit, S., et al., *Deletion of Thymidine Kinase Activity from L Cells Resistant to Bromodeoxyuridine*. Exp Cell Res, 1963. **31**: p. 297-312.
80. Graf, L.H., Jr., P. Kaplan, and S. Silagi, *Efficient DNA-mediated transfer of selectable genes and unselected sequences into differentiated and undifferentiated mouse melanoma clones*. Somat Cell Mol Genet, 1984. **10**(2): p. 139-51.
81. Chiang, E.Y. and I. Stroynowski, *The role of structurally conserved class I MHC in tumor rejection: contribution of the Q8 locus*. J Immunol, 2006. **177**(4): p. 2123-30.
82. Storkus, W.J., et al., *Reversal of natural killing susceptibility in target cells expressing transfected class I HLA genes*. Proc Natl Acad Sci U S A, 1989. **86**(7): p. 2361-4.
83. Aldrich, C.J., et al., *Identification of a Tap-dependent leader peptide recognized by alloreactive T cells specific for a class Ib antigen*. Cell, 1994. **79**(4): p. 649-58.
84. McGrath, M.E., *The lysosomal cysteine proteases*. Annu Rev Biophys Biomol Struct, 1999. **28**: p. 181-204.
85. Nagano, N., M. Ota, and K. Nishikawa, *Strong hydrophobic nature of cysteine residues in proteins*. FEBS Lett, 1999. **458**(1): p. 69-71.
86. Zeng, L., et al., *A structural basis for antigen presentation by the MHC class Ib molecule, Qa-1b*. J Immunol, 2012. **188**(1): p. 302-10.
87. Winn, M.D., *An overview of the CCP4 project in protein crystallography: an example of a collaborative project*. J Synchrotron Radiat, 2003. **10**(Pt 1): p. 23-5.
88. Buck, C.B., et al., *The human immunodeficiency virus type 1 gag gene encodes an internal ribosome entry site*. J Virol, 2001. **75**(1): p. 181-91.
89. Russell, R.B. and G.J. Barton, *Multiple protein sequence alignment from tertiary structure comparison: assignment of global and residue confidence levels*. Proteins, 1992. **14**(2): p. 309-23.

90. Aldrich, C.J., et al., *T cell recognition of Q<sub>A</sub>-1b antigens on cells lacking a functional Tap-2 transporter*. J Immunol, 1992. **149**(12): p. 3773-7.
91. Lowen, L.C., C.J. Aldrich, and J. Forman, *Analysis of T cell receptors specific for recognition of class IB antigens*. J Immunol, 1993. **151**(11): p. 6155-65.
92. Brunner, K.T., et al., *Quantitative assay of the lytic action of immune lymphoid cells on 51-Cr-labelled allogeneic target cells in vitro; inhibition by isoantibody and by drugs*. Immunology, 1968. **14**(2): p. 181-96.
93. McMahan, C.W. and D.H. Raulet, *Expression and function of NK cell receptors in CD8+ T cells*. Curr Opin Immunol, 2001. **13**(4): p. 465-70.
94. Lu, L., et al., *Regulation of activated CD4+ T cells by NK cells via the Q<sub>a</sub>-1-NKG2A inhibitory pathway*. Immunity, 2007. **26**(5): p. 593-604.
95. Braud, V.M., et al., *Expression of CD94-NKG2A inhibitory receptor is restricted to a subset of CD8+ T cells*. Trends Immunol, 2003. **24**(4): p. 162-4.
96. Vance, R.E., et al., *Implications of CD94 deficiency and monoallelic NKG2A expression for natural killer cell development and repertoire formation*. Proc Natl Acad Sci U S A, 2002. **99**(2): p. 868-73.
97. Strong, R.K., et al., *HLA-E allelic variants. Correlating differential expression, peptide affinities, crystal structures, and thermal stabilities*. J Biol Chem, 2003. **278**(7): p. 5082-90.



CURRICULUM VITAE FOR Ph.D. CANDIDATES  
The Johns Hopkins University School of Medicine

Kasra X. Ramyar

June 2014

**Educational History:**

Ph.D. Expected 2014	Program in Immunology Mentor: Mark Soloski, Ph.D.	Johns Hopkins School of Medicine
B.S. 1993	Biology	Johns Hopkins University

**Other Professional Experience:**

Research Associate 2013-	Dept. of Biochemistry & Molecular Biophysics	Kansas State University
Research Associate 2008- 2013	Dept. of Cell Biology & Biophysics	University of Missouri Kansas City

**Publications:**

Garcia, B. L., B. J. Summers, **K. X. Ramyar**, A. Tzekou, Z. Lin, D. Ricklin, J. D. Lambris, J. H. Laity and B. V. Geisbrecht. "A Structurally Dynamic N-Terminal Helix Is a Key Functional Determinant in Staphylococcal Complement Inhibitor (Scin) Proteins." *J Biol Chem* 288, no. 4 (2013): 2870-81.

Skaff, D. A., **K. X. Ramyar**, W. J. McWhorter, M. L. Barta, B. V. Geisbrecht and H. M. Miziorko. "Biochemical and Structural Basis for Inhibition of Enterococcus Faecalis Hydroxymethylglutaryl-Coa Synthase, Mvas, by Hymeglusin." *Biochemistry* 51, no. 23 (2012): 4713-22.

Garcia, B. L., B. J. Summers, Z. Lin, **K. X. Ramyar**, D. Ricklin, D. V. Kamath, Z. Q. Fu, J. D. Lambris and B. V. Geisbrecht. "Diversity in the C3b [Corrected] Contact Residues and Tertiary Structures of the Staphylococcal Complement Inhibitor (Scin) Protein Family." *J Biol Chem* 287, no. 1 (2012): 628-40.

Garcia, B. L., **K. X. Ramyar**, D. Ricklin, J. D. Lambris and B. V. Geisbrecht. "Advances in Understanding the Structure, Function, and Mechanism of the Scin and Efb Families of Staphylococcal Immune Evasion Proteins." *Adv Exp Med Biol* 946, (2012): 113-33.

Bannantine, J. P., C. K. Lingle, J. R. Stabel, **K. X. Ramyar**, B. L. Garcia, A. J. Raeber, P. Schacher, V. Kapur and B. V. Geisbrecht. "Map1272c Encodes an Nlpc/P60 Protein, an Antigen Detected in Cattle with Johne's Disease." *Clin Vaccine Immunol* 19, no. 7 (2012): 1083-92.

Garcia, B. L., **K. X. Ramyar**, A. Tzekou, D. Ricklin, W. J. McWhorter, J. D. Lambris and B. V. Geisbrecht. "Molecular Basis for Complement Recognition and Inhibition Determined by Crystallographic Studies of the Staphylococcal Complement Inhibitor (Scin) Bound to C3c and C3b." *J Mol Biol* 402, no. 1 (2010): 17-29.

Garcia, B. L., A. Tzekou, **K. X. Ramyar**, W. J. McWhorter, D. Ricklin, J. D. Lambris and B. V. Geisbrecht. "Crystallization of Human Complement Component C3b in the Presence of a Staphylococcal Complement-Inhibitor Protein (Scin)." *Acta Crystallogr Sect F Struct Biol Cryst Commun* 65, no. Pt 5 (2009): 482-5.

Hammel, M., G. Sfyroera, S. Pyrpasopoulos, D. Ricklin, **K. X. Ramyar**, M. Pop, Z. Jin, J. D. Lambris and B. V. Geisbrecht. "Characterization of Ehp, a Secreted Complement Inhibitory Protein from *Staphylococcus Aureus*." *J Biol Chem* 282, no. 41 (2007): 30051-61.

Lassen, K. G., **K. X. Ramyar**, J. R. Bailey, Y. Zhou and R. F. Siliciano. "Nuclear Retention of Multiply Spliced Hiv-1 Rna in Resting Cd4+ T Cells." *PLoS Pathog* 2, no. 7 (2006): e68.

Hammel, M., **K. X. Ramyar**, C. T. Spencer and B. V. Geisbrecht. "Crystallization and X-Ray Diffraction Analysis of the Complement Component-3 (C3) Inhibitory Domain of Efb from *Staphylococcus Aureus*." *Acta Crystallogr Sect F Struct Biol Cryst Commun* 62, no. Pt 3 (2006): 285-8.

Cho, H. S., K. Mason, **K. X. Ramyar**, A. M. Stanley, S. B. Gabelli, D. W. Denney, Jr. and D. J. Leahy. "Structure of the Extracellular Region of Her2 Alone and in Complex with the Herceptin Fab." *Nature* 421, no. 6924 (2003): 756-60.

Leahy, D. J., C. E. Dann, 3rd, P. Longo, B. Perman and **K. X. Ramyar**. "A Mammalian Expression Vector for Expression and Purification of Secreted Proteins for Structural Studies." *Protein Expr Purif* 20, no. 3 (2000): 500-6.

Korb, L. C., S. Mirshahidi, **K. Ramyar**, A. A. Sadighi Akha and S. Sadegh-Nasseri. "Induction of T Cell Anergy by Low Numbers of Agonist Ligands." *J Immunol* 162, no. 11 (1999): 6401-9.

Merdes, A., **K. Ramyar**, J. D. Vechio and D. W. Cleveland. "A Complex of Numa and Cytoplasmic Dynein Is Essential for Mitotic Spindle Assembly." *Cell* 87, no. 3 (1996): 447-58.